

1-1-2014

# Cxcr2 Macromolecular Complex In Pancreatic Cancer: A Potential Therapeutic Target In Tumor Growth

Shuo Wang  
*Wayne State University,*

Follow this and additional works at: [http://digitalcommons.wayne.edu/oa\\_dissertations](http://digitalcommons.wayne.edu/oa_dissertations)

 Part of the [Cell Biology Commons](#)

---

## Recommended Citation

Wang, Shuo, "Cxcr2 Macromolecular Complex In Pancreatic Cancer: A Potential Therapeutic Target In Tumor Growth" (2014).  
*Wayne State University Dissertations*. Paper 934.

This Open Access Dissertation is brought to you for free and open access by DigitalCommons@WayneState. It has been accepted for inclusion in Wayne State University Dissertations by an authorized administrator of DigitalCommons@WayneState.

**CXCR2 MACROMOLECULAR COMPLEX IN PANCREATIC CANCER:  
A POTENTIAL THERAPEUTIC TARGET IN TUMOR GROWTH**

by

**SHUO WANG**

**DISSERTATION**

Submitted to the Graduate School

of Wayne State University,

Detroit, Michigan

in partial fulfillment of the requirements

for the degree of

**DOCTOR OF PHILOSOPHY**

2014

MAJOR: BIOCHEMISTRY AND  
MOLECULAR BIOLOGY

Approved by:

---

Advisor

Date

---

---

---

---

**© COPYRIGHT BY**

**SHUO WANG**

**2014**

**All Rights Reserved**

**DEDICATION**

to my parents

for their unconditional love and support.

## **ACKNOWLEDGEMENTS**

I would like sincerely and grateful thank my dissertation advisor, Dr. Chunying Li, for his guidance, training, understanding and patience during my graduate studies at Wayne State University. His mentorship was superb by providing a well-rounded training plan allowing me to obtain adequate experimental experience and also encouraging me to develop my own individuality and independence. I would also like to thank all the group members I have been working with: Yanning Wu, Annette Stewart, Yuning Hou, Marcello P. Castelvetero, and Xiaoqing Guan.

I would also like to thank Dr. Timothy Stemmler, Dr. Jianjun Wang, and Dr. Xuequn Chen for their valuable suggestions, accessibilities and all kinds of help on my graduate studies.

I would also like to thank everyone in the department with whom I have the most meaningful years at Wayne State.

## TABLE OF CONTENTS

|   |           |
|---|-----------|
| Dedication .....  | ii        |
| Acknowledgements .....  | iii       |
| List of Abbreviations .....   | viii      |
| List of Tables .....  | xii       |
| List of Figures.....  | xiii      |
| <b>Chapter I – Introduction .....</b>   | <b>1</b>  |
| 1.1 Overview of CXCR2 Chemokine Receptor.....                                     | 1         |
| 1.1.1 Chemokines and Chemokine Receptors .....                                    | 1         |
| 1.1.2 CXCR2 Structure .....   | 2         |
| 1.1.3 CXCR2 Ligands and Signaling .....   | 3         |
| 1.1.4 Roles of CXCR2 Biological Axis .....  | 5         |
| 1.2 CXCR2 in Diseases and Its Clinical Significance .....                         | 5         |
| 1.2.1 CXCR2 in inflammatory diseases .....  | 5         |
| 1.2.2 CXCR2 in Cancer .....   | 8         |
| 1.3 CXCR2 Antagonists and Therapeutic Implications .....                          | 9         |
| 1.4 CXCR2 Macromolecular Complex – Identification and Therapeutic Potential ..... | 14        |
| <b>Chapter II – CXCR2 Macromolecular Complex in Pancreatic Cancer .....</b>       | <b>20</b> |
| 2.1 Introduction .....  | 20        |
| 2.1.1 Overview of Pancreatic Cancer .....   | 20        |
| 2.1.2 Biological Axis of CXCR2 in Pancreatic Cancer .....                         | 20        |
| 2.1.3 PDZ proteins and PDZ domain-mediated protein-protein interaction .....      | 21        |
| 2.2 Materials and Methods .....   | 23        |

|  |    |
|--|----|
| 2.2.1 Antibodies and Reagents .....  | 23 |
| 2.2.2 Bacterial Strains, plasmid constructions, and mutagenesis .....  | 25 |
| 2.2.3 Protein Expression and Purification .....  | 27 |
| 2.2.4 Cell Culture .....   | 31 |
| 2.2.5 DNA Transfection .....   | 32 |
| 2.2.6 Western Blot Analysis .....  | 32 |
| 2.2.7 GST Pull-down Assay .....  | 33 |
| 2.2.8 Pair-wise Binding Assay .....  | 33 |
| 2.2.9 Macromolecular Complex Assembly Assay .....  | 34 |
| 2.2.10 Co-Immunoprecipitation Assay .....  | 35 |
| 2.2.11 Cell Proliferation Assay .....  | 35 |
| 2.2.12 Cell Invasion Assay .....   | 36 |
| 2.2.13 Pancreatic Cancer-induced angiogenesis of endothelial cells .....   | 37 |
| 2.2.14 Xenografts of Human Pancreatic Cancer cells in Immunodeficient Mice .....   | 37 |
| 2.2.15 Immunohistochemistry and Quantification of Proliferation Index .....  | 38 |
| 2.2.16 Statistical Analysis .....  | 38 |
| 2.3 Results .....  | 39 |
| 2.3.1 Bacterial Expression and Protein Purification .....  | 39 |
| 2.3.2 Overexpression of CXCR2 in human pancreatic cancer cells .....   | 42 |
| 2.3.3 Endogenous CXCR2 and PLC- $\beta$ 3 in human pancreatic cancer cells preferentially<br>Interacts with NHERF1 ..... | 42 |
| 2.3.4 CXCR2 and PLC- $\beta$ 3 Interact with NHERF1 in a Direct and PDZ Motif-Dependent<br>Manner .....                  | 44 |
| 2.3.5 CXCR2 interacts with both PDZ domains of NHERF1 (PDZ1 and PDZ2) .....  | 46 |

|  |           |
|--|-----------|
| 2.3.6 Endogenous PLC- $\beta$ 3 in human pancreatic cancer cells preferentially interacts with NHERF1-PDZ2 .....   | 49        |
| 2.3.7 NHERF1 Clusters CXCR2 and PLC- $\beta$ 3 into a Macromolecular Complex both <i>In Vitro</i> and in human pancreatic cancer cells .....                         | 52        |
| 2.3.8 CXC Chemokine/CXCR2 Biological Axis Promotes Pancreatic Cancer Cell Proliferation .....  | 54        |
| 2.3.9 Disrupting the CXCR2 Macromolecular Complex Inhibits Pancreatic Cancer Proliferation .....   | 56        |
| 2.3.10 Inhibitory effect of EF1060 on MIA PaCa-2 proliferation .....   | 59        |
| 2.3.11 Disrupting the CXCR2 Macromolecular Complex Blocks Pancreatic Cancer Cell Invasion .....  | 62        |
| 2.3.12 Disrupting the CXCR2 Macromolecular Complex Blocks Pancreatic Cancer-induced angiogenesis .....   | 62        |
| 2.3.13 Disrupting the CXCR2 Macromolecular Complex Inhibits Pancreatic Tumor Growth <i>In Vivo</i> .....   | 66        |
| 2.4 Discussion .....   | 68        |
| <b>Chapter III – Crystallographic Analysis of NHERF1-PLC<math>\beta</math>3 Interaction Provides Structural Basis for CXCR2 Signaling in Pancreatic Cancer .....</b> | <b>71</b> |
| 3.1 Introduction .....   | 71        |
| 3.2 Materials and Methods .....  | 79        |
| 3.2.1 Protein Expression and Purification .....  | 79        |
| 3.2.2 Crystallization, Data Collection and Structure Determination .....   | 80        |
| 3.2.3 Protein Data Bank Accession Number .....   | 82        |
| 3.3 Results .....  | 82        |
| 3.4 Discussion.....  | 86        |
| <b>Chapter IV – Conclusion and Future Directions.....</b>  | <b>88</b> |
| 4.1 Conclusion .....   | 88        |



|  |     |
|--|-----|
| 4.2 Future Directions .....  | 89  |
| 4.2.1 Investigation of the effect of the CXCR2 macromolecular complex in CXCR2 Signaling .....                                     | 89  |
| 4.2.2 Further Characterization of Interactions between NHERF1 and CXCR2 by Flourescence Recovery After Photobleaching (FRAP) ..... | 91  |
| Appendix: Correspondance .....   | 96  |
| References .....   | 98  |
| Abstract .....   | 111 |
| Autobiographical Statement .....   | 113 |

## LIST OF ABBREVIATIONS

|        |   |
|--------|---|
| AAA    | PDZ motif mutants (last three amino acids of PDZ motifs of CXCR2/PLC- $\beta$ 3 were replaced by amino acids AAA using mutagenesis) |
| AAV2   | Adeno-Associated Virus, Serotype 2  |
| ALI    | Acute Lung Injury   |
| ARDS   | Acute Respiratory Distress Syndrome   |
| BALF   | Bronchoalveolar Lavage Fluid  |
| BK     | Bradykinin  |
| BSA    | Bovine Serum Albumin  |
| cAMP   | Cyclic Adenosine Monophosphate  |
| CCK    | Cholecystokinin   |
| CCR2   | Chemokine (C-C Motif) Receptor 2  |
| CF     | Cystic Fibrosis   |
| CFTR   | Cystic Fibrosis Transmembrane Conductance Regulator   |
| co-IP  | Co-Immunoprecipitation  |
| COPD   | Chronic Obstructive Pulmonary Disease   |
| C-tail | Last 45 amino acids (or 100 amino acids) of the C-terminus of CXCR2 (or PLC- $\beta$ 3)   |
| CXCL1  | Chemokine (C-X-C Motif) Ligand 1  |
| CXCL5  | Chemokine (C-X-C Motif) Ligand 5  |
| CXCL8  | Chemokine (C-X-C Motif) Ligand 8  |
| CXCR2  | Chemokine (C-X-C Motif) Receptor 2  |

|                |   |
|----------------|---|
| DAG            | 1, 2-Diacylglycerol   |
| DMSO           | Dimethyl Sulfoxide  |
| <i>E. coli</i> | Escherichia Coli  |
| ENA-78         | Epithelial-Derived Neutrophil-Activating Peptide 78                           |
| EPC            | Endothelial Progenitor Cell   |
| ERM            | Ezrin-Radixin-Moesin  |
| EYFP           | Enhanced Yellow Fluorescent Protein   |
| FBS            | Fetal Bovine Serum  |
| FL             | Full-length   |
| FLAG           | Flag-tag (or Flag octapeptide) with the protein sequence of<br>DYKDDDDK       |
| FRAP           | Flourescence Recovery After Photobleaching                                    |
| GAIP           | Guanosine Triphosphatase-Activating Protein                                   |
| GAPDH          | Glyceraldehyde 3-Phosphate Dehydrogenase                                      |
| GFP            | Green Fluorescent Protein   |
| GIPC           | GAIP-Interacting Protein, C Terminus  |
| GPCR           | G-Protein Coupled Receptor  |
| GRO $\alpha$   | Growth-Related Oncogene $\alpha$  |
| GST            | Glutathione S-Transferase   |
| GTPase         | Hydrolase Enzymes That Can Bind And Hydrolyze Guanosine<br>Triphosphate (GTP) |
| HA             | Hemagglutinin   |
| HEK293         | Human Embryonic Kidney 293 Cells  |

|                   |  |
|-------------------|--|
| HUVEC             | Human Umbilical Vein Endothelial Cells   |
| I/R-I             | Ischemia Reperfusion Injury  |
| IBD               | Inflammatory Bowel Diseases  |
| IL-8              | Interkeukin-8 (as known as CXCL8)  |
| IL-8RB (= CXCR2)  | Interkeukin-8 Receptor Type B  |
| IP <sub>3</sub>   | Inositol-1,4,5-Trisphosphate   |
| IPTG              | Isopropyl β-D-1-Thiogalactopyranoside  |
| IQGAP1            | Ras GTPase-activating-like protein   |
| kDa               | Kilo Dalton  |
| LASP-1            | LIM and SH3 protein-1  |
| LB Broth medium   | Luria-Bertani Broth medium   |
| LIC               | Ligation Independent Cloning   |
| LPAR2             | Lysophosphatidic Acid Receptor 2   |
| MAPK              | Mitogen Activated Protein Kinase   |
| MPO               | Myeloperoxidase  |
| MTT               | 3-(4,5-Dimethylthiazol-2-yl)-2,5-Diphenyltetrazolium Bromide   |
| NHERF1            | Sodium-Hydrogen Antiporter 3 Regulator 1   |
| OD <sub>600</sub> | Optical density of a sample measured at wavelength of 600nm  |
| PAGE              | Polyacrylamide Gel Electrophoresis   |
| PDAC              | Pancreatic Ductal Adenocarcinoma   |
| PDGFR             | Platelet-Derived Growth Factor Receptor  |
| PDZ               | Post Synaptic Density Protein (PSD95), Drosophila Disc Large Tumor Suppressor (Dlg1), and Zonula Occludens-1 Protein (Zo-1); |

|                  |   |
|------------------|---|
|                  | <b>PSD-95/DIga/ZO-1</b>   |
| PGP              | tri-peptide Proline-Glycine-Proline                             |
| PI3K             | Phosphoinositide 3-Kinase                                       |
| PIP <sub>2</sub> | Phosphatidylinositol 4, 5- Bisphosphate                         |
| PLC              | Phospholipase C   |
| PLC-β            | Phospholipase C, β Isozyme                                      |
| PMN              | Polymorphonuclear Neutrophil                                    |
| PMSF             | Phenylmethylsulfonyl Fluoride                                   |
| PVDF             | Polyvinylidene Fluoride   |
| Rab              | Ras-related protein that in humans is encoded by the RAB8A gene |
| Rab11-FIP2       | Rab11-family interacting protein 2                              |
| S.O.C. medium    | Super Optimal Broth medium with Catabolite repression           |
| SCID             | Severe Combined Immunodeficiency                                |
| SDS              | Sodium Dodecyl Sulfate  |
| TIRFM            | Total Internal Reflection Fluorescence Microscope               |
| VASP             | Vasodilator-Stimulated Phosphoprotein                           |
| β2AR             | β2-Adrenergic Receptor  |
| ΔTTL/ΔTQL        | PDZ Motif Deletion Of CXCR2/PLC-β3                              |

## LIST OF TABLES

|  |    |
|--|----|
| Table 1-1 – CXCR2 Antagonists .....                            | 11 |
| Table 2-1 – Primes used in the current study .....             | 28 |
| Table 3-1 – Table 2-1 – Primes used in the current study ..... | 81 |

## LIST OF FIGURES

|             |  |    |
|-------------|--|----|
| Figure 1-1  | CXCR2 structure and receptor-ligand binding .....  | 4  |
| Figure 2-1  | Purification of the bacterially expressed GST-His-S-CXCR2-C-tail and His-S-PLC- $\beta$ 3-C-tail .....         | 40 |
| Figure 2-2  | Overexpression of CXCR2 in human pancreatic cancer cells .....   | 43 |
| Figure 2-3  | CXCR2 and PLC- $\beta$ 3 in PDAC cells preferentially interact with NHERF1.....                                | 45 |
| Figure 2-4  | CXCR2 and PLC- $\beta$ 3 interact with NHERF1 in a direct and PDZ motif-dependent manner .....                 | 47 |
| Figure 2-5  | CXCR2 interacts with both PDZ1 and PDZ2 of NHERF1 .....  | 48 |
| Figure 2-6  | Endogenous PLC- $\beta$ 3 in human pancreatic cancer cells preferentially interacts with NHERF1-PDZ2.....      | 50 |
| Figure 2-7  | NHERF1 clusters CXCR2 and PLC- $\beta$ 3 into a macromolecular complex <i>in vitro</i> and in PDAC cells ..... | 53 |
| Figure 2-8  | CXC Chemokine/CXCR2 Biological Axis Promotes Pancreatic Cancer Cell Proliferation .....                        | 55 |
| Figure 2-9  | Disrupting the CXCR2 Macromolecular Complex Inhibits Pancreatic Cancer Proliferation .....                     | 57 |
| Figure 2-10 | Inhibitory effect of EF1060 on MIA PaCa-2 proliferation.....   | 60 |
| Figure 2-11 | Disrupting the CXCR2 Macromolecular Complex Blocks Pancreatic Cancer Cell Invasion .....                       | 63 |
| Figure 2-12 | Disrupting the CXCR2 Macromolecular Complex Blocks Pancreatic Cancer-induced angiogenesis .....                | 64 |
| Figure 2-13 | Transduction efficiency of AAV2/2CMV constructs .....  | 67 |
| Figure 2-14 | Disrupting the CXCR2 Macromolecular Complex Inhibits Pancreatic Tumor Growth In Vivo .....                     | 69 |
| Figure 2-15 | Proposed mechanism of the NHERF1-mediated coupling of CXCR2  |    |

|            |   |    |
|------------|---|----|
|            | to PLC- $\beta$ 3 signaling in PDAC cells .....   | 74 |
| Figure 3-1 | Structure of NHERF1 PDZ1 in complex with the PLC $\beta$ 3<br>C-terminal sequence ENTQL ..... | 83 |
| Figure 3-2 | Structural comparison of NHERF1 PDZ1 and PDZ2.....  | 85 |



## Chapter 1

### Introduction

#### 1.1 Overview of CXCR2 Chemokine Receptor

##### 1.1.1 Chemokines and Chemokine Receptors

Chemokines are a family of small cytokines that are responsible for directed cellular chemotaxis. Chemokines can be divided into two categories: inflammatory chemokines that recruit leukocytes in response to physiological stimulus and homeostatic chemokines that are constitutively expressed, and responsible for the continuous basal level of cell migration and the architecture of secondary lymphoid organs<sup>1</sup>. Inflammatory chemokines and their receptors have pivotal roles in both innate and adaptive immunity in response to infection, tissue damage, and other physiological abnormalities. Homeostatic chemokines involve in the migration of B and T cells through specialized areas of secondary lymphoid organs, and migration of lymphocytes involved in immune surveillance<sup>2</sup>. In spite of the critical roles of chemokines and their receptors in the immune system, they have been documented to be actively involved in enormous pathologies<sup>1,3,4</sup>, including inflammatory diseases (inflammatory bowel disease, atherosclerosis), pulmonary diseases (chronic obstructive pulmonary disease (COPD), asthma), autoimmune diseases (psoriasis, rheumatoid arthritis, and multiple sclerosis), and cancers.

To date, approximately 50 chemokines and 20 corresponding chemokine receptors have been identified. Based on the conserved pattern of cysteine residues at N-

terminus, chemokines have been divided into four different subfamilies: C, CC, CXC, and CX<sub>3</sub>C, where C represents cysteine residue, and X represents any non-cysteine residue. In human, there are 7 CXC subfamily chemokine receptors (CXCR1 ~ CXCR7), and 15 cognate CXC chemokines (or CXCR ligands). CXCR2, a prototypical member of the CXC chemokine receptors, was first discovered as a neutrophil receptor<sup>5</sup>. Years of intensive research has also delineated its roles in a variety of diseases including cancer and inflammatory diseases. Furthermore, several pharmaceutical companies have identified a number of potent CXCR2 antagonists that have been evaluated in the clinical trials. However, many clinical trials of CXCR2 antagonists/inhibitors have not been successful due to the suboptimal clinical endpoints. Recent studies targeting compartmentalized interactions of CXCR2 complexes inside the cells open the door for development of a new class of CXCR2 inhibitors, which target the specific interactions between CXCR2 and its binding partners. This chapter focuses on the most recent progress about the interactions between CXCR2 and its interacting partners, and the fine-tuned regulation of CXCR2 compartmentalized signalings in inflammation, cancer, and angiogenesis.

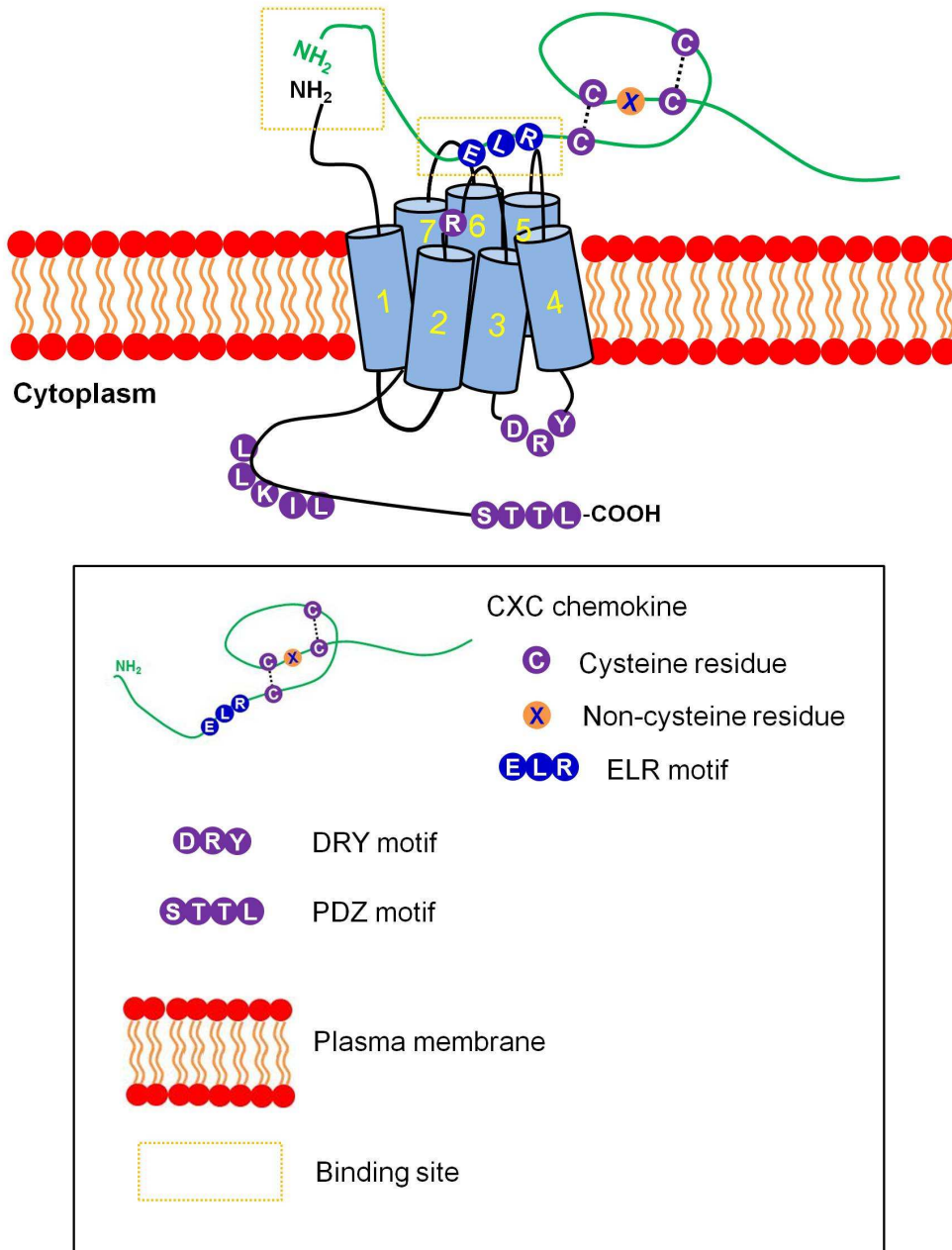
### **1.1.2 CXCR2 Structure**

CXCR2 was first designated as IL-8 receptor type B (IL-8RB) by Murphy and his colleagues<sup>5</sup>, sharing 77% identity with another closely-related receptor IL-8RA (also known as CXCR1) at the amino acid sequence level. CXCR2 is a G protein-coupled receptor which is composed of seven transmembrane domains, an extracellular N-terminal domain, three extracellular loops, three intracellular loops, and a cytoplasmic

C-terminus (Fig. 1 - 1). The extracellular N-terminal domain is involved in ligand binding, and the DRY (Asp-Arg-Tyr) motif in the second intracellular loop is the G protein docking site, and is responsible for intracellular downstream signaling upon ligand binding<sup>6</sup>. Also, the Asp 199 in the second extracellular loop<sup>7</sup> and an LLKIL motif in the C-terminus<sup>8</sup> are both required for receptor internalization.

### **1.1.3 CXCR2 Ligands and Signaling**

CXCR2 is the cognate receptor for the CXC chemokines CXCL1 ~ 3 and CXCL5 ~ 8 (also referred to as CXCR2 ligands)<sup>9</sup>. The characteristic ELR (Glu-Leu-Arg) motif located in the N terminus of the CXCR2 ligands are responsible for the ligand-receptor binding<sup>10</sup>, and is strongly associated with the leukocyte attraction<sup>11</sup>. Although further structural studies regarding the ligand-receptor interaction of CXCR2 are still in need, the binding mechanism has been proposed based on modeling and structural studies of CXCR4 and CCR2 binding modes<sup>12,13</sup>. Conceptually, the binding involves the binding between N-terminal residues from both the receptor and its ligands (preceding the 1<sup>st</sup> cysteine), followed by the interaction of the ELR motif of the ligands with the 2<sup>nd</sup> and 3<sup>rd</sup> extracellular loops of the receptor. N-terminus of the receptor is responsible for the binding selectivity and affinity<sup>14</sup>, whereas the ELR motif from the ligands enables the stabilization of the binding interaction and leads to the activation of the downstream signaling cascade<sup>15</sup>. Upon ligand-receptor binding, the heterotrimeric G protein is activated, whereby the  $\alpha$ -subunit and  $\beta\gamma$ -complex dissociate, leading to the activation or inhibition of a wide variety of downstream targets (phospholipase C, adenylyl cyclase, cAMP-dependent protein kinase, GTPases, PI3K, etc.). CXCR2 has been implicated in



**Fig, 1-1 CXCR2 Structure and Binding.** CXCR2 chemokine receptor consists of seven transmembrane domains, an extracellular N-terminal domain and an intracellular C-terminal domain. It contains a D-R-Y motif on the 2<sup>nd</sup> intracellular loop, and another LLKIL motif on the C-terminus functioning as protein docking site

activation of several signaling transduction pathways, including phospholipase C (PLC) pathway, PI3K pathway, and Rho, Rac and mitogen activated protein kinase (MAPK) pathways<sup>16</sup>.

#### **1.1.4 Roles of CXCR2 Biological Axis**

Signaling pathways evoked by the activation of CXCR2 have been borne out to play important roles in a variety of cellular responses, including cell migration, chemotaxis, cell adhesion, cellular morphological change, cytoskeletal rearrangement, etc<sup>17</sup>. The expression of CXCR2 on leukocytes, especially neutrophils, has been well-established for its roles in leukocyte homeostasis as well as the recruitment of leukocytes from bone marrow in respond to inflammation and injury<sup>18-20</sup>. CXCR2 had also been reported in preservation of oligodendrocyte function and myelination of neural tissues<sup>21</sup>. Furthermore, CXCR2 and its ligands have also been demonstrated to play essential roles in cutaneous wound healing<sup>22</sup>.

### **1.2 CXCR2 in Diseases and Its Clinical Significance**

#### **1.2.1 CXCR2 in inflammatory diseases**

Although the recruitment of neutrophils, which is regulated primarily by CXCR2, is important in response to acute inflammation and injury<sup>19,20</sup>, persistent or over-exuberant expression of CXCR2 and its ligands could subvert the protective effects of neutrophils into a manner that cause diseases, since excessive neutrophil influx and accumulation at the inflammation sites is well-believed to play crucial roles in pathogenic progression of clinical and experimental inflammatory diseases. Therefore, CXCR2 has been widely

demonstrated to play important role in various inflammatory diseases, including chronic obstructive pulmonary disease (COPD), acute lung injury (ALI), cystic fibrosis (CF), inflammatory bowel diseases (IBD), and ischemia-reperfusion injury. Increased expression of CXCR2 and its cognate CXC chemokines have been reported in recent clinical studies in various inflammatory disease systems, suggesting the clinical significance of CXC chemokine/CXCR2 biological axis.

It has been documented that CXCR2<sup>23,24</sup> and its cognate ligands (CXCL1<sup>25</sup>, CXCL5<sup>23</sup>, CXCL7<sup>23,24</sup>, CXCL8<sup>26</sup>, and PGP<sup>27</sup>) are significantly up-regulated in the patients with severe COPD compared with healthy smokers and patients with mild/moderate **COPD**. It has been reported that the patients with acute respiratory distress syndrome (**ARDS**) has a dramatically higher concentration CXCL1<sup>28</sup>, CXCL5<sup>28</sup> and CXCL8<sup>28-30</sup> in bronchoalveolar lavage fluid (BALF), and the level of the CXCL8: anti-CXCL8 antibody complexes profoundly correlated with the clinical disease activity<sup>31</sup> and mortality<sup>29</sup>. **CF** patients also showed significantly elevated levels of CXCL8 in sputum, BALF, and sera, and the high level of CXCL8 significantly correlated with clinical status<sup>32</sup>. Expression levels of CXCR2<sup>33,34</sup> and its cognate ligands, CXCL1<sup>33,34</sup>, CXCL2<sup>33</sup>, CXCL3<sup>33,34</sup>, CXCL5<sup>35</sup>, and CXCL8<sup>33,34,36-38</sup>, in the patients with **IBD** were substantially higher than the control individuals. Clinically, neutrophil-mediated reperfusion injury significantly increased mortality and morbidity when patients underwent **ischemia-reperfusion injury (I/R-I)** such as organ transplantation<sup>39,40</sup> and cardiopulmonary bypass<sup>41</sup>. CXCR2 cognate ligands, CXCL3<sup>42</sup>, CXCL7<sup>42</sup> and CXCL8<sup>42-44</sup> were enormously increased in the BALF from patients underwent lung transplantation compared to the control subjects,

and that high level of CXCL8 in the donor BALF profoundly correlated with the development of severe early graft dysfunction and with early recipient mortality<sup>44</sup>. Significantly increased CXCL8 was also detected in patients underwent cardiopulmonary bypass<sup>45</sup>.

Laboratory investigations also showed that CXCR2 deficiency or CXCR2 blockage prevented the Polymorphonuclear neutrophil (PMN) recruitment/accumulation in various experimental disease models. In **COPD** model, Weathington et al. reported that a CXCR2 specific peptide (PGP) failed to induce neutrophil accumulation in CXCR2<sup>-/-</sup> mice<sup>27</sup>. Miller et al. also reported that CXCR2 deficiency substantially decreased mucus secretion in the BALF, which is associated with chronic bronchitis. In **ALI**, animal studies have reported that PMN recruitment in the lung was significantly decreased in CXCR2<sup>-/-</sup> mice<sup>46-49</sup>. Kordonowy et al. also reported that ALI was attenuated in the obese mice, in which neutrophil CXCR2 expression was dramatically decreased<sup>50</sup>. Furthermore, blockade of CXCR2 by neutralizing antibody also markedly reduced neutrophil accumulation in ALI models<sup>51,52</sup>. In **IBD** model, Buanne *et al.* reported that PMN infiltration into mucosa was prominently reduced in CXCR2<sup>-/-</sup> mice with limited degree of mucosal damage and reduced clinical symptoms<sup>53</sup>. Elevated CXCR2 expression has been reported during post-lung transplantation **I/R-I** in rats<sup>42</sup>, and CXCR2 deficiency has demonstrated to reduce the impairment caused by I/R injury in different models<sup>54,55</sup>. Also, blockade of CXCR2 markedly prevented graft malfunction and inhibited neutrophil recruitment and accumulation in transplantation models<sup>42,56</sup>.

### 1.2.2 CXCR2 in Cancers

Overexpression of CXCR2 has been detected in patients with various cancers including breast cancer<sup>57</sup>, laryngeal squamous cell carcinoma<sup>58</sup>, colon cancer<sup>59</sup>, prostate cancer<sup>60,61</sup>, pancreatic cancer<sup>62,63</sup>, lung adenocarcinoma<sup>64</sup>, ovarian cancer (associated with patient survival)<sup>65</sup>, nasopharyngeal carcinoma<sup>66</sup> and brain tumor<sup>67</sup>. Besides, CXCR2 cognate ligands (CXCL1, CXCL5, and/or CXCL8) also overexpressed in patients with prostate cancer<sup>61</sup>, colon cancer<sup>59,68-70</sup>, breast cancer<sup>71,72</sup>, and pancreatic cancer<sup>73-75</sup>. Furthermore, overexpression of CXCR2 and/or its ligands prominently correlated with tumor stage, disease severity and patient survival in most cases.

Recent studies using CXCR2<sup>-/-</sup> mice have reported that CXCR2 deficiency profoundly prevented primary tumor growth and spontaneous metastases in lung cancer<sup>76</sup>, inhibited human melanoma tumor growth and experimental lung metastasis<sup>77</sup>, and suppressed human prostate tumor growth *in vivo*<sup>78</sup>. Blockade of CXCR2, by either neutralizing antibodies or short hairpin RNA (shRNAs), also significantly suppressed the proliferation, invasion and tumor growth *in vitro* and *in vivo* in many cancer models<sup>67,79-82</sup>.

Recent advances also suggest that CXCR2 not only contributed to the cancer cell biology, but also played important roles in the interplay between tumor cell and tumor microenvironment. For example, Jamieson *et al.* reported that inflammation-driven and spontaneous tumorigenesis in skin and intestine has been distinctively subsided in CXCR2<sup>-/-</sup> mice, in which tumor-associated leukocyte recruitment has also been attenuated<sup>83</sup>.



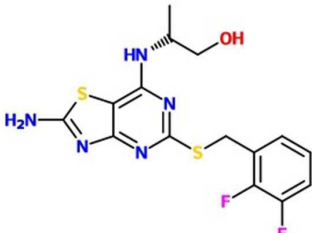
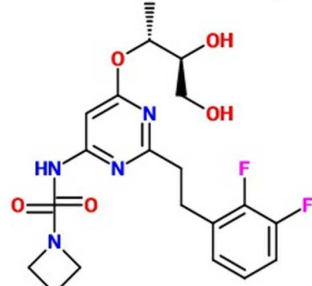
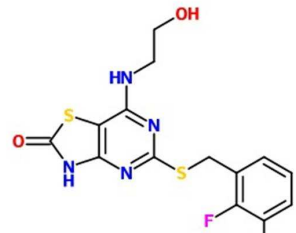
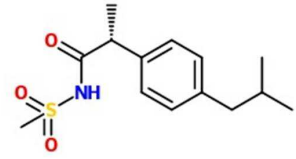
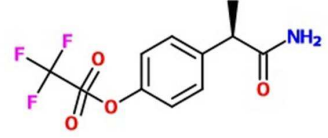
### 1.3 CXCR2 Antagonists and Therapeutic Implications

Given the essential role of CXCR2 biological axis in inflammatory diseases and cancers, pharmacological studies targeting CXCR2 has dramatically increased over the last decade. Several pharmaceutical companies have developed potent and selective CXCR2 antagonists, and laboratory investigations have achieved significant progress on CXCR2 antagonists in various disease models. Chapman et al. reported that **SCH-527123**, one of the CXCR2 allosteric inhibitors, significantly inhibited the neutrophil recruitment, mucus production, and goblet cell hyperplasia in a murine COPD model<sup>84</sup>. SCH-563705, another CXCR2 antagonist with similar structure with SCH-527123, has been demonstrated to reduce the arthritis disease severity *in vivo*<sup>85</sup>, and block the mammosphere formation *ex vivo*<sup>71</sup>. Singh et al. demonstrated the inhibitory effect of **SCH-479833**, with similar structure as SCH-527123, on tumor growth and angiogenesis in melanoma<sup>86</sup> and colon cancer<sup>87</sup> animal models. **SB225002**, a well-established competitive CXCR2 inhibitor, has also been reported to exert the inhibitory effect in inflammatory disease and cancer models. Braber et al. reported that SB225002 significantly inhibited CXCL1-induced increase of myeloperoxidase (MPO) levels in pulmonary tissue<sup>88</sup>. SB-225002 has also been demonstrated to significantly reduce MPO activity, BALF neutrophil accumulation, and edma formation in the injured lung<sup>89</sup>. Herbold et al. demonstrated the inhibitory effect of SB225002 in alveolar neutrophil and exudate macrophage recruitment in mice in a lung injury model<sup>49</sup>. In breast cancer models, SB-225002 has also been reported to inhibit mammary epithelial cell migration<sup>90</sup> and breast cancer cell invasion<sup>91</sup>. Two groups also reported **SB656933**,

another allosteric CXCR2 inhibitor, and its predecessor SB332235, could block the neutrophil activation, recruitment, and accumulation in COPD models<sup>88,92,93</sup>. **SB265610**, another allosteric CXCR2 inhibitor, has also been reported to suppress mammary tumor cell migration, myeloid cell recruitment and lung metastasis in breast cancer models<sup>80,94,95</sup>. Another CXCR2 inhibitor, **SB-468477** developed by Glaxo-Smith-Kline, has been shown to inhibit monocyte migration in response to selective CXCR2 ligands, CXCL1, CXCL5 and CXCL7<sup>96</sup>. **Repertaxin**, a CXCR2 inhibitor also known as Reparixin, was reported to block the neutrophil accumulation in a lung injury model, and abate the pancreatic cancer tumor growth *in vivo*<sup>97</sup>. **DF2162**, another allosteric CXCR2 inhibitor developed by Dompé S.P.A., has been reported to inhibit the arthritis *in vivo* with diminished neutrophil infiltration, oedema formation, and hypernociception<sup>98-100</sup>. Besides the effect on arthritis, DF2162 was also demonstrated to reduce the airway neutrophil transmigration, and improve lung pathology in lung fibrosis model<sup>101</sup>. **G31P**, as known as CXCL8(3–72)K11R, is an orthosteric inhibitor of CXCR2, which has been reported to fully abolish Benzo(a)pyrene triggered neutrophil recruitment in BALFs<sup>102</sup>. Liu et al. reported that G31P significantly suppressed prostate cancer cell proliferation both *in vitro* and *in vivo*<sup>103</sup>. **AZ10397767**, developed by AstraZeneca as a thiazolopyrimidine-based CXCR2 antagonist, has been shown to suppress lung cancer growth with decreased neutrophil infiltration<sup>104</sup>, and sensitize prostate cancer cells to chemotherapy<sup>105</sup>. Furthermore, some of the CXCR2 antagonists have been progressed into clinical trials<sup>106,107</sup>. Some of the well-tested CXCR2 antagonists have been summarized in Table 1-1.

Table. 1-1 Summary of CXCR2 Antagonists

| Compound   | Structure | Type       | Company         | Clinical Trials                               |
|------------|-----------|------------|-----------------|---|
| SCH-527123 |           | Allosteric | Schering-Plough | Psoriasis<br>Asthma<br>COPD                   |
| SCH-563705 |           | Allosteric | Schering-Plough | N/A   |
| SCH-479833 |           | Allosteric | Schering-Plough | N/A   |
| SB656933   |           | Allosteric | GlaxoSmithKline | Ulcerative Colitis<br>COPD<br>Cystic Fibrosis |
| SB332235   |           | Allosteric | GlaxoSmithKline | N/A   |
| SB265610   |           | Allosteric | GlaxoSmithKline | N/A   |
| SB225002   |           | Allosteric | GlaxoSmithKline | N/A   |
| SB468477   |           |            | GlaxoSmithKline |   |

| Compound   | Structure   | Type                      | Company      | Clinical Trials   |
|------------|---|---------------------------|--------------|---|
| Compound 6 |    |                           | AstraZeneca  |   |
| AZD-5069   |    |                           | AstraZeneca  | COPD (Phase II)<br>Bronchiectasis (Phase II)            |
| AZ10397767 |   | Thiazolo-pyrimidine-based | AstraZeneca  | N/A   |
| Reparixin  |  | Allosteric                | Dompé S.P.A. | Islet Transplantation<br>Ischemia-Reperfusion<br>Injury |
| DF2162     |  | Allosteric                | Dompé S.P.A. | N/A   |

**SCH-527123**, developed by Schering-Plough, has been evaluated in several neutrophil dominant diseases including psoriasis (NCT00684593, phase II), asthma (NCT00688467, Phase II; NCT00632502, Phase II) and COPD (NCT01068145, Phase I; NCT00441701, Phase II). Holz *et al.* has reported that SCH-527123 caused significant attenuation of ozone-induced neutrophilia in healthy subjects<sup>108</sup>. **Reparixin**, developed by Dompé S.P.A., has also been tested in phase II clinical trials of I/R-I after lung and kidney transplantation, and in phase III clinical in pancreatic islet transplantation. **SB-656933**, the derivative of **SB-332235**<sup>109</sup> developed by GlaxoSmithKline, has also been assessed in several phase I/II COPD clinical trials. Moss *et al.* reported that SB656933 was well-tolerated in adult CF patients, and significantly suppressed sputum neutrophil and elatase<sup>110</sup>. AZD-5069, developed by AstraZeneca, has also been evaluated in phase II clinical trials in COPD and bronchiectasis patients<sup>111</sup>.

In spite of the availability of several databases of clinical trials, scant results of completed clinical trials have been publicly released. Termination or discontinuation of the trials might result from the difficulty in patient recruitment, financial issues, or failure to reach clinical end points<sup>107</sup>. Furthermore, small molecule drugs/antagonists targeting at chemokine receptors still face several challenges that have been well-discussed in the excellent review paper by Proudfoot *et al.*, including the interspecies difference in antagonist potency, redundancy in receptor-ligand pairing and subsequent biological functions, suboptimal pharmacokinetic and toxicity profiles, and the inadequate ultimate curative effects<sup>107</sup>.

#### **1.4 CXCR2 Macromolecular Complex – Identification and Therapeutic Potential**

Besides the challenges mentioned above, emphasis is also placed on identifying novel CXCR2 inhibitors, which can be more tissue-specific and/or disease-specific<sup>112</sup>, because CXCR2 functions in normal physiology (including early tumor surveillance and immune system physiology) have to be protected in any antagonist that will be advanced to clinical trials. Recent studies aiming at protein-protein interactions involving CXCR2 have explored some novel avenues for innovative drug discovery. It has been documented that chemokine receptors couple not only to G proteins but also to additional non-G proteins, especially the scaffolding proteins, which could provide binding sites for downstream effector proteins<sup>113</sup>, and direct CXCR2 to operate in specific signaling networks. With no doubt it would be beneficial if we could identify novel CXCR2-interacting proteins or tissue/disease specific interacting partners of CXCR2, which could enhance the CXCR2 signaling in certain disease conditions. By disrupting these protein-protein interactions of CXCR2, we may develop more effective treatment options.

Recent advances have already revealed the functional importance of the CXCR2-interacting partners in CXCR2 trafficking, recycling, signal transduction, and it has also been suggested that different repertoires of adaptor/scaffolding proteins binding to CXCR2 and other chemokine receptors at varying spatiotemporal points are, at least partially, responsible for the versatile biological/cellular responses in different disease conditions<sup>114</sup>. Richmond group has identified several CXCR2-interacting proteins, which associates with CXCR2 and modulate CXCR2 trafficking, signaling, and CXCR2-

mediated cellular functions. Hsc/Hsp70 interacting protein (Hip) interacts with a C-terminal domain of CXCR2 (KILAIHGLI; i.e. a.a 327 ~ a.a 335), and affects CXCR2-mediated chemotaxis<sup>115</sup>. Several Ras-related proteins (Rab), including Rab5, Rab11a, and Rab11-family interacting protein 2 (Rab11-FIP2), and Rho GTP-binding protein (RhoB) were also shown to bind CXCR2, and play important roles in CXCR2 trafficking, recycling and CXCR2-mediated chemotaxis<sup>116-118</sup>.  $\beta$ -arrestin 2, a member of arrestin family of adaptor proteins, has been demonstrated to bind phosphorylated carboxyl-regions of CXCR1 and CXCR2, and modulate receptor internalization and activation of signal transduction pathways<sup>119,120</sup>. Besides  $\beta$ -arrestin 2, other scaffolding proteins, such as vasodilator-stimulated phosphoprotein (VASP)<sup>121</sup>, LIM and SH3 protein-1 (LASP-1)<sup>122</sup>, and Ras GTPase-activating-like protein (IQGAP1)<sup>114</sup>, were also identified by proteomics approaches to associate with CXCR2, and regulate CXCR2-mediated signaling and chemotaxis. Furthermore, it has been unveiled that the C-terminal cytoplasmic domain of CXCR2, which contains several specific motifs (amino acid sequences) such as LLKIL motif<sup>8</sup>, PDZ motif (-STTL)<sup>123</sup> and phosphorylation sites, is responsible for CXCR2 signaling, post-endocytic sorting, and/or CXCR2-mediated cellular chemotaxis. These studies not only led to identification of novel CXCR2-interacting partners and the critical motifs in CXCR2 responsible for the binding, but also revealed the functional significance of the coordinated regulation of CXCR2 signaling by these CXCR2-interacting partners, suggesting the therapeutic potential for targeting CXCR2-specific protein interactions.

Recently, we have also identified a PDZ domain-containing protein, Na<sup>+</sup>/H<sup>+</sup> exchange regulatory cofactor (NHERF1), as a novel CXCR2-interacting protein. NHERF1 associates with CXCR2 by PDZ interaction, and clusters the downstream effector, PLC-β<sub>2</sub>, into a CXCR2 macromolecular complex (CXCR2•NHERF1•PLC-β<sub>2</sub>) in neutrophils<sup>124</sup>. The formation of this CXCR2 complex is PDZ motif-dependent (i.e. -STTL-COOH for CXCR2; -ESRL-COOH for PLC-β<sub>2</sub>). An exogenous CXCR2 C-terminal domain containing PDZ motif (last 45 amino acids or last 13 amino acids) was demonstrated to compete and disrupt the physical interaction between CXCR2 and NHERF1, and also were shown to impair the CXCR2-mediated intracellular calcium mobilization, chemotaxis, and transepithelial migration in neutrophils. We also identified another CXCR2 macromolecular complex (CXCR2•NHERF1•PLC-β<sub>3</sub>) in human pancreatic ductal adenocarcinoma cells (PDACs), gene delivery or peptide delivery of exogenous CXCR2 C-terminal domain (last 45 or 13 amino acids) impaired cancer cell invasion and cell proliferation *in vitro* and *in vivo*<sup>125</sup>.

Most recently, we also demonstrated the importance of CXCR2 PDZ-mediated protein interactions in the function of endothelial progenitor cells (EPCs)<sup>126</sup>. By using an exogenous CXCR2 C-tail peptide or DNA construct (containing CXCR2 PDZ motif), CXCR2-mediated intracellular calcium mobilization in EPC, EPC *in vitro* migratory responses and neovessel formation, and EPC *in vivo* angiogenesis were significantly impaired. Our findings not only identified the existence and biological functions of the CXCR2 complex, but also revealed the therapeutic potential of targeting PDZ-mediated CXCR2 macromolecular complex in inflammation, cancer, and angiogenesis.



Although the scaffolding proteins have been demonstrated to regulate the CXCR2 signalings in diseases; however, it has been proved that eradication of the scaffolding proteins would not simply achieve the desired inhibitory effect in disease conditions. For example, although the  $\beta$ -arrestin 2 plays crucial roles in mediating CXCR2-signaling<sup>119,120</sup>, eradication of  $\beta$ -arrestin 2, unexpectedly, caused enhanced CXCR2 signaling and functional endpoints *in vitro* and *in vivo*<sup>127</sup>. This warrants the necessity of unveiling more structural details of the interaction between CXCR2 and its interacting partners to develop new therapeutic strategies. Therefore, we further investigated the structural basis of the NHERF1 PDZ1 domain in complex with the C-terminal sequence of CXCR2 at 1.1 Å resolution<sup>128</sup>. We not only determined that the positions 0 and -2 of the PDZ motif (position 0 referring to the extreme C-terminal residue) possess the ability to form networks of hydrogen bonds and hydrophobic interactions with NHERF1-PDZ1 domain, which are responsible for the stabilization and specificity of PDZ1-CXCR2 interaction, but also observed that the interaction between NHERF1-PDZ1 and CXCR2 at position -1 and -3 of the PDZ motif are very different from other PDZ1-PDZ motif interactions (i.e. PDZ1-CFTR, PDZ1-  $\beta$ 2AR, and PDZ1-PDGFR). Specifically, the orientation, the rotameric states, and binding preference of His29 and Arg40 in the NHERF1 PDZ1 domain is very different in PDZ1-CXCR2 interaction than in PDZ1-CFTR, PDZ1- $\beta$ 2AR, and PDZ1-PDGFR interactions. The unveiled structural basis suggests that even though both -1 and -3 residues in PDZ motif were less stringently specified than 0 and -2 residues in the PDZ domains, they could still interact with a few key residues in the PDZ motif-binding pocket specifically, which endow -1 and -3

residues with critical roles in PDZ motif recognition and selection within a network of NHERF-scaffolded interactions. Also, the conformation and rotameric states of the residues in the PDZ motif-binding pocket are also important in different side chain recognition of the PDZ motif and specific interaction. Our most recent study has also demonstrated the presence of the substantial structural flexibility in the PDZ1 peptide-binding pocket, which provides potential strategies for drug design against the NHERF1 PDZ1 domain<sup>129</sup>.

Our findings of the functional significance and therapeutic potential of the interaction between CXCR2 and NHERF1 in inflammation, tumorigenesis, and angiogenesis may be valuable in the development of innovative strategies for targeted drug discovery. However, the complexity of the NHERF1 interaction network and its versatile roles in regulation of many cellular processes essential to normal physiology<sup>130,131</sup> poses a challenge for designing CXCR2 inhibitors that are specific to the CXCR2-NHERF1 interaction without cross-inhibiting any of the other NHERF1-coordinated signaling events. Therefore, the specificity and selectivity of the novel CXCR2 inhibitors targeting on the CXCR2-NHERF1 interaction is dependent upon the understanding of the structural features that how the PDZ motif and critical residues in PDZ binding pocket work in coordination to determine the PDZ motif recognition and specificity of the interaction, and upon the exploitation of these features to differentiate CXCR2 from other NHERF1-interacting proteins. Further structural studies regarding identification of critical residues, from both PDZ motif and PDZ binding pocket, which are responsible for CXCR2 recognition, would be beneficial to design novel inhibitors that disrupt

CXCR2-NHERF1 interaction specifically without affecting other NHERF1 interaction and NHERF1-scaffolded signaling complex.

## Chapter II

### CXCR2 Macromolecular Complex in Pancreatic Cancer

© 2013 Neoplasia Press (Translational Oncology)

#### 2.1 Introduction

##### 2.1.1 Overview of Pancreatic Cancer

Pancreatic cancer, the most lethal malignancy of the gastrointestinal tract with 5-year survival rates of less than 5%, is the fourth leading cause of cancer-related deaths in both men and women in the United States<sup>132</sup>. The most common type of pancreatic cancer is pancreatic ductal adenocarcinoma (PDAC). Chemoresistance, early metastases and late clinical presentation in this incurable human malignancy result in no effective methods for early prognosis as well as a lack of effective systemic therapies with reduced side effects<sup>133,134</sup>. Therefore, a more comprehensive understanding of the biology of PDAC and the mechanisms/factors that promote invasion and tumor growth may help identify new molecular targets for the development of diagnostics and/or therapeutics of pancreatic cancer.

##### 2.1.2 Biological Axis of CXCR2 in Pancreatic Cancer

CXC-chemokine receptor 2 (CXCR2) is the cognate receptor for the CXC-chemokines, CXCL1 ~ 3 and CXCL5 ~ 8<sup>9</sup>. The CXC-chemokine/CXCR2 signaling has been reported to promote malignant cancer progression in many cancer types including pancreatic cancer<sup>135-139</sup>. It has been documented that the elevated expression of CXCL5 and

CXCL8 is correlated with poor differentiation, histopathologic grade and advanced clinical grade pancreatic adenocarcinomas in patients<sup>74,140</sup>. Recent studies also suggest that CXCR2 is expressed in various PDAC cell lines<sup>141-144</sup> and is primarily involved in enhancing the proliferation and survival of cancer cells via the autocrine and/or paracrine effect<sup>74,141,144</sup>. More importantly, increased expression of CXCR2 and its ligands has been shown in higher grades and stages of pancreatic adenocarcinomas in patients<sup>63,140</sup>, indicating that CXCR2 is involved in the exacerbation of tumors and could be a promising target for developing selective and effective treatments for pancreatic cancer. As a G-protein coupled receptor (GPCR), CXCR2 couples to the pertussis toxin-sensitive  $G_i$  proteins to stimulate phosphatidylinositide-specific phospholipase C (PLC) activities<sup>145</sup>. Agonist-induced activation of PLC- $\beta$ , one of the six families of PLC isozymes, catalyzes the hydrolysis of phosphatidylinositol 4, 5-bisphosphate (PIP<sub>2</sub>), generating 1, 2-diacylglycerol (DAG) and inositol-1, 4, 5-trisphosphate (IP<sub>3</sub>) which activates PKC isoforms and triggers the release of Ca<sup>2+</sup> from internal sources, respectively.

### **2.1.3 PDZ proteins and PDZ domain-mediated protein-protein interaction**

PDZ (PSD-95/DlgA/ZO-1) domains are ubiquitous protein-protein recognition modules that form peptide-binding pockets and generally mediate physical interaction with the carboxyl termini of a wide variety of proteins (such as membrane receptors, ion channel, etc.) that terminate in consensus binding motifs (referred to as PDZ motif)<sup>146,147</sup>. PDZ domains are important to nucleate the formation of compartmentalized multi-protein complexes that are critical for efficient and specific cell signaling<sup>148</sup>. These domains are

able to specifically recognize and bind short carboxyl-terminal peptides of a variety of proteins (membrane receptors, ion channel families, etc.). The specific C-terminal sequence motifs are usually 4 ~ 5 residues in length, and are referred to as PDZ motifs. The nomenclature for the PDZ motif is described as follows: the extreme C-terminal residue is referred to as the P<sub>0</sub> residue; subsequent residues towards the N-terminal are termed P<sub>-1</sub>, P<sub>-2</sub>, P<sub>-3</sub>, etc. Comprehensive peptide library screens suggest that P<sub>0</sub> and P<sub>-2</sub> residues at the C-terminus of the membrane receptors are most critical for recognition and physical interaction between membrane receptors and PDZ domain-containing proteins (also referred to as PDZ scaffold proteins or PDZ proteins)<sup>149</sup>. In general, particular hydrophobic P<sub>0</sub> residues, such as Valine (V) or Leucine (L), are preferred, although sequence variations of PDZ domains could change the size and shape preference<sup>150,151</sup>. Also, variations in the P<sub>-2</sub> binding pocket result in distinct preferences for hydroxylated, charged or hydrophobic amino acids. In class I PDZ domains, hydroxylated side chain of either a Serine (S) or Threonine (T) is favored at P<sub>-2</sub> due to a specific hydrogen bond that is formed from a histidine residue<sup>152</sup>.

A variety of PDZ domain-containing proteins (also referred to as PDZ scaffold/adaptor proteins) have been reported to nucleate the formation of compartmentalized multi-protein complexes that are critical for efficient and specific cell signaling<sup>153-157</sup>. Some PDZ scaffold proteins, such as Na<sup>+</sup>/H<sup>+</sup> exchange regulatory factors (NHERF1 & NHERF2) and PDZ domain containing 1 (PDZK1), preferentially associate with the surface membrane of epithelial cells and interact with membrane receptors and their downstream effectors. PLC-β is one of the downstream effectors for GPCR signaling,

and it has been reported to specifically bind with the PDZ scaffold proteins via PDZ-based interaction since all PLC- $\beta$  isoforms possess consensus PDZ motifs, -X-S/T-X-L/V-COOH (X represents any amino acid), at their carboxyl termini<sup>158-161</sup>. Therefore, the specificity of agonist-induced PLC- $\beta$  activation and subsequent intracellular signaling might be dependent upon the specific interactions of PLC- $\beta$  with particular PDZ scaffold proteins<sup>162</sup>. Similar to PLC- $\beta$  isoforms, CXCR2 also possesses a consensus PDZ motif (-S-T-T-L-COOH) at its carboxyl termini. Previous studies by us and others have demonstrated that the PDZ motif of CXCR2 is involved in the regulation of intracellular signaling and cell functions in neutrophils<sup>163</sup> as well as post-endocytic sorting and cellular chemotaxis in CXCR2-overexpressing HEK293 cells<sup>123</sup>. Hence, the PDZ motif of CXCR2 can, theoretically, mediate potential interaction with certain PDZ scaffold proteins, which subsequently binds relevant downstream effectors, forming multi-protein macromolecular complexes. However, the molecular mechanism(s) as to how this potential CXCR2 macromolecular complex are formed and/or regulated, as well as what role the CXCR2 complex might play in PDAC growth and progression have not been determined.

## **2.2 Materials and Methods**

### **2.2.1 Antibodies and Reagents**

Anti-human CXCR2, NHERF1, PLC- $\beta$ 3, and GAPDH antibodies were purchased from Santa Cruz Biotechnology (Santa Cruz, CA). Recombinant human chemokines, CXCL8/IL-8, CXCL5/ENA-78, and CXCL1/GRO $\alpha$ , were obtained from ProSpec-Tany Technogene (East Brunswick, NJ). Growth factor reduced Matrigel matrix, glutathione

agarose beads and Transwell inserts were purchased from BD Bioscience (Franklin Lakes, NJ). MTT (3-(4,5-Dimethylthiazol-2-yl)-2,5-diphenyltetrazolium bromide) and protease inhibitors (Aprotinin, Leupeptin, Pepstatin A, and phenylmethylsulfonyl fluoride) were purchased from Sigma-Aldrich (St. Louis, MO). Human CXCR2 C-tail peptides (biotin-conjugated at N-terminus): wild-type "WT" (biotin-FVGSSSGHTSTTL), PDZ motif deletion mutant " $\Delta$ TTL" (biotin-FVGSSSGHTS) and PDZ motif mutant "AAA" (biotin-FVGSSSGHTSAAA) were synthesized by Genemed Synthesis Inc. (San Antonio, TX) and used as reported before<sup>163</sup>. Chariot<sup>TM</sup> peptide/protein delivery reagent was purchased from Active Motif (Carlsbad, CA). S-protein agarose and streptavidin beads were purchased from Novagen/EMD Millipore (Billerica, MA). Coomassie Brilliant Blue, Bradford protein assay kit and Western Blot apparatus were obtained from Bio-Rad Laboratories, Inc. (Hercules, CA). Polyacrylamide gel for Western Blot analysis was purchased from Genscript Corp. (Piscataway Township, NJ). Fetal bovine serum (FBS) and antibiotics, Ampicillin sodium salt, Kanamycin sulfate, and Puromycin dihydrochloride, were purchased from Fisher Scientific (Pittsburgh, PA). Penicillin and Streptomycin were purchased from Invitrogen/Life Technologies (Carlsbad, CA). The plasmid pcDNA3.1(+)-FLAG-PLC- $\beta$ 3 was obtained from the laboratory of Dr. Theresa M. Filtz (Oregon State University), and used for construct generation was described before<sup>164</sup>. Bacterial stock of plasmid DNA of pGEX-4T-1-NHREF1, pGEX-4T-1-NHERF2, pGEX-4T-1-PDZK1, pGEX-4T-1-NHERF1-PDZ1, pGEX-4T-1-NHERF1-PDZ2, and pGEX-4T-1-PDZ1&2 were obtained from Dr. Anjaparavanda P. Naren's laboratory at The University of Tennessee Health Science Center (current institution: Cincinnati



Children's Hospital Medical Center). All the pGEX-4T-1 plasmids were used to generate purified proteins with GST tag (see section 2.2.3).

### 2.2.2 Bacterial Strains, plasmid constructions, and mutagenesis

*E. coli* strain NovaBlue GigaSingles™ Competent cells (genotype: *endA1 hsdR17(r<sub>k12</sub><sup>-</sup> m<sub>k12</sub><sup>+</sup>)supE44thi-1 recA1 gyrA96relA1 lacF'[proA<sup>+</sup>B<sup>+</sup>lac<sup>q</sup>ZΔM15::Tn10(Tc<sup>R</sup>)]*, Novagen/EMD Millipore, Billerica, MA) was used for molecular cloning. Strain DH5α™ (genotype: *F<sup>-</sup> Φ80lacZΔM15 Δ(lacZYA-argF) U169 recA1 endA1 hsdR17 (rK<sup>-</sup>, mK<sup>+</sup>) phoA supE44 λ<sup>-</sup> thi-1 gyrA96 relA1)* was obtained from Dr. Anjaparavanda P. Naren's laboratory at The University of Tennessee Health Science Center, and was used for molecular cloning. *E. coli* strain BL21 (DE3) (genotype: *[F ompT hsdS<sub>B</sub> (r<sub>B</sub>-m<sub>B</sub>-) gal dcm (DE3 [lacI lacUV5-T7 gene1 ind1 Sam7 nin5]*; New England Biolabs) was used for protein expression and purification.

Plasmid vector, pGEX-4T-1, which contains a Glutathione S-transferase tag (GST-tag) in frame and upstream of the multiple cloning site, was purchased from GE Healthcare (formerly Amersham Biosciences). Plasmid vector, pET-41, which contains a GST-His-S tag in frame and upstream of the multiple cloning site, was purchased from Novagen /EMD Millipore (Billerica, MA). Plasmid vectors, pET-30 and pTriEx-4, which both contain His-S tag in frame and upstream of the multiple cloning site, were purchased from Novagen/EMD Millipore (Billerica, MA). Plasmid vectors, pGEX-4T-1, pET-30, and pET-41, were used to generate purified proteins fused with GST tag, His-S tag, and GST-His-S tag, respectively.

The construct, pcDNA3.1(+)-3HA-CXCR2 (full length), was purchased from Missouri University of Science and Technology cDNA Resource Center (Prod# CXCR20TN00, Rolla, MO), and used as a template to create the following constructs by ligation independent cloning (LIC) kit from Novagen/EMD Millipore (Billerica, MA): pET-30-hCXCR2-C-tail (Wild-type), pET30-hCXCR2-C-tail (PDZ motif deletion), pET-30-hCXCR2-C-tail (PDZ motif mutation), pET-41-hCXCR2-C-tail (Wild-type), pET-41-hCXCR2-C-tail (PDZ motif deletion), pET41-hCXCR2-C-tail (PDZ motif deletion), pTriEx4-hCXCR2-C-tail (Wild-type), pTriEx4-hCXCR2-C-tail (PDZ motif deletion), pTriEx4-hCXCR2-C-tail (PDZ motif mutation). The primers used for plasmid constructions were summarized in Table 2.1. The PCR conditions used were as follows: 1 minute denaturation at 95°C, 35 amplification cycles with an annealing temperature of 55°C, and final extension of 72°C for 5 minutes. PCR products were run on a 1.5% DNA agarose gel. PCR products of the correct size were excised from the gel, extracted and purified using Wizard<sup>®</sup> SV Gel and PCR Clean-Up System (Promega, Madison, WI). The plasmids were purified by the PureYield<sup>™</sup> DNA preparation system (Promega).

The construct pcDNA3.1(+)-FLAG-PLC- $\beta$ 3-FL that encodes the full length of human PLC- $\beta$ 3, was used as a template to create the following PLC- $\beta$ 3 constructs by ligation independent cloning (LIC) kit from Novagen/EMD Millipore (Billerica, MA): pET-30-hPLC- $\beta$ 3-C-tail (Wild-type), pET30-hPLC- $\beta$ 3-C-tail (PDZ motif deletion), pET-30-hPLC- $\beta$ 3-C-tail (PDZ motif mutation), pET-41-hPLC- $\beta$ 3-C-tail (Wild-type), pET-41-hPLC- $\beta$ 3-C-tail (PDZ motif deletion), pET41-hPLC- $\beta$ 3-C-tail (PDZ motif deletion), pTriEx4-hPLC- $\beta$ 3-

C-tail (Wild-type), pTriEx4-hPLC- $\beta$ 3-C-tail (PDZ motif deletion), pTriEx4-hPLC- $\beta$ 3-C-tail (PDZ motif mutation). The primers used for plasmid constructions were also summarized in Table 2.1. All the plasmids were sent for DNA sequencing (Genewiz, South Plainfield, NJ) to ensure the accurate DNA sequence.

### 2.2.3 Protein Expression and Purification

Aforementioned pET41 constructs (GST-His-S-tagged) and pET30 constructs (His-S-tagged) were transformed into *E. Coli* BL21 (DE3) cells for protein expression. A heat-shock method was used in bacterial transformation. Briefly, a sudden increase of temperature (42°C for 30s) creates pores in the plasma membrane of the bacterial competent cells, allowing the plasmid DNA entering the competent cells. A rich medium, S.O.C. medium, was used for the recovery of the *E. Coli* competent cells, maximizing the transformation efficiency of competent cells. SOC medium contains 0.5% Yeast Extract, 2% Tryptone, 10mM NaCl, 2.5mM KCl, 10mM MgCl<sub>2</sub>, 10mM MgSO<sub>4</sub>, and 20mM glucose.

GST-tagged proteins were purified from transformed *E. Coli* BL21 (DE3) bacteria. A 5ml overnight culture in Luria-Bertani broth medium (Fisher Scientific, Pittsburgh, PA) was made from a glycerol stock. The overnight culture was diluted into the large scale LB Broth medium (500ml), and culture was grown in LB Broth medium with 15 $\mu$ g/ml kanamycin at 37°C with constant shaking until it reached an OD<sub>600</sub> of 0.6~ 1.0. The protein expression was induced using isopropyl  $\beta$ -D-1-thiogalactopyranoside (IPTG) with 200 $\mu$ M final concentration at 37 °C with constant shaking for 3hrs. Bacteria were pelleted by centrifugation at 5,000g for 15min. Bacterial pellets were frozen at -80 °C

Table 2.1 Primers used in this study

| Plasmid  |              | Sequence                                    |
|--|--------------|---|
| pET30/41/pTriEx4-CXCR2-C-tail (WT)                           | Forward (5') | GACGACGACAAGATGTTTCATT<br>GGCCAGAAG         |
|  | Reverse (5') | GAGGAGAAGCCCGGTTTAGA<br>GAGTAGTGGAAGT       |
| pET30/41/pTriEx4-CXCR2-C-tail ( $\Delta$ TTL)                | Forward (5') | GACGACGACAAGATGTTTCATT<br>GGCCAGAAG         |
|  | Reverse (5') | GACGGATCCTTAGAGAGTAGT<br>GGA                |
| pET30/41/pTriEx4-CXCR2-C-tail (AAA)                          | Forward (5') | CAGGGCACACTTCCGCTGCTG<br>CCTAAACCGGGCTTCTCC |
|  | Reverse (5') | GGAGAAGCCCGGTTTAGGCA<br>GCAGCGGAAGTGTGCCCTG |
| pET30/41/pTriEx4-CXCR2-C-tail (ATA)                          | Forward (5') | CAGGGCACACTTCCGCTACTG<br>CCTAAACCGGGCTTCTCC |
|  | Reverse (5') | GGAGAAGCCCGGTTTAGGCA<br>GTAGCGGAAGTGTGCCCTG |
| pET30/41/pTriEx4-hPLC- $\beta$ 3-full-length (WT)            | Forward (5') | GACGACGACAAGATGGCGGG<br>CGCCCAG             |
|  | Reverse (5') | GAGGAGAAGCCCGGTTAGAG<br>CTGCGTGTTC          |
| pET30/41/pTriEx4-hPLC- $\beta$ 3-full-length ( $\Delta$ TTL) | Forward (5') | GACGACGACAAGATGGCGGG<br>CGCCCAG             |
|  | Reverse (5') | GAGGAGAAGCCCGGTTAGTTC<br>TCCTCCTGGCTC       |
| pET30/41/pTriEx4-hPLC- $\beta$ 3-C-tail (WT)                 | Forward (5') | GACGACGACAAGATGGTCAAC<br>TCCATCCGT          |
|  | Reverse (5') | GAGGAGAAGCCCGGTTAGAG                        |

|   |              |  |
|---|--------------|--|
|   |              | CTGCGTGTTC   |
| pET30/41/pTriEx4-hPLC- $\beta$ 3-C-tail ( $\Delta$ TTL) | Forward (5') | GACGACGACAAGATGGTCAAC<br>TCCATCCGT                                   |
|   | Reverse (5') | GAGGAGAAGCCCGGTTAGTTC<br>TCCTCCTGGCTC                                |
| pET30/41/pTriEx4-hPLC- $\beta$ 3-C-tail (AAA)           | Forward (5') | GACGACGACAAGATGGTCAAC<br>TCCATCCGT                                   |
|   | Reverse (5') | GAGGAGAAGCCCGGTCAAGC<br>AGCAGCGTTCTC                                 |
| Human CXCR2 (Reverse-transcriptase PCR)                 | Forward (5') | AACATGGGCAACAATACAGCA  |
|   | Reverse (5') | TGAGGACGACAGCAAAGATG   |
| Human PLC- $\beta$ 3 (Reverse-transcriptase PCR)        | Forward (5') | AGTTCCAGAACAGACAGGTG   |
|   | Reverse (5') | TTCTTATGCTTGTCCTCAT  |
| Human NHERF1 (Reverse-transcriptase PCR)                | Forward (5') | GAGACCAAGCTGCTGGTG   |
|   | Reverse (5') | GGCCAGGGAGATGTTGAAG  |
| Human GAPDH (Reverse-transcriptase PCR)                 | Forward (5') | ATGTTCCAGGAGCGAGATCC   |
|   | Reverse (5') | ACCACTGACACGTTGGCAGT   |
| hNHERF1-pLKO.1-shRNA1                                   | Forward (5') | CCGGCAGGGAAACTGACGAG<br>TTCTTCTCGAGAAGAAGTCTCGT<br>CAGTTTCCCTGTTTTTG |
|   | Reverse (5') | AATTCAAAAACAGGGAAACTG<br>ACGAGTTCTTCTCGAGAAGAA<br>CTGGTCAGTTTCCCTG   |
| hNHERF1-pLKO.1-shRNA2                                   | Forward (5') | CCGGCAGAAGGAGAACAGTC<br>GTGAACTCGAGTTCACGACTG<br>TTCTCCTTCTGTTTTTG   |
|   | Reverse (5') | AATTCAAAAACAGAAGGAGAA<br>CAGTCGTGAACTCGAGTTCAC<br>GACTGTTCTCCTTCTG   |

overnight, and resuspended in lysis buffer (Tris base, NaCl) supplemented with protease inhibitors (aprotinin [1 $\mu$ g/ml], leupeptin [1 $\mu$ g/ml], pepstatin [1 $\mu$ g/ml], phenylmethylsulfonyl fluoride (PMSF) [500 $\mu$ M], and Lysozyme [100 $\mu$ g/ml]). The bacterial pellets were sonicated on ice, and allowed to mix at 4°C for 30 minutes. Subsequently, 10% Triton-X was added to the suspension and allowed to mix at 4°C for 30 minutes. The bacterial debris was then pelleted down by centrifugation at 27,000g for 20 minutes at 4°C. Glutathione agarose beads (50% slurry) were then added to the cleared supernatant and allowed to mix for 2 hour at 4°C. Glutathione agarose beads were pelleted down by centrifugation at 800g and washed by TBS (25mM Tris, 137mM NaCl, 2.7mM KCl, PH = 7.4) for 5 times. Proteins were eluted from the glutathione agarose beads using 50mM glutathione (PH 7.5), and the excessive glutathione was subsequently dialyzed away by centrifugation in the Amicon<sup>®</sup> Centrifugal Filters (Molecular Weight Cut-Off: 3kDa, EMD/Millipore, Billerica, MA). The concentration of purified proteins was estimated using the Bradford protein estimation assay (Bio-Rad). A 20 $\mu$ l sample of the protein was eluted using Laemmli sample buffer and run on a polyacrylamide gel to visualize the quantity and quality of the purified protein. Laemmli sample buffer contains 60mM Tris-base, 10% (v/v) glycerol, and 2% SDS (electrophoresis grade).

His-S-tagged proteins were purified using a similar protocol with a few changes. Cobalt beads (50% slurry) were added to the cleared supernatant and allowed to mix at 4°C for 30 minutes instead of glutathione agarose beads. Proteins were eluted from the cobalt

beads using His binding buffer (500mM NaCl, 80mM Tris-base, 25mM Imidazole, PH=7.4)

#### **2.2.4 Cell Culture**

Human pancreatic ductal adenocarcinoma cell lines (PANC-1, MIA PaCa-2, AsPC-1, BxPC-3 and HPAC) and Human Embryonic Kidney 293 cells (HEK293) were obtained from American Type Culture Collection (Manassas, VA). Normal human pancreatic duct epithelial (HPDE) cells, pancreatic cancer cell lines, Colo357 and L3.6pl, were obtained from Dr. Paul J Chiao at the University of Texas MD Anderson Cancer Center (Houston, TX). PDAC cells (PANC-1, MIA PaCa-2, HPAC, AsPC-1, BxPC-3, Colo357, and L3.6pl) and HEK293 cells were cultured in Dulbecco's modified Eagle's medium (Thermo Scientific, Rockford, IL) containing 4.5g/l D-glucose and L-glutamine supplemented with 10% fetal bovine serum (FBS), 100 units/ml penicillin, and 100µg/ml streptomycin at 37°C in humidified air with 5% CO<sub>2</sub>. HPDE cells were cultured in keratinocyte serum-free medium (Invitrogen/Life Technologies, Carlsbad, CA) supplemented with 5ng/ml epidermal growth factor, 50µg/ml bovine pituitary extract, 100 units/ml penicillin, and 100µg/ml streptomycin. PANC-1, MIA PaCa-2, AsPC-1, BxPC-3 and HPAC were derived from different pancreatic cancer patients with adenocarcinoma of the pancreas. All the PDAC cells were subcultured as a ratio of 1:6 ~ 1:8, and cryopreserved by the complete medium with 5% (v/v) DMSO in liquid nitrogen. Human Umbilical Vein Endothelial cells (HUVEC) were obtained from American Type Culture Collection (Manassas, VA). HUVEC cells were cultured in EBM-2 medium supplemented with 5% FBS, human recombinant Epidermal Growth Factor, hydrocortisone, human Fibroblast

Growth Factor Basic with heparin, Vascular Endothelial Growth Factor, human recombinant Insulin-like Growth Factor, Ascorbic Acid, and Gentamicin (Amphotericin-B) (Fisher Scientific, Pittsburgh, PA). The HUVEC cells were cryopreserved by the 70% (v/v) complete medium, 20% (v/v) FBS, and 10% (v/v) DMSO.

### **2.2.5 DNA Transfection**

Lipofectamine<sup>TM</sup> 2000 transfection reagent (Invitrogen/Life Technologies, Carlsbad, CA) was used for the DNA transfection. Briefly, cells were seeded on tissue culture dishes until 70% ~ 80% confluency. On the transfection day, the cells were washed and cultured with basal medium (without serum and antibiotics). The transfection complex was set up in two tubes. The first tube contained the Opti-MEM medium (Invitrogen/Life Technologies, Carlsbad, CA) and DNA, and the second tube contained Opti-MEM medium with Lipofectamin<sup>TM</sup> 2000 transfection reagent based on the optimum condition provided by the manufacturer. The transfection complex was then added to the cell culture dishes, and incubated at 37°C for 6 hours. Then, the medium was cultured in the complete growth medium for 24 ~ 48 hours for the studies.

### **2.2.6 Western Blot Analysis**

Cells were lysed in lysis buffer (50 mM Tris - pH 8.0, 150 mM NaCl, 1% Nonidet P-40, 0.5% sodium deoxycholate, 0.1% SDS) supplemented with a mixture of protease inhibitors (containing 1 mM phenylmethylsulfonyl fluoride, 1 µg/ml aprotinin, 1 µg/ml pepstatin and 1 µg/ml leupeptin). Protein concentration of the cleared supernatant (17,000 x g, 15 min) was estimated by Bradford protein assay (Bio-Rad). Proteins were



eluted in Laemmli sample buffer containing  $\beta$ -mercaptoethonal, separated by SDS-PAGE (7.5% or 4–15%), and immunoblotted using indicated antibodies. The signal was detected by SuperSignal<sup>®</sup> West Pico (or Femto) substrate (Thermo Scientific, Rockford, IL). The blots were visualized and recorded using a BioSpectrum 500 Imaging system (UVP, Upland, CA). The images were analyzed using ImageJ software (National Institutes of Health, Bethesda, MD).

### **2.2.7 GST Pull-down Assay**

GST pull-down assay was performed as previously described<sup>163</sup>. Briefly, fresh PDAC cells were lysed in binding buffer (PBS + 0.2% Triton X-100, supplemented with a mixture of protease inhibitors (aprotinin [1 $\mu$ g/ml], leupeptin [1 $\mu$ g/ml], pepstatin [1 $\mu$ g/ml], phenylmethylsulfonyl fluoride (PMSF) [500 $\mu$ M]). Cell lysate was mixed at 4°C for 15 minutes and centrifuged at 17,000g for 15 minutes to retrieve the cleared supernatant. The cleared supernatant was equally mixed with GST alone or various GST-PDZ fusion proteins (GST-NHERF1, GST-NHERF2, or GST-PDZK1) at 4°C for 2 hrs. The mixture was pulled down by glutathione agarose beads (BD Biosciences) at 4°C overnight. The glutathione agarose beads were centrifuged at 700g for 1 minute and washed three times with binding buffer. The proteins were eluted in Laemmli sample buffer containing  $\beta$ -mercaptoethonal (5%). The eluents were separated by SDS-PAGE, transferred to a PVDF membrane by Western Blot apparatus (Bio-Rad) and immunoblotted with anti-CXCR2 or anti-PLC- $\beta$ 3 antibodies (Santa Cruz Biotechnology, Santa Cruz, CA).

### **2.2.8 Pair-wise Binding Assay**

Purified GST-NHERF1 was mixed with various purified His-S-PLC- $\beta$ 3 C-tail fragments (WT, or PDZ motif mutants,  $\Delta$ TQL, AAA), or CXCR2 C-tail peptides (biotin-conjugate at N-terminus; WT, or PDZ motif mutants,  $\Delta$ TTL, AAA) in binding buffer (PBS + 0.2% Triton X-100 + protease inhibitors (aprotinin [1 $\mu$ g/ml], leupeptin [1 $\mu$ g/ml], pepstatin [1 $\mu$ g/ml], phenylmethylsulfonyl fluoride (PMSF) [500 $\mu$ M])) at 22-24°C for 1 hr. The mixtures were incubated with S-protein agarose (for His-S-tagged fusion proteins), or streptavidin beads (for biotin-conjugated peptides) for 2 hrs. The beads were centrifuged at 700g for 1 minute and washed three times with binding buffer. The bound proteins were eluted with Laemmli sample buffer containing  $\beta$ -mercaptoethanol (5%). The eluents were resolved and separated by SDS-PAGE, transferred to a PVDF membrane by Western Blot apparatus (Bio-Rad) and immunoblotted with anti-NHERF1 antibody (Santa Cruz Biotechnology).

### **2.2.9 Macromolecular Complex Assembly Assay**

Purified His-S-tagged CXCR2 C-tail fragments (WT, PDZ motif mutants  $\Delta$ TTL or AAA) or His-S-tagged PLC- $\beta$ 3 C-tail fragments (WT, PDZ motif mutants  $\Delta$ TQL or AAA) were mixed with GST-NHERF1 (or GST alone) in 200  $\mu$ l of binding buffer (PBS + 0.2% Triton X-100 + protease inhibitors (aprotinin [1 $\mu$ g/ml], leupeptin [1 $\mu$ g/ml], pepstatin [1 $\mu$ g/ml], phenylmethylsulfonyl fluoride (PMSF) [500 $\mu$ M])), and the complex was pulled down with S-protein agarose. This step is also referred to as pair-wise binding as described above. The dimeric complex was then mixed with the lysates of PDAC cells expressing endogenous full-length PLC- $\beta$ 3 and CXCR2 for 3 hrs at 4°C. The S-protein agarose were centrifuged at 700g for 1 minute and washed extensively with binding buffer. The

bound proteins were then eluted by Laemmli sample buffer containing  $\beta$ -mercaptoethanol (5%), resolved and separated by SDS-PAGE, transferred to a PVDF membrane by Western Blot apparatus (Bio-Rad) and immunoblotted using anti-PLC- $\beta$ 3 or anti-CXCR2 antibodies (Santa Cruz Biotechnology, Santa Cruz, CA).

#### **2.2.10 Co-Immunoprecipitation Assay**

A co-immunoprecipitation kit (Thermo Scientific/Pierce, Rockford, IL) was used to immobilize the normal IgG control and anti-CXCR2 IgG to the resin according to manufacturer's instruction. PDAC cells were lysed in binding buffer (PBS + 0.2% Triton X-100 + protease inhibitors (aprotinin [1 $\mu$ g/ml], leupeptin [1 $\mu$ g/ml], pepstatin [1 $\mu$ g/ml], phenylmethylsulfonyl fluoride (PMSF) [500 $\mu$ M])), and cleared cell lysates (17,000  $\times$  g, 15 min) were processed for co-immunoprecipitation (co-IP) as reported before<sup>155,163</sup>. The co-precipitated protein complex was resolved and separated by SDS-PAGE, and probed for NHERF1 and PLC- $\beta$ 3. For the reverse co-IP, anti-PLC- $\beta$ 3 IgG was used to immunoprecipitate the complex. The co-precipitated protein complex was separated by SDS-PAGE and probed for NHERF1 and CXCR2. The signal was detected by SuperSignal<sup>®</sup> West Pico (or Femto) substrate (Thermo Scientific, Rockford, IL).

#### **2.2.11 Cell Proliferation Assay**

Cell proliferation was assessed by MTT assay as reported before<sup>74</sup>. In brief, PDAC cells were seeded in 96-well plates ( $7 \times 10^3$  cells per well) and allowed to adhere overnight. Then, the cells were fed with serum-free fresh media with or without 100 ng/mL of CXCR2 ligands (CXCL1, CXCL5 or CXCL8). After indicated growth periods, cells were

incubated with 20 $\mu$ l of MTT solution (1 mg/ml) at 37°C for 3.5 hrs and then incubated with MTT solvent (4 mM HCl, 0.1% Nonidet P-40 in isopropanol) under constant mixing protected from light for 15 min at 22-24°C. Spectrophotometric absorbance of the samples at 590 nm was determined by a microplate reader (Bio-Rad). In parallel, Colo357 and HPAC cells were transfected with various pTriEx4 plasmids (vector alone, CXCR2 C-tail  $\Delta$ TTL, or CXCR2 C-tail WT) or delivered with CXCR2 C-tail peptides (WT or  $\Delta$ TTL) for 24-48 hours prior to the MTT assay as indicated.

Another peptide inhibitor targeting the interaction between CXCR2 and NHERF1, EF1060, was synthesized in Dr. Spaller's laboratory (Dartmouth College, NH). EF1060 is myristoylated at N-terminus and bears the last eight amino acids of the C-terminal sequence of CXCR2 (N-myristoyl-SGHTSTTL), as shown in Figure 2-10 A. MTT (3-(4,5-Dimethylthiazol-2-yl)-2,5-diphenyltetrazolium bromide) was purchased from Sigma-Aldrich (St Louis, MO). EF1060 was dissolved in DMSO. Cell proliferation was assessed by MTT assay as reported before<sup>74</sup>. In brief, MIA PaCa-2 cells were seeded in 96-well plates ( $7 \times 10^3$  cells per well) and allowed to adhere overnight. The cells were treated with EF1060 with control groups (DMSO and non-treatment). After indicated growth periods, cells were incubated with 20  $\mu$ l of MTT solution (1 mg/ml) at 37°C for 3.5 hrs and then incubated with MTT solvent (4 mM HCl, 0.1% Nonidet P-40 in isopropanol) under constant mixing protected from light for 15 min at 22 ~ 24°C. Spectrophotometric absorbance of the samples at 590 nm was determined by a microplate reader (Bio-Rad).

### **2.2.12 Cell Invasion Assay**

PDAC cells were plated at a density of  $1.5 \times 10^5$  cells per well in 24-well plate. Cells were transfected with various pTriEx4 plasmids (vector alone, CXCR2 C-tail  $\Delta$ TTL, or CXCR2 C-tail WT). After 48 hrs' incubation, *in vitro* invasion assay was performed using Transwell inserts (BD Biosciences) with 8.0  $\mu$ m pore size. Briefly,  $1 \times 10^5$  transfected PDAC cells were suspended in serum-free medium and seeded onto the Transwell inserts pre-coated with diluted (1:3) Matrigel. The Transwell inserts were then placed into 24-well plates filled with the same medium containing 100 ng/ml CXCL8. After 16 hrs' incubation, the upper surface of the Transwell inserts were wiped with a cotton swab and the invaded cells were fixed and stained with Diff-Quick stain (IMEB Inc., San Marcos, CA). The number of invading cells was counted under an inverted microscope ( $\times 50$ ) in 3 randomly selected fields per well. The data were analyzed by ImageJ software (National Institutes of Health, Bethesda, MD) and Microsoft Excel software. In separate experiments, PDAC cells were delivered with CXCR2 C-tail peptides (WT or  $\Delta$ TTL) for 24 hrs, and the cell invasion was assessed as described above.

### **2.2.13 Pancreatic Cancer-induced angiogenesis of endothelial cells**

The PANC-1 cells were transfected with various pTriEx4 plasmids (vector alone, CXCR2 C-tail  $\Delta$ TTL, or CXCR2 C-tail WT) or delivered with CXCR2 C-tail peptides (WT or  $\Delta$ TTL) for 24-48 hrs prior to the angiogenesis assay. The transfected PANC-1 cells were seeded onto the Transwell inserts with 0.4 $\mu$ m pore size, and allowed to adhere for 3hrs. Growth Factor Reduced Matrigel (Fisher Scientific, Pittsburgh, PA) was used to mimic the extracellular matrix, and was diluted with the basal EBM-2 medium, and

allowed to form the gel in the 24-well plates for 2 hours at 37°C. HUVEC cells were treated with basal EBM-2 medium (serum- and growth factors-free) for 3 hours prior to the angiogenesis assay, and were seeded onto the diluted Matrigel. Then, the transfected PANC-1 cells on the Transwell inserts were placed onto the 24-well plates containing the HUVEC cells. After indicated periods, tube formation was examined under the microscope. The lengths of the tube formed by HUVEC cells were measured by ImageJ software (National Institutes of Health, Bethesda, MD), and analyzed by Microsoft Excel software.

#### **2.2.14 Xenografts of Human Pancreatic Cancer cells in Immunodeficient Mice**

Three GFP-tagged AAV2 constructs, AAV2/2CMV-GFP, AAV2/2CMV-GFP-CXCR2 C-tail  $\Delta$ TTL and AAV2/2CMV-GFP-CXCR2 C-tail WT (customized by the Gene Transfer Vector Core, University of Iowa) were used to transduce HPAC cells. CB17 severe combined immunodeficient (CB17-SCID) mice (female, 4 ~ 6 weeks old) were randomly divided into four groups ( $n = 10-12$ ), and each mouse received 200  $\mu$ l serum-free DMEM containing  $3 \times 10^6$  HPAC cells (transduced or non-transduced) subcutaneously in the unilateral flank area. The mice were subjected to measurement of subcutaneous tumors every other day and monitored for changes in body weight and other side effects. Tumor volume was calculated by the formula  $(L \times W^2)/2$ , where  $L$  and  $W$  are the tumor length and width (in mm), respectively. To avoid severe discomfort in the control group, animals were euthanized after 4 weeks. Tumor tissues were harvested for histological analysis and immunohistochemical staining. Tumor volume in SCID mice was plotted against time, and the final tumor weights were measured after the mice

were euthanized. All the animal studies were accomplished under the protocol approved by Wayne State University Institutional Animal Care and Use Committee.

### **2.2.15 Immunohistochemistry and Quantification of Proliferation Index**

Tumor tissue from the xenografts was fixed by 4% paraformaldehyde (PH = 7.5) and embedded within paraffin. Paraformaldehyde-fixed and paraffin-embedded sections (5  $\mu\text{m}$ ) were stained with Ki-67 antibody (Ventana Medical Systems, Tucson, AZ) as reported<sup>165</sup>. Results were expressed as percentage of Ki-67 positive cells per 200 x magnification (Ki-67<sup>+</sup> cell number/total cell number). A total of 10 sections from each experimental group were examined by Zeiss Axiophot epifluorescence microscope (Carl Zeiss) and analyzed by Image-Pro Plus 6.0 software (Media Cybernetics, UK).

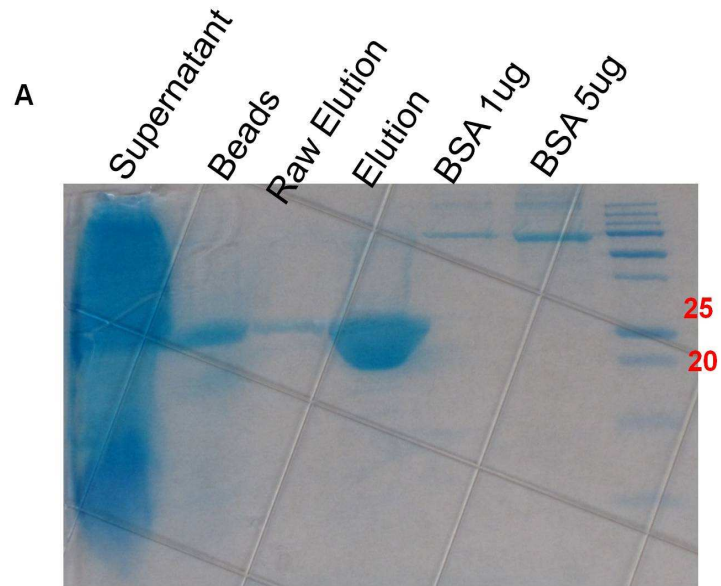
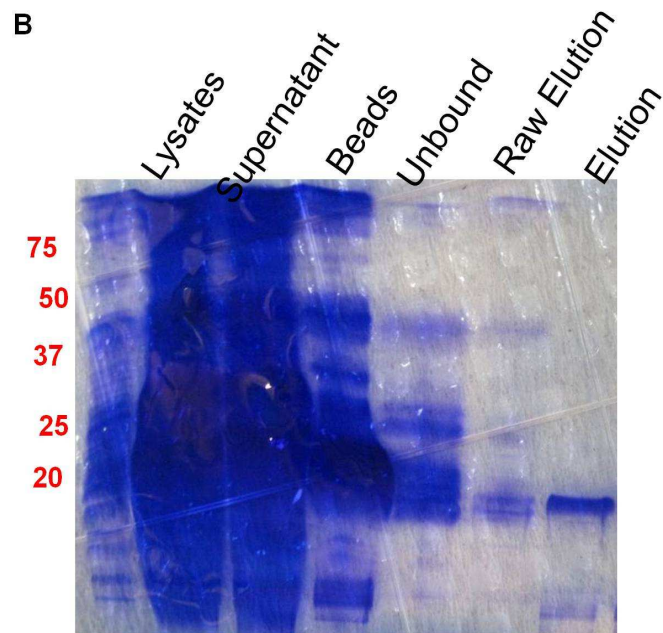
### **2.2.16 Statistical Analysis**

Data are presented as mean  $\pm$  SE of at least three independent experiments. Statistical significance of differences was assessed with the Student's t-test. A value of  $P < 0.05$  was considered statistically significant.

## **2.3 Results**

### **2.3.1 Bacterial Expression and Protein Purification**

High quality of recombinant His-S-CXCR2-C-tail (wild-type, PDZ motif deletion, PDZ motif mutation) and His-S-PLC- $\beta$ 3-C-tail proteins (wild-type, PDZ motif deletion, PDZ motif mutation) were produced as described in section 2.2.3. Figure 2-1 showed the purification of the bacterially expressed His-S-PLC- $\beta$ 3-C-tail (Fig. 2-1 A) and His-S-

His-S-PLC- $\beta$ 3-C-tail

His-S-CXCR2-C-tail



**Fig. 2-1: Purification of the bacterially expressed His-S-PLC- $\beta$ 3-C-tail and His-S-CXCR2-C-tail.** Figure 2-1 showed a Coomassie stained SDS-PAGE showing the bacterially expressed and purified (A) His-S-PLC- $\beta$ 3-C-tail and (B) His-S-CXCR2-C-tail proteins. “Supernatant” indicates the proteins in the supernatant prior to the Glutathione beads binding; “Unbound” indicates the proteins in the supernatant that did not bind to the glutathione beads; “Beads” indicates the proteins left with the beads; “Raw-Elution” indicates the eluted proteins prior to the dialysis; “Elution” indicates the eluted proteins. Molecular Weights: BSA ~ 66.5kDa; His-S-PLC- $\beta$ 3-C-tail ~ 20kDa, His-S-CXCR2-C-tail ~ 16kDa.

CXCR2-C-tail (Fig. 2-2 B). All the fractions were stained with Coomassie Brilliant Blue (Bio-Rad).

### **2.3.2 Overexpression of CXCR2 in human pancreatic cancer cells**

The expression of CXCR2 in normal human pancreatic duct epithelial (HPDE) cells and several PDAC cell lines (HPAC, Colo357, PANC-1, and MIA PaCa-2) were examined and compared by Western blotting as described in section 2.2.6. All the five PDAC cell lines tested in our study showed significantly increased CXCR2 expression (both protein and mRNA) as compared to HPDE cells (Fig. 2-2), which is in agreement with the previous clinical study that reported an up-regulation of IL-8/CXCL8 and its receptors in both pancreatic adenocarcinomas and neuroendocrine tumors<sup>140</sup>.

### **2.3.3 Endogenous CXCR2 and PLC- $\beta$ 3 in human pancreatic cancer cells preferentially interacts with NHERF1**

In a recent study, we demonstrated that the consensus PDZ motif at the carboxyl terminus of CXCR2 mediates PDZ-based interactions with certain PDZ scaffold proteins (such as NHERF1, NHERF2) in neutrophils<sup>163</sup>. In order to investigate if endogenous CXCR2 in PDAC cells binds to any PDZ scaffold proteins, we performed a pull-down assay<sup>163</sup> as described in Materials and Methods. As shown in Fig. 2-3 A, we observed interactions between CXCR2 and the membrane-associated PDZ proteins NHERF1 and NHERF2 in Colo357, L3.6pl, and HPAC cells, among which NHERF1 has a higher binding affinity for CXCR2 as compared with NHERF2. However, neither GST (the negative control) nor PDZK1 was found to bind to endogenous CXCR2 in these PDAC cell lines (Fig. 2-3 A).

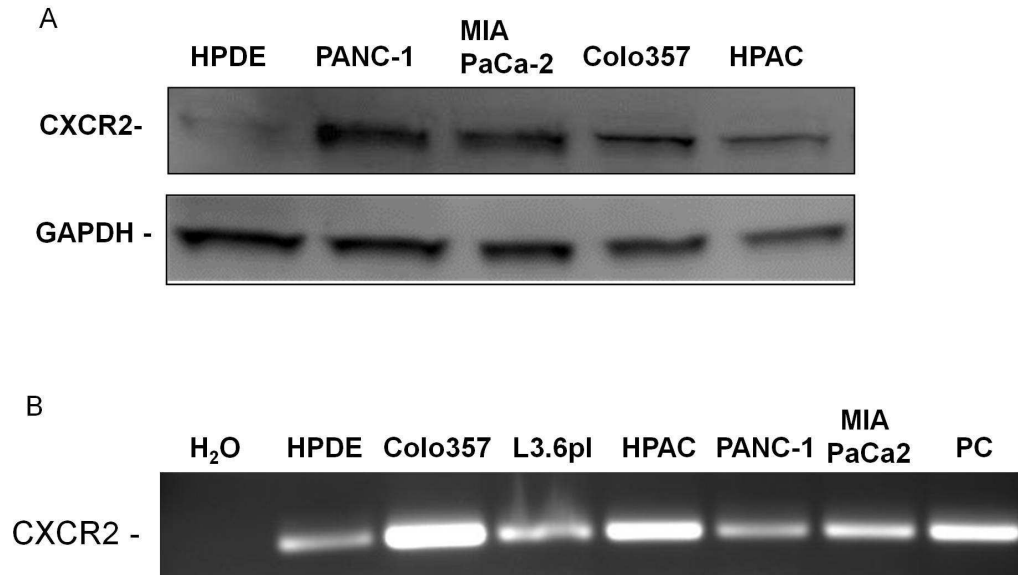


**Fig. 2-2: Overexpression of CXCR2 in human pancreatic cancer cells.** (A) CXCR2 is overexpressed in human pancreatic cancer cells. Expression levels of CXCR2 in normal pancreatic ductal epithelial cell (HPDE) and several PDAC cell lines (HPAC, Colo357, PANC-1, and MIA PaCa-2) were examined by Western blot analysis. Blot analysis of GAPDH was used as internal control. (B) The mRNA expression of CXCR2 of HPDE, Colo357, L3.6pl, HPAC, PANC-1, and MIA PaCa-2 cells were examined by Reverse-Transcriptase PCR, in which SuperScript™ System (Invitrogen) was used. Positive control (PC) of CXCR2 for RT-PCR is plasmid pcDNA3.1-3HA-CXCR2 (full-length). *Wang, S. et al. CXCR2 macromolecular complex in pancreatic cancer: a potential therapeutic target in tumor growth. Translational oncology 6, 216-225 (2013). © 2013 Neoplasia Press.*

CXCR2 couples to the pertussis toxin-sensitive  $G_i$  to stimulate phosphatidylinositide-specific phospholipase C (PLC) activities<sup>145</sup>. Similar to CXCR2, all human PLC- $\beta$  isoforms possess consensus class I PDZ motifs at their carboxyl termini<sup>162</sup>. Our previous study has demonstrated that PLC- $\beta$ 3, containing a PDZ motif (TQL-COOH), overexpressed in HEK293 cells interact with NHERF1 and NHERF2<sup>163</sup>. Here, we explored the potential interactions between PDZ scaffold proteins (NHERF1, NHERF2 and PDZK1) and endogenous PLC- $\beta$ 3 in PDAC cell lines. By similar GST pull-down experiments, we observed that endogenous PLC- $\beta$ 3 in PDAC cells bind to both NHERF1 and NHERF2; however, it did not bind to PDZK1 or to GST alone (Fig. 2-3 B). Moreover, in comparison to NHERF2, NHERF1 appears to interact with PLC- $\beta$ 3 with a higher affinity in most of the PDAC cell lines we tested (Fig. 2-3 B). In addition, the binding between endogenous PLC- $\beta$ 3 in PDAC cells and NHERF1 increased with increasing amounts of NHERF1 in a dose-dependent manner (Fig. 2-3 C).

#### **2.3.4 CXCR2 and PLC- $\beta$ 3 Interact with NHERF1 in a Direct and PDZ Motif-Dependent Manner**

The data resulting from the GST pull-down studies presented above (Fig. 2-3) did not provide information whether the interactions between CXCR2 or PLC- $\beta$ 3 and NHERF1 are direct, as cell lysates contain large numbers of other proteins as well. In order to test if CXCR2 or PLC- $\beta$ 3 binds NHERF1 directly or by other intermediary proteins, and to test the PDZ motif dependence, we performed a pair-wise binding assay that detects a direct interaction between purified proteins *in vitro*<sup>163</sup>. Purified His-S fusion proteins containing the C-tail fragments (last 45 amino acids) of CXCR2 WT, C-tail  $\Delta$ TTL (with

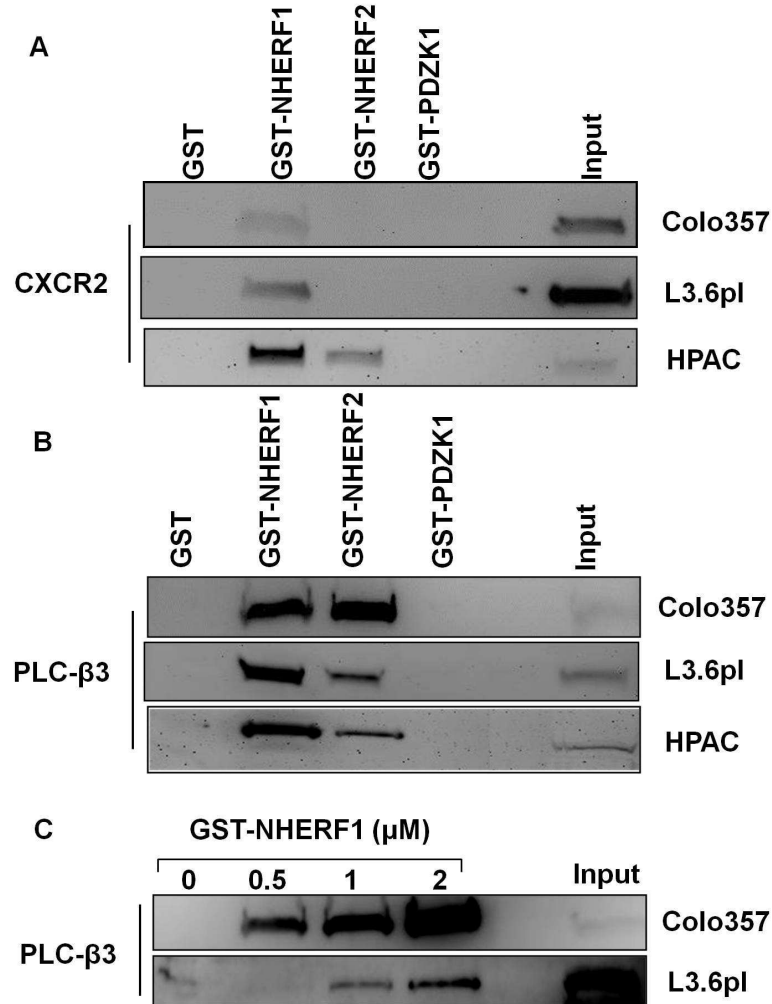


**Figure 2-3: CXCR2 and PLC-β3 in PDAC cells preferentially interact with NHERF1.** (A) Endogenous CXCR2 (from indicated PDAC cells) was pulled down by PDZ scaffold protein (NHERF1, NHERF2, or PDZK1). The membrane was blotted with anti-CXCR2 antibody. GST was used as a negative control. (B) Endogenous PLC-β3 (from indicated PDAC cells) was pulled down by PDZ scaffold protein (NHERF1, NHERF2, or PDZK1). The membrane was blotted with anti-PLC-β3 antibody. The GST was used as a negative control. (C) Endogenous PLC-β3 was pulled down by NHERF1 in a dose-dependent manner. Input is 5% of the total cell lysates. *Wang, S. et al. CXCR2 macromolecular complex in pancreatic cancer: a potential therapeutic target in tumor growth. Translational oncology 6, 216-225 (2013).* © 2013 Neoplasia Press.

PDZ motif TTL deleted), or C-tail AAA or ATA (with PDZ motif TTL mutated to AAA or ATA) were mixed with GST-NHERF1, and the mixtures were pulled down by S-protein-agarose (the S-protein can specifically bind to the S-tag within the fusion proteins). The protein complex was immunoblotted with anti-NHERF1 antibody. We observed that the CXCR2 C-tail directly interacts with NHERF1 in a PDZ motif-dependent manner, as the interaction between NHERF1 and CXCR2 C-tail lacking the PDZ motif ( $\Delta$ TTL) or CXCR2 C-tail with PDZ motif mutations (AAA or ATA) was remarkably reduced (Fig. 2-4A). We also observed that PLC- $\beta$ 3 C-tail (containing the PDZ motif) directly binds to NHERF1 in a PDZ motif-dependent manner, as the interaction between NHERF1 and PLC- $\beta$ 3 C-tail lacking the PDZ motif ( $\Delta$ TQL) or PLC- $\beta$ 3 C-tail with PDZ motif mutation (AAA) was almost completely abolished compared to wild-type (WT) PLC- $\beta$ 3 C-tail (Fig. 2-4 B).

### **2.3.5 CXCR2 interacts with both PDZ domains of NHERF1 (PDZ1 and PDZ2)**

We also showed that CXCR2 interacts with both PDZ domains of NHERF1 (PDZ1 and PDZ2) in the GST pull-down assays, with PDZ2 exhibiting higher binding affinities (Fig. 2-5)<sup>128</sup>. Specifically, CXCR2 overexpressed in HEK293 cells were pulled down by using various purified GST-NHERF1 fractions (GST-PDZ1, GST-PDZ2, and GST-PDZ1-2). Whereas no CXCR2 was detected in the negative control lane containing GST alone, significant amounts of CXCR2 were found in the lanes containing PDZ1 domain (GST-PDZ1), PDZ2 domain (GST-PDZ2), and both PDZ domains together (GST-PDZ1-PDZ2) (Fig. 2-5). To test whether the PDZ-CXCR2 interactions are direct, we performed an *in vitro* pair-wise binding assay with a biotinylated peptide containing the last 13 amino

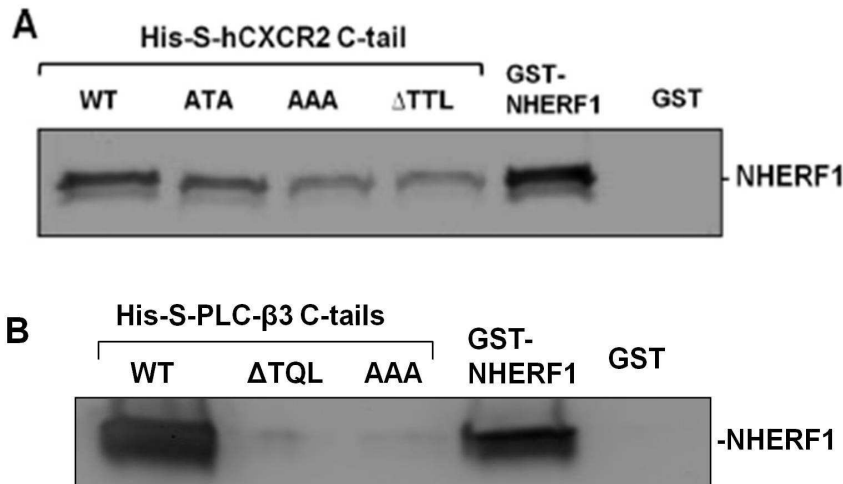


**Fig. 2-4: CXCR2 and PLC-β3 interact with NHERF1 in a direct and PDZ motif-dependent manner. (A)** Pair-wise binding between GST-NHERF1 and His-S-hCXCR2 C-tail (containing the last 45 amino acids) WT, PDZ motif deletion (ΔTTL), or PDZ motif mutants (ATA and AAA). The complex was pulled down by S-protein agarose and immunoblotted with anti-NHERF1 IgG. Purified GST or GST-NHERF1 (20 ng) were loaded as negative or positive control for the anti-NHERF1 antibody, respectively. *Wu, Y., Wang, S. et al. A chemokine receptor CXCR2 macromolecular complex regulates neutrophil functions in inflammatory diseases. The Journal of biological chemistry 287, 5744-5755, doi:10.1074/jbc.M111.315762 (2012) . © 2012 by American Society for Biochemistry and Molecular Biology. (B)* Pair-wise binding between GST-NHERF1 and His-S-hPLC-β3 C-tails (containing the last 100 amino acids) WT, PDZ motif deletion (ΔTQL), or PDZ motif mutant (AAA). The complex was pulled down by S-protein agarose and immunoblotted with anti-NHERF1 antibody. *Wang, S. et al. CXCR2 macromolecular complex in pancreatic cancer: a potential therapeutic target in tumor growth. Translational oncology 6, 216-225 (2013). © 2013 Neoplasia Press.*

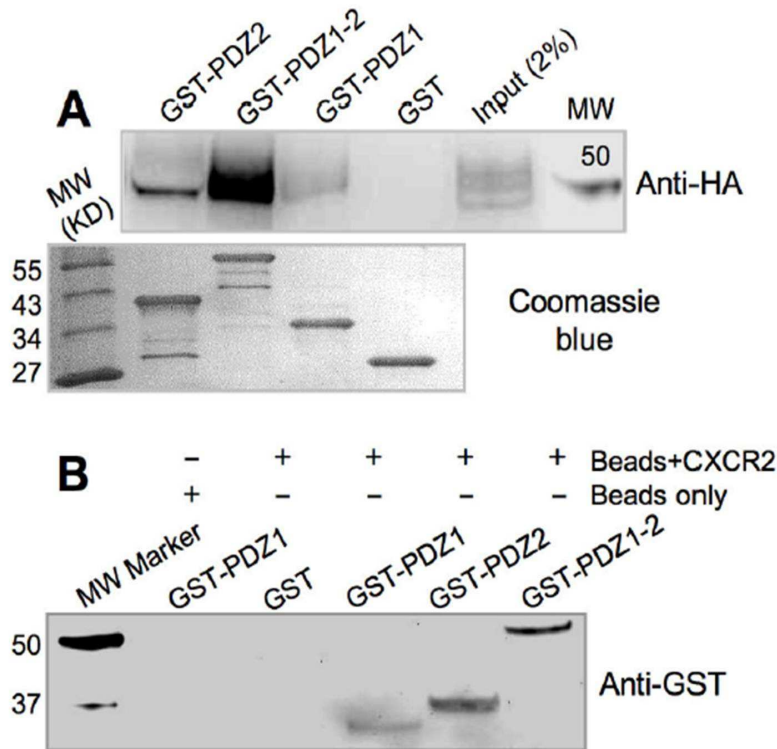


**Fig. 2-5: CXCR2 interacts with both PDZ1 and PDZ2 of NHERF1.** **A)** GST pull-down of CXCR2 with PDZ domains of NHERF1. Lysates of HEK293 cells overexpressing HA-tagged CXCR2 were used to interact with various purified GST-fused NHERF1 fractions (GST-PDZ1, GST-PDZ2, GST-PDZ1-PDZ2, and GST alone), where GST alone served as a negative control. Binding experiments were analyzed by SDS-PAGE and visualized by immunoblotting using anti-HA antibodies. The amount of beads-immobilized GST proteins in each reaction is shown in the lower panel. **B)** Biotin pair-wise binding assays to detect direct interaction between CXCR2 and NHERF1. A biotinylated peptide corresponding to the last 13 residues of CXCR2 was used to interact with various purified GST-fused NHERF1 fractions (GST-PDZ1, GST-PDZ2, GST-PDZ1-PDZ2, and GST alone). Binding was resolved by SDS-PAGE and immunoblotted with anti-GST antibodies. Lu, G. R., Wu, Y., Jiang, Y., Wang, S. et al. *Structural Insights into Neutrophilic Migration Revealed by the Crystal Structure of the Chemokine Receptor CXCR2 in Complex with the First PDZ Domain of NHERF1*. *Plos One* 8, doi:ARTN e76219 DOI 10.1371/journal.pone.0076219 (2013)



acids of CXCR2 (Biotin-FVGSSSGHTSTTL-COOH). Similar binding results were observed in the experiments where CXCR2 interacts with both PDZ domains of NHERF1 (Fig. 2-5).

### **2.3.6 Endogenous PLC- $\beta$ 3 in human pancreatic cancer cells preferentially interacts with NHERF1-PDZ2**

We also demonstrated that endogenous PLC- $\beta$ 3 in various PDAC cells (PANC-1, MIA PaCa-2, AsPC-1, BxPC-3, and HPAC) preferentially interacts with PDZ2 domain of NHERF1. Specifically, the total cell lysates of PDAC cells (PANC-1, MIA PaCa-2, AsPC-1, BxPC-3, and HPAC) were mixed with various purified GST-NHERF1 fractions (GST-PDZ1, GST-PDZ2, and GST-PDZ1-2), and GST-NHERF1 full length. By the GST pull-down assays, we observed that the PLC- $\beta$ 3 endogenously expressed in all the PDAC cell lines preferentially interacts with PDZ2 domain with higher binding affinity (Fig. 2-6 A). It's also worth mentioning that the binding affinity between PLC- $\beta$ 3 and PDZ2 domain is even stronger than the binding between PLC- $\beta$ 3 and full-length NHERF1. Morales and colleagues have demonstrated a head-to-tail intramolecular interaction between the PDZ2 domain and the C-terminal ezrin-radixin-moesin (ERM)-binding region that could mask the association between NHERF1 and other PDZ domain ligands<sup>166,167</sup>. The higher binding affinity of PDZ2 domain compared to the full-length NHERF1 protein is in agreement with the findings by Georgescu group. We also demonstrated the PLC- $\beta$ 3 interacts with both PDZ1 and PDZ2 domains of NHERF1 directly by a pair-wise binding study (Fig. 2-6 B). Also, the PDZ2 domain has a slight higher binding affinity.

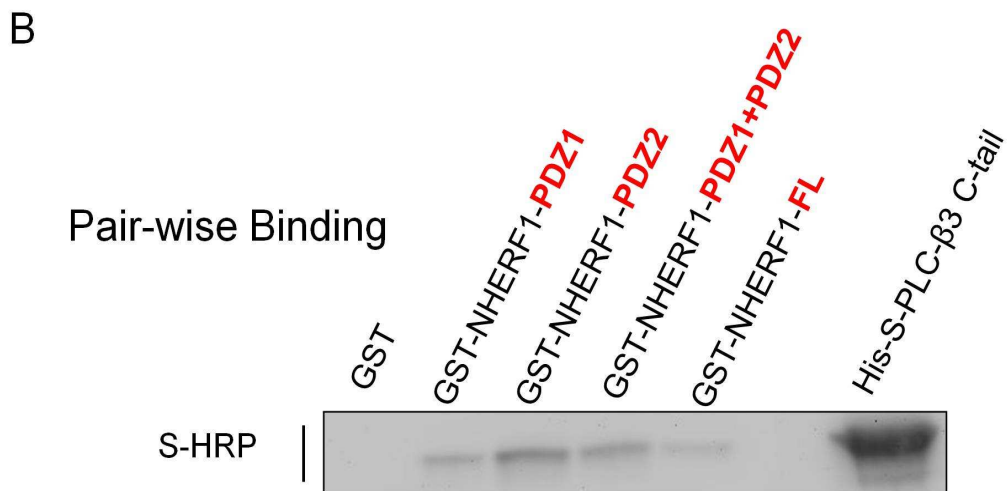
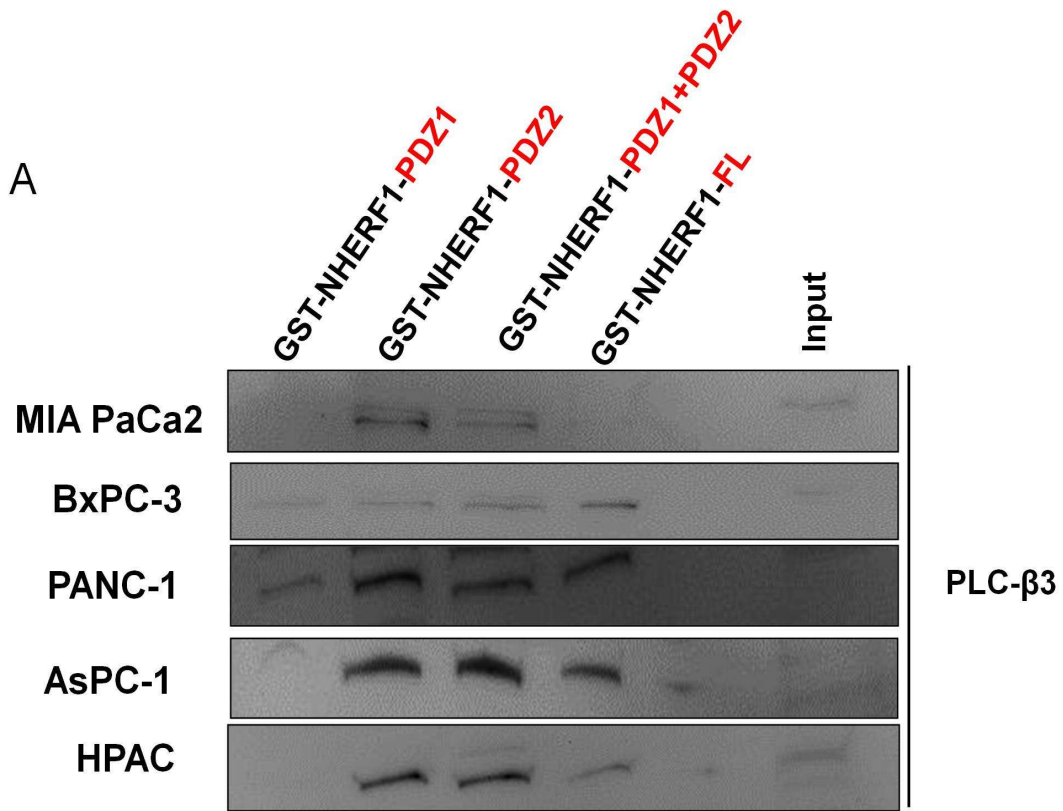


**Fig. 2- 6: Endogenous PLC- $\beta$ 3 in human pancreatic cancer cells preferentially interacts with NHERF1-PDZ2.** (A) GST pull-down of endogenous PLC- $\beta$ 3 with PDZ domains of NHERF1. Lysates of various PDAC cells (PANC-1, MIA PaCa-2, AsPC-1, BxPC-3, and HPAC) were used to interact with GST fusion proteins (GST-PDZ1, GST-PDZ2, and GST-PDZ1-PDZ2). GST alone served as a negative control. Binding experiments were analyzed by SDS-PAGE and visualized by immunoblotting using anti-PLC- $\beta$ 3 antibodies. (B) Pair-wise binding assays to detect direct interaction between purified PLC- $\beta$ 3 and NHERF1. His-S-PLC- $\beta$ 3-C-terminal (containing the last 100 amino acids) was used to interact with various purified GST-fused NHERF1 fractions (GST-PDZ1, GST-PDZ2, GST-PDZ1-PDZ2, GST-NHERF1-FI and GST alone). Binding was resolved by SDS-PAGE and immunoblotted with anti-S protein HRP. Jiang, Y., Wang, S. et al. *Crystallographic Analysis of NHERF1-PLC $\beta$ 3 Interaction Provides Structural Basis for CXCR2 Signaling in Pancreatic Cancer*. *Biochemical and biophysical research communications*, doi:10.1016/j.bbrc.2014.03.028 (2014). © 2014 Elsevier.

### **2.3.7 NHERF1 Clusters CXCR2 and PLC- $\beta$ 3 into a Macromolecular Complex both *In Vitro* and in human pancreatic cancer cells**

Results from the above GST pull-down experiments demonstrated that both endogenous CXCR2 and PLC- $\beta$ 3 in PDAC cells preferentially interact with NHERF1 (Fig. 2-3 A and 2-3 B), and PLC- $\beta$ 3 binds to NHERF1 in a direct and PDZ motif-dependent manner (Fig. 2-4 B), similar to the interaction between CXCR2 and NHERF1 as we previously reported<sup>163</sup>. Hence, we hypothesized that NHERF1 might nucleate CXCR2 and PLC- $\beta$ 3 forming a macromolecular complex in a PDZ motif-dependent manner and this complex might be critical for efficient and specific signaling mediated by CXC-chemokine/CXCR2 biological axis in PDAC cells. Towards this end, we sought to determine if we could detect a macromolecular complex containing CXCR2, NHERF1, and PLC- $\beta$ 3 *in vitro*. Using an *in vitro* macromolecular complex assembly assay (Fig. 2-7A)<sup>163</sup>, we observed the existence of a complex composed of CXCR2 C-tail, NHERF1 and endogenous PLC- $\beta$ 3 in PDAC cells (Fig. 2-7 B). Furthermore, we demonstrated that CXCR2 C-tail did not bind to PLC- $\beta$ 3 directly, and the macromolecular complex was not formed by CXCR2 C-tail PDZ motif mutants ( $\Delta$ TTL or AAA), indicating that the formation of the CXCR2 macromolecular complex is PDZ motif-dependent (Fig. 2-7 B). In addition, we detected a similar complex consisting of PLC- $\beta$ 3 C-tail (containing the PDZ motif TQL), NHERF1, and endogenous CXCR2 from PDAC cells (data not shown).

Results from the above demonstrated that a CXCR2 macromolecular complex exists *in vitro*; however, it did not provide the evidence whether this complex exists in native

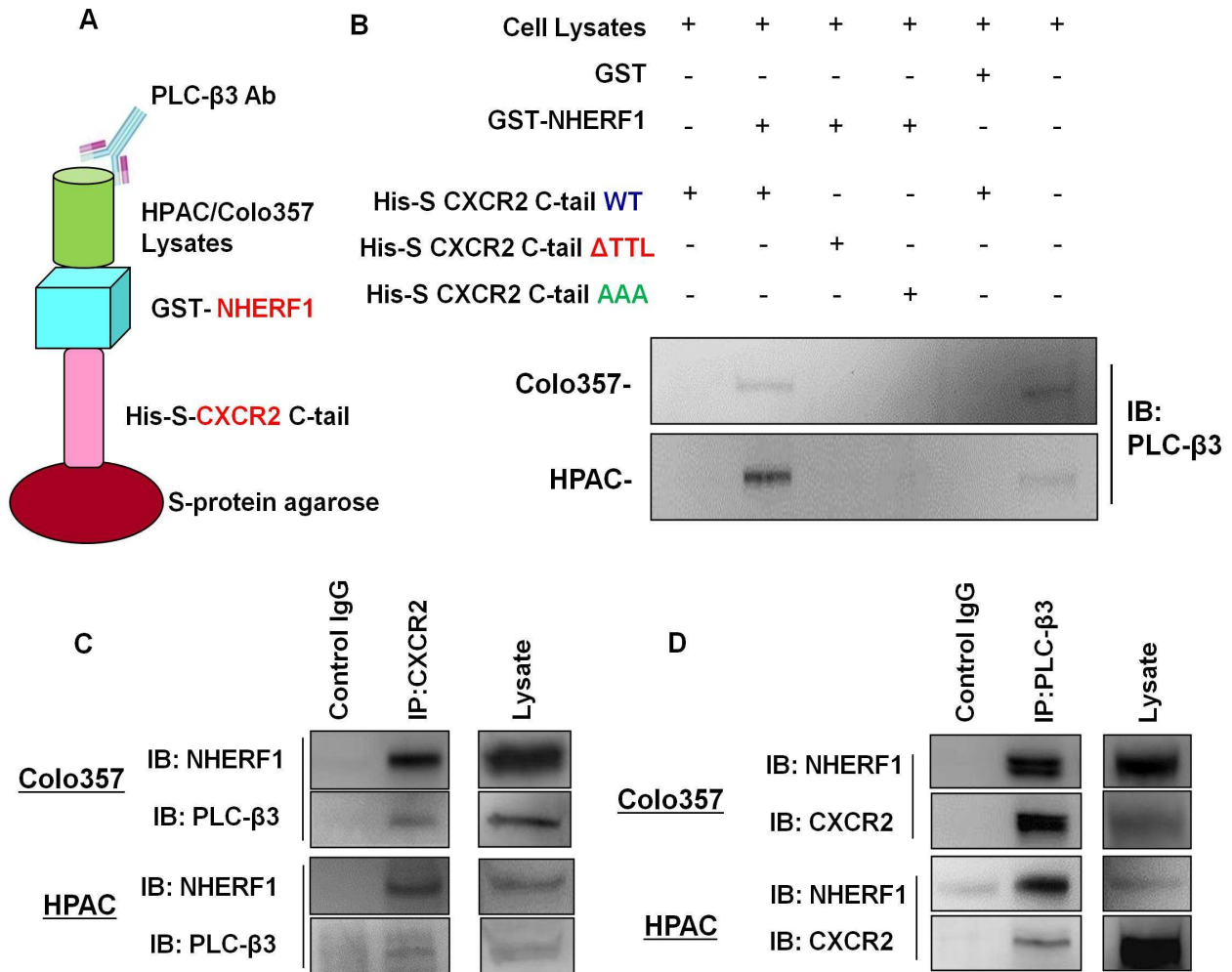


**Fig. 2-7: NHERF1 clusters CXCR2 and PLC- $\beta$ 3 into a macromolecular complex in vitro and in PDAC cells.** (A) Pictorial representation of *in vitro* macromolecular complex assembly (refer to section 2.2.9). (B) *In vitro* macromolecular complex assembly of CXCR2 C-tails (WT,  $\Delta$ TTL, or AAA), GST-NHERF1, and endogenous PLC- $\beta$ 3 (from Colo357 and HPAC cells). (C) Endogenous PLC- $\beta$ 3 and NHERF1 were co-immunoprecipitated with CXCR2 from Colo357 and HPAC cells. (D) Endogenous CXCR2 and NHERF1 were co-precipitated with PLC- $\beta$ 3 from Colo357 and HPAC cells. *Wang, S. et al. CXCR2 macromolecular complex in pancreatic cancer: a potential therapeutic target in tumor growth. Translational oncology 6, 216-225 (2013). © 2013 Neoplasia Press.*

membranes of PDAC cells that endogenously express all the relevant interacting proteins. To address this issue, co-immunoprecipitation was performed using either anti-CXCR2 or anti-PLC- $\beta$ 3 antibodies as described in section 2.2.10. We observed that NHERF1 and PLC- $\beta$ 3 in PDAC cells were co-immunoprecipitated with CXCR2 (Fig. 2-7 C). Similarly, CXCR2 and NHERF1 were also co-precipitated with PLC- $\beta$ 3 from PDAC cells (Fig. 2-7 D), indicating that there is likely to be a macromolecular complex composed of endogenous CXCR2, NHERF1 and PLC- $\beta$ 3 on the surface membranes of Colo357 and HPAC cells.

### **2.3.8 CXCR2 Chemokine/CXCR2 Biological Axis Promotes Pancreatic Cancer Cell Proliferation**

To examine the effect of CXCR2 signaling on PDAC cell proliferation, PDAC cells were treated with CXCR2 ligands followed by the MTT cell proliferation assay as described in section 2.2.11. As illustrated in Fig. 2-8 A, HPAC cells showed significantly elevated cell proliferative activities in response to both CXCL8 and CXCL1 ( $P < 0.05$ ), and CXCL5 also promoted HPAC proliferation, though without statistical significance ( $P = 0.07$ ). Proliferation of Colo357 cells was significantly augmented by CXCL5 ( $P < 0.05$ ), and also by CXCL8 and CXCL1 though without statistical significance ( $P = 0.09$  and  $0.2$ , respectively) (Fig. 2-8 B). It has been reported that Colo357 cells showed a significant high level of CXCL5 secretion<sup>73</sup>, and it has also been documented that CXCL5 is overexpressed in the pancreatic cancer patients compared to the normal individuals, which is associated with the poor survival in patients<sup>74</sup>. Our results underpinned the autocrine effects of CXCL5 on Colo357 cell proliferation. However, the normal pancreatic duct HPDE cells did not demonstrate significantly increased growth

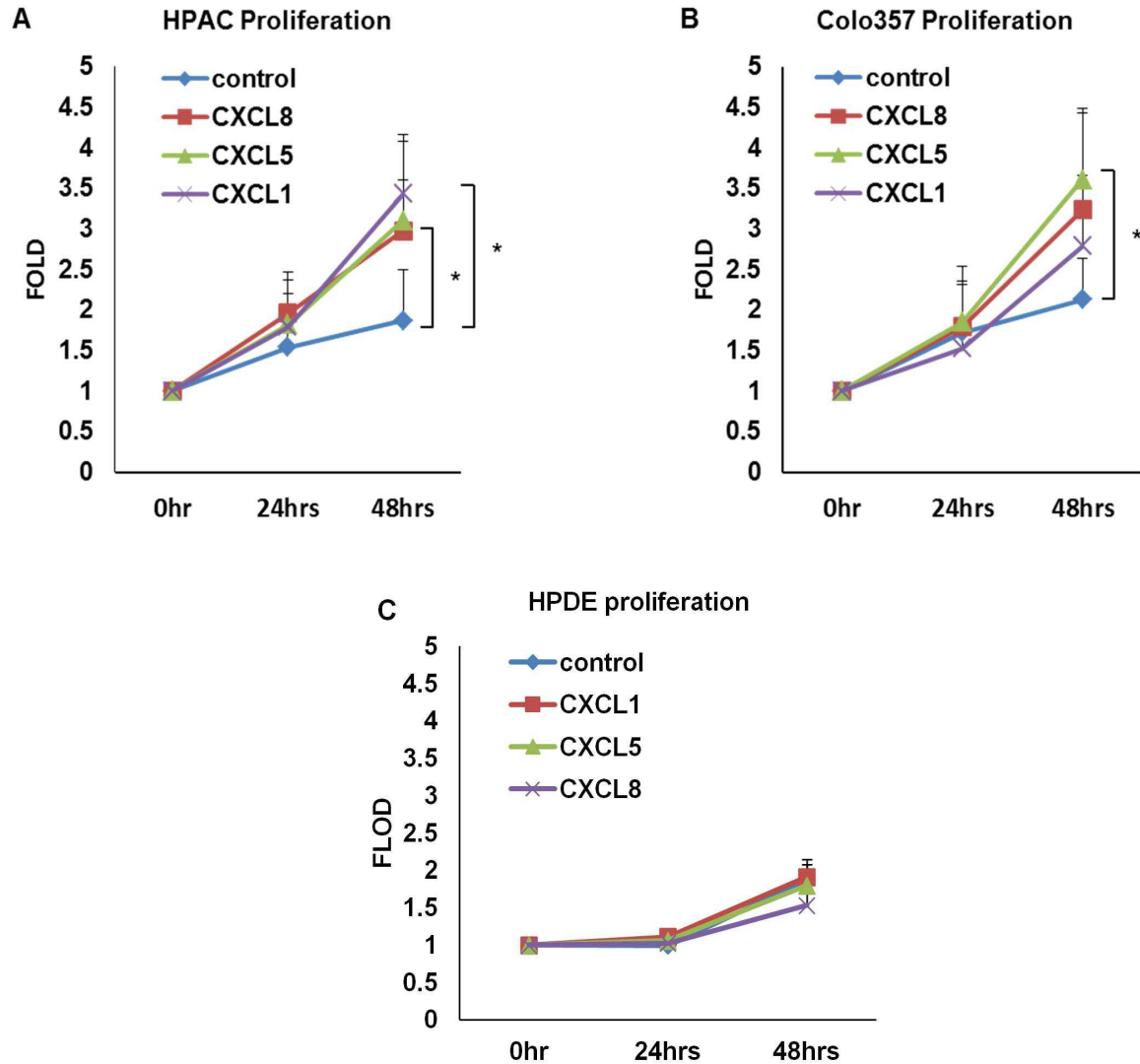


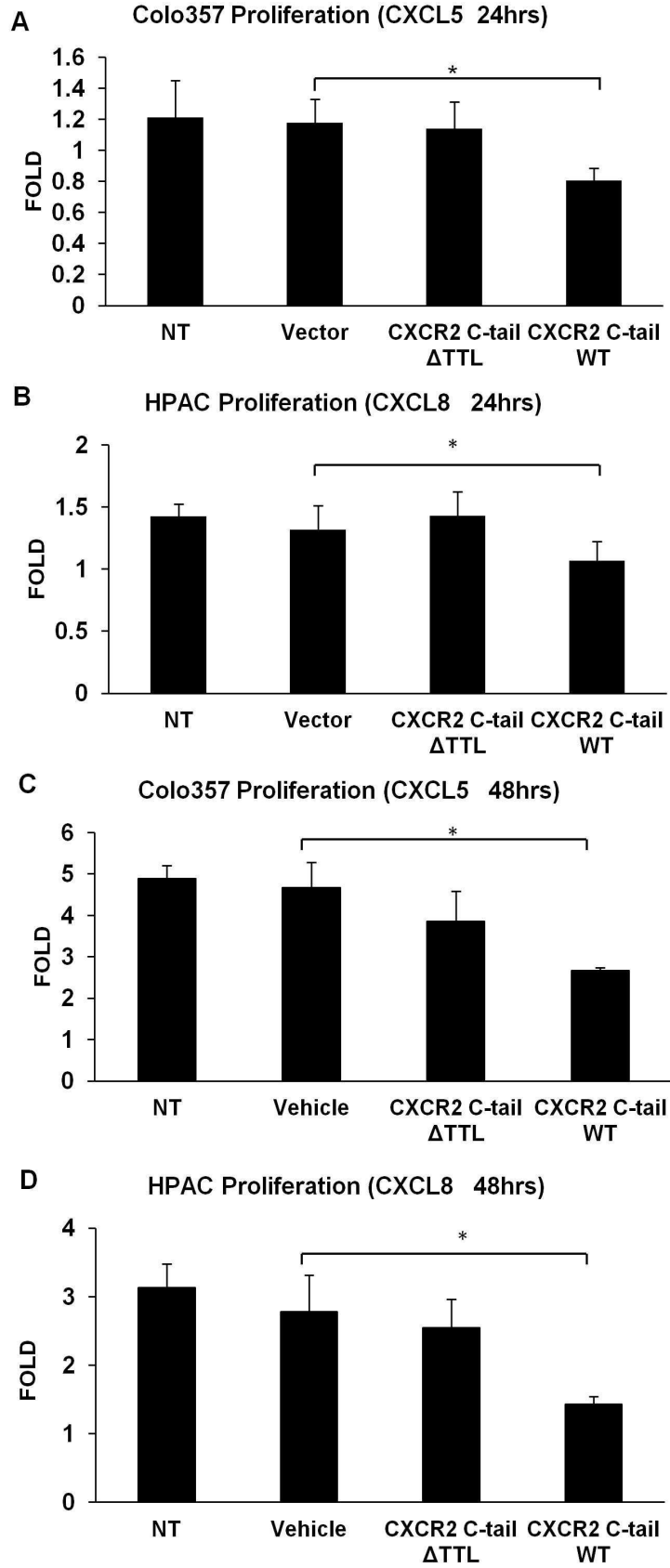
**Fig. 2-8: CXC Chemokine/CXCR2 Biological Axis Promotes Pancreatic Cancer Cell Proliferation.** (A) HPAC, (B) Colo357, and (C) HPDE cell proliferation in response of CXCL1/CXCL5/CXCL8 (100 ng/ml) was assessed and quantified by MTT assay and expressed as relative to the initial time point (0 hour). *Wang, S. et al. CXCR2 macromolecular complex in pancreatic cancer: a potential therapeutic target in tumor growth. Translational oncology 6, 216-225 (2013). © 2013 Neoplasia Press.*

stimulated by the treatment of either of these CXCR2 ligands (CXCL1, CXCL5, or CXCL8) (Fig. 2-8 C), indicating that CXCR2 biological axis significantly promoted pancreatic cancer cell proliferation.

### **2.3.9 Disrupting the CXCR2 Macromolecular Complex Inhibits Pancreatic Cancer Proliferation**

Given that the CXC-chemokine/CXCR2 biological axis plays an important role in PDAC cell proliferation (Fig. 2-8 A and 2-8 B), and here we also demonstrated that the PDZ motif of CXCR2 is essential for the physical coupling of CXCR2 to PLC- $\beta$ 3 mediated by NHERF1 into a macromolecular signaling complex (Fig. 2-7 B); therefore, it is possible that perturbation of the CXCR2 macromolecular complex might affect CXCR2 ligand-induced PDAC cell proliferation. In a recent study, we utilized a CXCR2 C-tail peptide (containing the PDZ motif) to disrupt the CXCR2 PDZ motif-mediated interaction with NHERF1 and observed a functional inhibition of CXCR2 ligand-induced cell migration in neutrophils<sup>163</sup>. We went on to evaluate the functional significance of this CXCR2 macromolecular complex in the CXCR2 ligand-induced PDAC cell proliferation. We transfected HPAC and Colo357 cells with plasmids encoding CXCR2 C-tail (WT or PDZ deletion  $\Delta$ TTL), and evaluated cell proliferative activities. As shown in Fig. 2-9 A, in response to CXCL5, Colo357 transfected with plasmid containing CXCR2 C-tail WT showed significantly reduced proliferative activities as compared to cells transfected with the vector alone or CXCR2 C-tail  $\Delta$ TTL, suggesting that disrupting CXCR2 macromolecular complex inhibits CXCR2 ligand-induced Colo357 growth, and PDZ motif on the C-terminus of CXCR2 is important for PDAC cell proliferation. HPAC





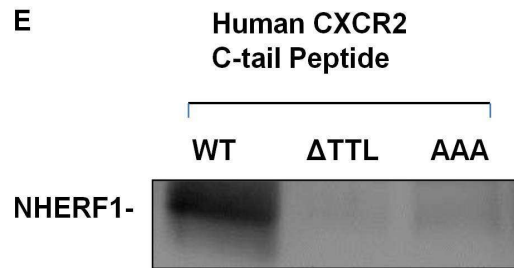


**Fig. 2-9: Disrupting the CXCR2 Macromolecular Complex Inhibits Pancreatic Cancer Proliferation.** Cell proliferation in response to indicated chemokines (CXCL5 or CXCL8; 100 ng/ml) in Colo357 and HPAC cells, which were transfected with plasmids expressing CXCR2 C-tail WT or  $\Delta$ TTL (A, B) or pre-delivered with CXCR2 C-tail-specific peptide WT or  $\Delta$ TTL (C, D). (E) Pair-wise binding between GST-NHERF1 and various biotin-conjugated CXCR2 C-tail-specific peptide (containing last 13 amino acids) WT,  $\Delta$ TTL, or AAA. The complex was pulled down by streptavidin agarose and immunoblotted with anti-NHERF1 antibody. Columns/dots, means of quintuplicates; bars, SEM; \*P < 0.05. NT, cells not transfected or pre-delivered with peptides. *Wang, S. et al. CXCR2 macromolecular complex in pancreatic cancer: a potential therapeutic target in tumor growth. Translational oncology 6, 216-225 (2013). © 2013 Neoplasia Press.*

transfected with CXCR2 C-tail WT showed significantly decreased cell proliferation in response to CXCL8 (Fig. 2-9 B). In addition, we delivered the CXCR2 C-tail peptides (WT and  $\Delta$ TTL) used in our previous studies<sup>163</sup> to Colo357 and HPAC cells, and we also observed significantly reduced cell proliferation stimulated by CXCL5 (Fig. 2-9 C) and CXCL8 (Fig. 2-9 D). Furthermore, using the pair-wise binding assay, we also demonstrated that the CXCR2 C-tail peptide interacts with NHERF1 in a direct and PDZ motif-dependent manner, because the CXCR2 WT peptide interacts with NHERF1, while the PDZ deletion peptide ( $\Delta$ TTL) or mutation peptide (AAA) failed to bind to NHERF1 (Fig. 2-9 E).

### **2.3.10 Inhibitory effect of EF1060 on MIA PaCa-2 proliferation**

The peptide inhibitor, EF1060, was dissolved in DMSO as 200mM stock with good solubility. Initially, concentration (500 ng/ml) of EF1060 was used to compare with the peptide synthesized by Genemed Synthesis (Biotin-CXCR2 C-tail; 13 a.a.). Significant change in cell proliferation was not detected at the peptide concentration of 500ng/ml (of 96-well plate) (Fig. 2-10 B).

However, by using similar peptide concentration (200 $\mu$ g/ml) that was previously reported by Dr. Spaller's group, significant reduction in cell proliferation by EF1060 has been observed compared with DMSO control (Fig. 2-10 C).

It is noteworthy that, EF1060, when used at low concentration (in Fig. 2-10 B) without Chariot, seemed to have inhibitory effect on cell proliferation, although had not achieved statistical significance given the small sample number. Meanwhile, EF1060 significantly

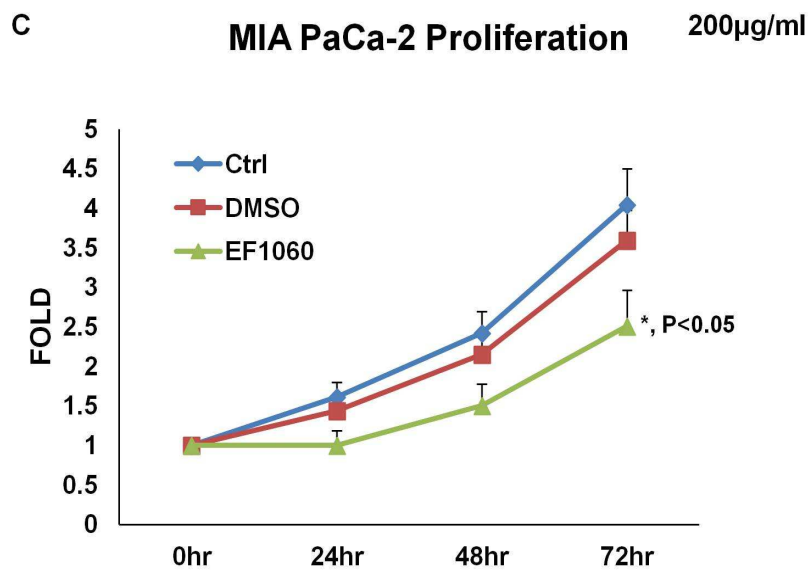
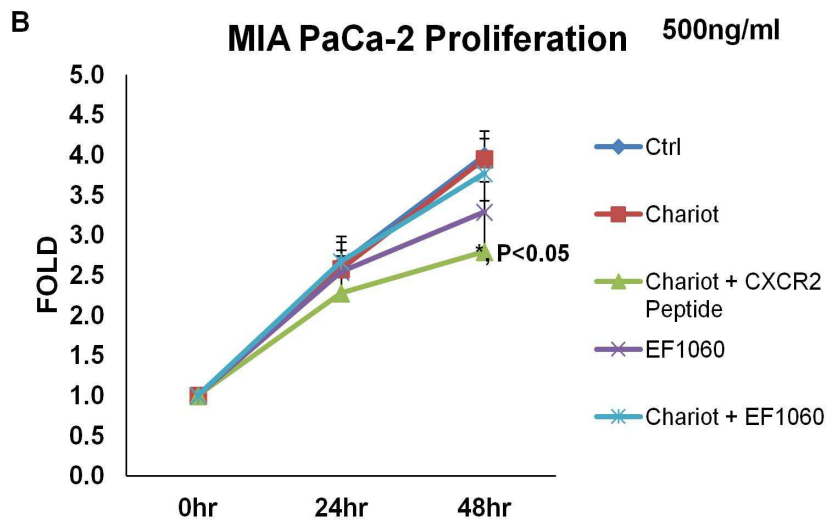
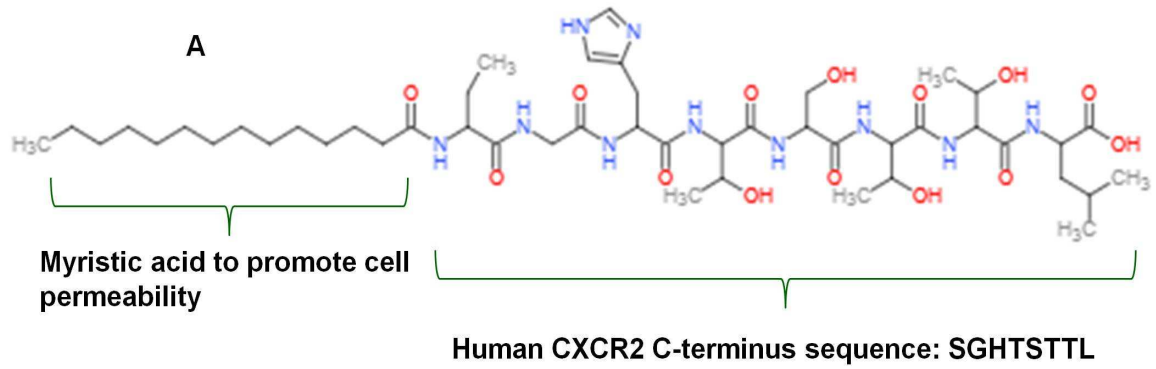


**Fig. 2-10 Inhibitory effect of EF1060 on MIA PaCa-2 proliferation.**

A) Structure of the peptide inhibitor EF1060 .

B) Peptide concentration is 500ng/ml. Ctrl: no Chariot or peptide; Chariot: only Chariot; Chariot + CXCR2 peptide (biotin- CXCR2 C-tail 13 a.a. (section 2.2.1) delivered by Chariot™); EF1060: EF1060, no Chariot added; Chariot + EF1060: EF1060, delivered by Chariot.

\* $P < 0.05$  compared with Chariot only.

C) Peptide Concentration is 200µg/ml. No Chariot agent added to all the groups. Ctrl: no Chariot or peptide; DMSO: same amount of DMSO as used in peptide; EF1060: EF1060 (dissolved in DMSO). \* $P < 0.05$  compared with DMSO only.

inhibited cell proliferation when used at high concentration without Chariot (as in Fig.2-10 C). However, when used at low concentration (in Fig. 2-10 B), EF1060 (+ Chariot™) had no effect on cell proliferation, which suggests that EF1060 with myristoylation at N-terminus might not require the commercial peptide delivery system.

### **2.3.11 Disrupting the CXCR2 Macromolecular Complex Blocks Pancreatic Cancer Cell Invasion**

We then examined the effect of disrupting CXCR2 signaling complex on the invasive capability of PDAC cells. HPAC cells were transfected with plasmids encoding CXCR2 C-tail (WT or  $\Delta$ TTL) and used to evaluate the invasive potency by an *in vitro* invasion assay as reported before<sup>73</sup>. As illustrated in Fig. 2-11, gene delivery of CXCR2 C-tail WT sequence, but not the  $\Delta$ TTL PDZ deletion sequence, significantly inhibited invasion of HPAC cells through Matrigel induced by CXCL8, implicating that the PDZ motif of CXCR2 is important for PDAC cell invasion.

### **2.3.12 Disrupting the CXCR2 Macromolecular Complex Blocks Pancreatic Cancer-induced angiogenesis**

We next investigated the effect of disrupting CXCR2 macromolecular complex on the capability of PDAC cell-induced angiogenesis. PANC-1 cells were transfected with plasmids encoding CXCR2 C-tail (WT or  $\Delta$ TTL) and used to evaluate the tumor-induced angiogenesis potential by an *in vitro* tube formation assay as described in section 2.2.13. Figure 2-12 showed that gene delivery of CXCR2 C-tail WT sequence, but not the  $\Delta$ TTL

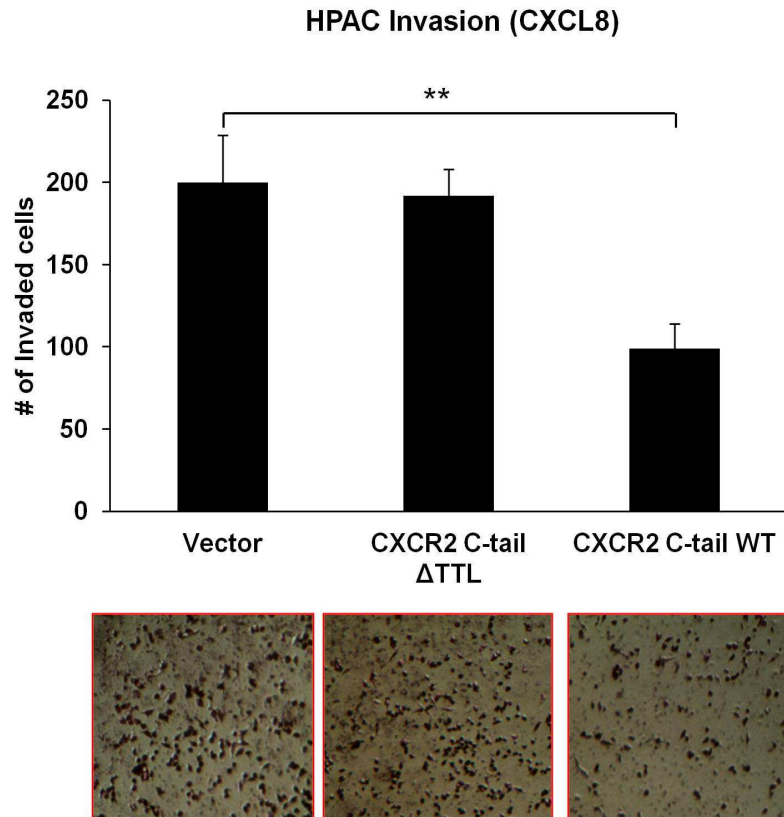


**Fig. 2-11 Disrupting the CXCR2 Macromolecular Complex Blocks Pancreatic Cancer Cell Invasion.** Gene delivery of CXCR2 C-tail sequence significantly inhibits malignant invasion of pancreatic cancer cell. HPAC cells were transfected with pTriEx4 vector alone, pTriEx4 CXCR2 C-tail PDZ motif deletion ( $\Delta$ TTL), or pTriEx4 CXCR2 C-tail WT. Invasion through the Transwell inserts pre-coated with Matrigel of transfected HPAC cells was initiated by CXCL8 (100 ng/ml) and quantified by microscopy. Columns, means of triplicates; bars, SEM; \*\*P < 0.01. *Wang, S. et al. CXCR2 macromolecular complex in pancreatic cancer: a potential therapeutic target in tumor growth. Translational oncology 6, 216-225 (2013). © 2013 Neoplasia Press.*

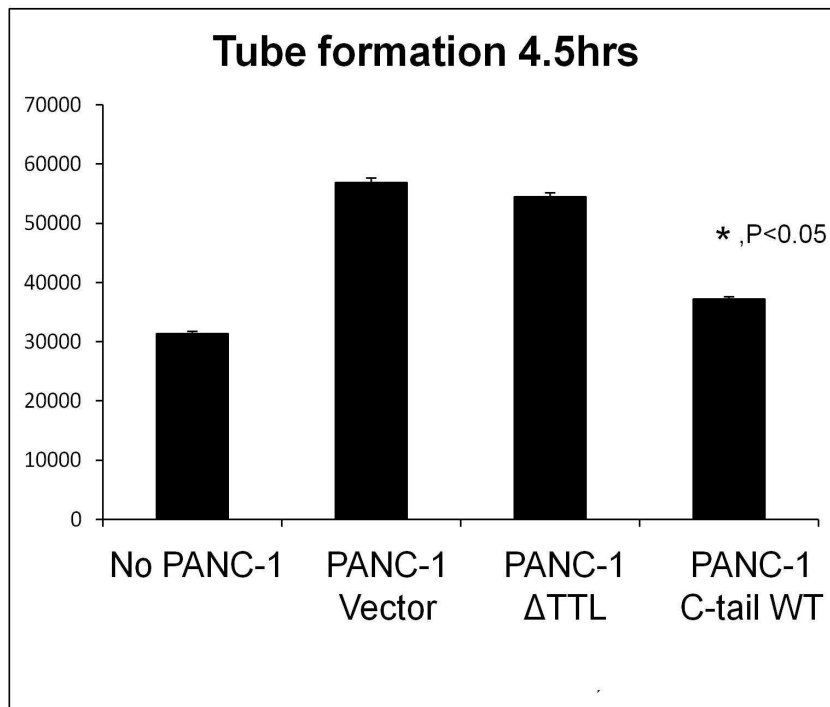
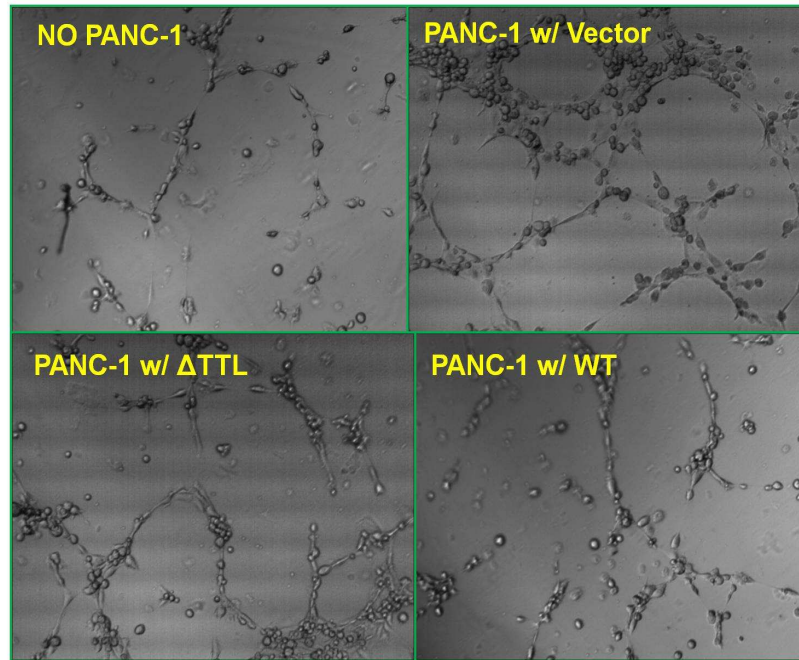




**Fig. 2-12 Disrupting the CXCR2 Macromolecular Complex Blocks Pancreatic Cancer-induced angiogenesis.** Gene delivery of CXCR2 C-tail sequence significantly inhibits pancreatic cancer cell-induced angiogenesis. PANC-1 cells were transfected with pTriEx4 vector alone, pTriEx4 CXCR2 C-tail PDZ motif deletion ( $\Delta$ TTL), or pTriEx4 CXCR2 C-tail WT. HUVEC cells on the growth factors-reduced Matrigel were co-cultured with transfected PANC-1 cells. Tube lengths were measured and quantified by ImageJ software. Columns, means of triplicates; bars, SEM; \*\*P < 0.05.

PDZ deletion sequence or pTriEx4 vector alone, significantly suppressed the tube formation of HUVEC cells induced by the PANC-1 cells, indicating the CXCR2 macromolecular complex through PDZ binding is important for PDAC-induced angiogenesis.

### **2.3.13 Disrupting the CXCR2 Macromolecular Complex Inhibits Pancreatic Tumor Growth *In Vivo***

To analyze the functional significance of the CXCR2 macromolecular complex in PDAC growth *in vivo*, a subcutaneous xenograft induced by HPAC cells in CB17-SCID mice was developed to determine whether disrupting the CXCR2 signaling complex could lead to inhibition of tumor growth *in vivo*. HPAC cells that were transduced with Adeno-Associated Virus (Serotype 2) expressing GFP - human CXCR2 C-tails (WT or  $\Delta$ TTL) or GFP alone, or non-transduced cells, were injected subcutaneously into CB17-SCID mice. The transduction efficiency was inspected visually under the fluorescence microscope (Fig. 2-13). Tumor volume was measured every other day starting at day 12 (when the tumor became palpable). At day 28, all mice were euthanized, and tumors were excised and final tumor weights were determined by the scale. We found that HPAC cells expressing GFP alone or GFP-CXCR2 C-tail  $\Delta$ TTL grew into sizable tumors underneath the skin that were comparable to non-transduced cells (Fig 2-14 A). However, HPAC cells expressing GFP-CXCR2 C-tail WT grew into significantly smaller tumors compared with the cancer cells expressing GFP vector alone or GFP-CXCR2 C-tail  $\Delta$ TTL, or non-transduced cells (Fig 2-14 A). Furthermore, the HPAC cells, transduced with GFP-CXCR2 C-tail WT, showed significantly reduced final tumor weight

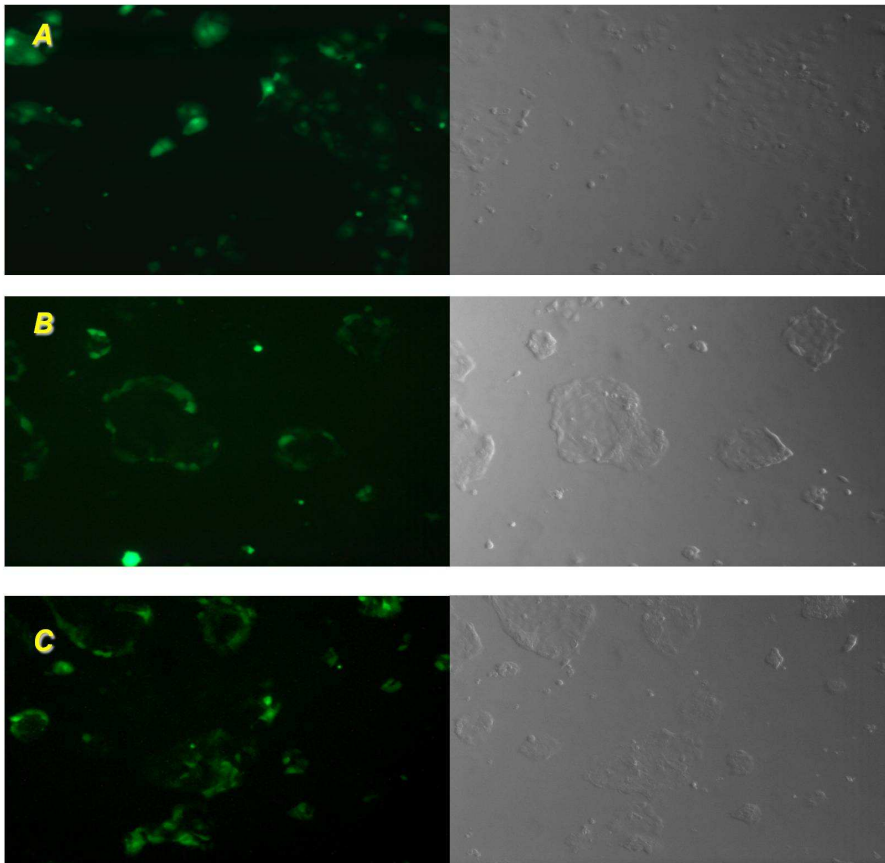


**Fig. 2-13 AAV2/2CMV Transduction Efficiency on HPAC cells.** A) HPAC were transduced with AAV2/2CMV-GFP vector; B) HPAC cells were transduced with AAV2/2CMV-GFP-hCXCR2 ( $\Delta$ TTL); C) HPAC cells were transduced with AAV2/2CMV-GFP-hCXCR2 (WT).

compared to the 3 other groups (Fig. 2-14 B). This result suggests an inhibitory effect of exogenous CXCR2 C-tail (containing the PDZ motif) on human pancreatic tumor development and progression *in vivo*. We then demonstrated that the proliferation index, determined by Ki-67 expression, in the group of mice injected with HPAC cells expressing GFP–CXCR2 C-tail WT was significantly lower ( $p < 0.01$ ) compared to the 3 other groups (non-transduction group, AAV2-GFP group, and AAV2-GFP-CXCR2 C-tail  $\Delta$ TTL group) (Fig. 2-14 C and D). Collectively, our data indicates the potential therapeutic effect of disrupting the CXCR2 macromolecular complex on the primary tumor of PDAC in a subcutaneous mouse model. It is noteworthy that in the group of mice injected with HPAC cells expressing GFP–CXCR2 C-tail WT did not show significant reduced *in vivo* tumor-induced angiogenesis compared to other groups.

## 2.4 Discussion

CXC-chemokines (such as CXCL1/GRO- $\alpha$ , CXCL8/IL-8, CXCL5/ENA-78) and their cognate receptor CXCR2 have been reported to play a critical role in tumor growth and tumor invasion and tumor-induced angiogenesis, as blockade of the CXC-chemokines/CXCR2 biological axis reduced tumorigenesis and angiogenesis in many human cancers including pancreatic cancer<sup>63,73,75,168</sup>. However, most of the interventional approaches have been conducted by systemic blockade or depletion of CXCR2 and/or its ligands, which might cause global undesired effects on other vital functions, as CXCR2 had also been reported in many essential normal cellular functions, such as in preservation of oligodendrocyte function and myelination of neural tissues<sup>21</sup>. This issue warrants the necessity of a more comprehensive understanding of the

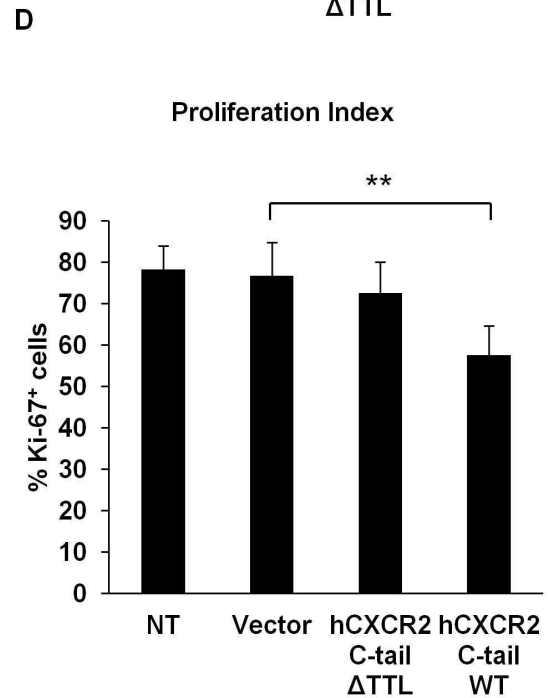
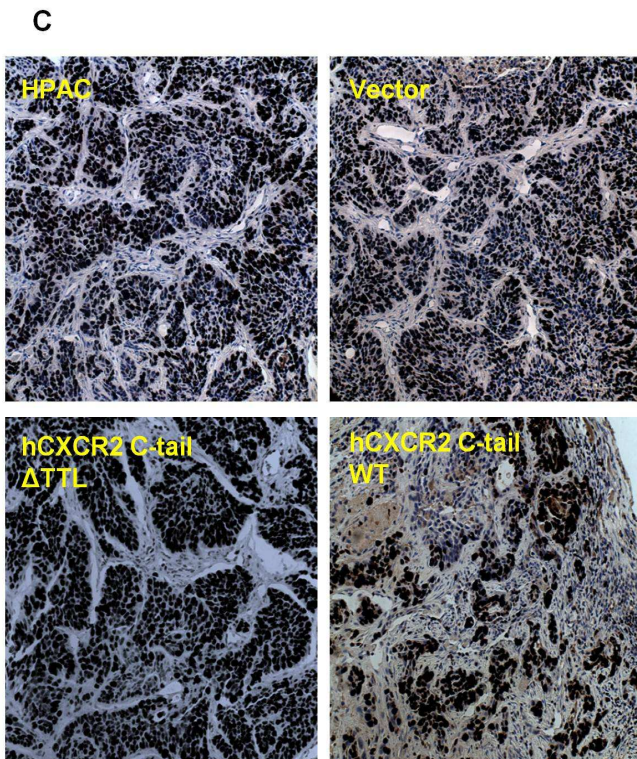
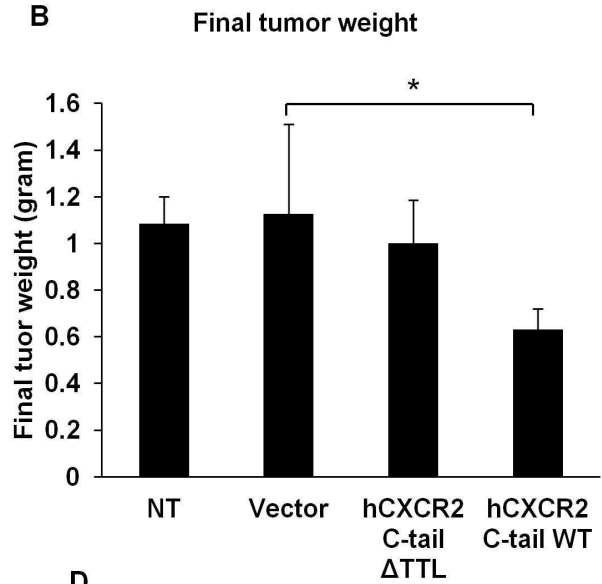
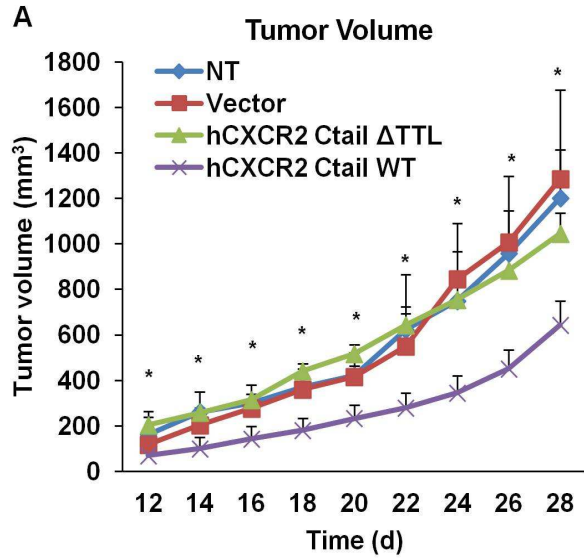


**Fig. 2-14 Disrupting the CXCR2 Macromolecular Complex Inhibits Pancreatic Tumor Growth *In Vivo*.** Disrupting the CXCR2 macromolecular complex inhibits pancreatic tumor growth *in vivo*. Gene delivery of CXCR2 c-tail sequence inhibits PDAC tumor growth *in vivo*. Tumor volume (A) was measured according to the formula  $(1/2 \times L \times W^2)$  every other day; and final tumor weights (B) were measured, averaged, and compared after 4 weeks. Proliferation index (D) was expressed as percentages of Ki-67<sup>+</sup> cells (see details in sections 2.2.14 and 2.2.15); and representative Ki-67<sup>+</sup> immunohistochemical images (200 $\times$ ) are shown in (C). \*P < 0.05; \*\*P < 0.01. NT, non-transduced cells. *Wang, S. et al. CXCR2 macromolecular complex in pancreatic cancer: a potential therapeutic target in tumor growth. Translational oncology 6, 216-225 (2013). © 2013 Neoplasia Press.*

molecular mechanisms of CXCR2 and its signaling, on the basis of which, selective and cell-specific therapeutic targets could be identified.

CXCR2 possesses a consensus PDZ motif at their carboxyl termini, and the PDZ motif has been reported to modulate cellular chemotaxis<sup>123</sup>. Recently, we demonstrated that the PDZ motif of CXCR2 plays an important role in regulating neutrophil functions as disrupting the interaction mediated by PDZ motif via using an exogenous peptide mimic (mapping CXCR2 PDZ motif) significantly inhibited CXCR2-mediated calcium mobilization and neutrophilic transepithelial migration<sup>163</sup>. In the present study, we identified the PDZ scaffold protein NHERF1 as a previously unrecognized interacting partner for CXCR2 in PDAC cells, and we also demonstrated the existence of a PDZ-based CXCR2 macromolecular signaling complex containing endogenous CXCR2, NHERF1 and PLC- $\beta$ 3 in PDAC cells. Furthermore, we provided functional evidence showing that disrupting the CXCR2 complex significantly inhibited the malignant cellular functions (i.e. proliferation and invasion) *in vitro* and pancreatic tumor growth *in vivo*.

Controversy exists regarding the expression of CXCR2 in human pancreatic cancer cell lines. Despite some studies reported that CXCR2 was not detected in some human PDAC cell lines (such as PANC-1, MIA PaCa-2, AsPC-1, BxPC-3 and HPAF-II)<sup>73,165,169</sup>, other groups reported the detection of CXCR2 and/or the autocrine effect of CXCR2 ligands in various human PDAC cells<sup>74,141-144,170</sup> (such as PANC-1, MIA PaCa-2, Capan-1, Capan-2, SUI-2, HuP-T4, Bx-PC-3, Panc03.27), and pancreatic tumors specimens from patients<sup>63,140</sup>. In the present study, we also detected the expression of CXCR2 in

PANC-1, MIA PaCa-2, HPAC, Colo357, and L3.6pl cells in Western blotting (Fig. 2-2 A) by using the same antibody Frick *et al* used to detect the CXCR2 expression in patient specimens<sup>63</sup>. RT-PCR results from our study also confirmed the expression of CXCR2 in these cell lines (Fig. 2-2 B). One possible reason for the failure of some groups to detect CXCR2 in PDAC cell lines might be that expression level of CXCR2 varies in different conditions. Yamamoto *et al* reported that CXCR2 is up-regulated in an orthotopic colon cancer model compared to the subcutaneous model<sup>171</sup>. Hussain *et al* also reported that the expression level of CXCR2 correlates with tumor grade and stage in pancreatic adenocarcinomas<sup>140</sup>.

PLC- $\beta$  is the major isozyme that has been well-studied to participate in GPCR-mediated signaling and modulate the physiological responses, such as promoting cell growth in many cancer types<sup>172-174</sup>. Each PLC- $\beta$  subtype has its distinct expression pattern and physiological relevance<sup>172</sup>. Among the four subtypes of PLC- $\beta$ , PLC- $\beta$ 3 is expressed in a wide range of cells and tissues<sup>174</sup>, and exhibits the highest affinity to G $\beta\gamma$  subunits and subsequent activation by G $\beta\gamma$  subunits<sup>175</sup>. A growing body of evidence suggests that PDZ scaffold proteins are involved in the modulation of PLC- $\beta$  isoforms in the PDZ motif-dependent manner. PLC- $\beta$ 3, with its PDZ motif (-STQL-COOH), was reported to bind to PDZ domains of NHERF2 and Shank2 via its PDZ motif at its carboxyl termini, in mouse small intestine<sup>161</sup> and in the postsynaptic density region in neuronal cells<sup>158</sup>, respectively. It has also been shown that PLC- $\beta$ 3 was down-regulated in jejuna villus cells in NHERF1- knockout mice<sup>160</sup>. Results from our present study revealed that PLC- $\beta$ 3 preferentially binds to NHERF1 in PDAC cells in a direct and PDZ motif-dependent



pattern. Therefore, the specificity and diversity of agonist-induced PLC- $\beta$  activity and its downstream signaling may be regulated by the specific interactions of PLC- $\beta$  isoforms and certain PDZ scaffold proteins.

There is accumulating evidence suggesting that the formation of spatial compact macromolecular signaling complexes beneath the plasma membrane enables the membrane receptors to transduce signals into cell interior and thereafter influence cell behavior with higher specificity and efficiency<sup>163,176-179</sup>. These findings have therapeutic implications in various diseases including inflammatory diseases, genetic diseases and cancer<sup>153-159</sup>. Our present study revealed a PDZ motif-dependent CXCR2 macromolecular signaling complex, in which CXCR2 and PLC- $\beta$ 3 were bridged by NHERF1, in the PDAC cells (Fig. 2-15). Results from our study also demonstrated the functional importance of the CXCR2 complex in pancreatic cancer cell functions *in vitro* and *in vivo*, as disturbing the CXCR2 complex by using an exogenous CXCR2 C-tail sequence (containing the PDZ motif) significantly attenuated malignant cell proliferation and cell invasion of PDAC cells and tumor growth *in vivo*. Our present study introduced a new concept of the CXCR2 macromolecular complex mediated via PDZ-based interactions, and we elucidated the molecular evidence and functional importance of this CXCR2 complex in pancreatic cancer progression. Moreover, by investigating a network of protein complexes rather than CXCR2 alone in pancreatic cancer, our results reveal a novel molecular target for the development of specific therapeutic strategies and agents that could combat pancreatic cancer.

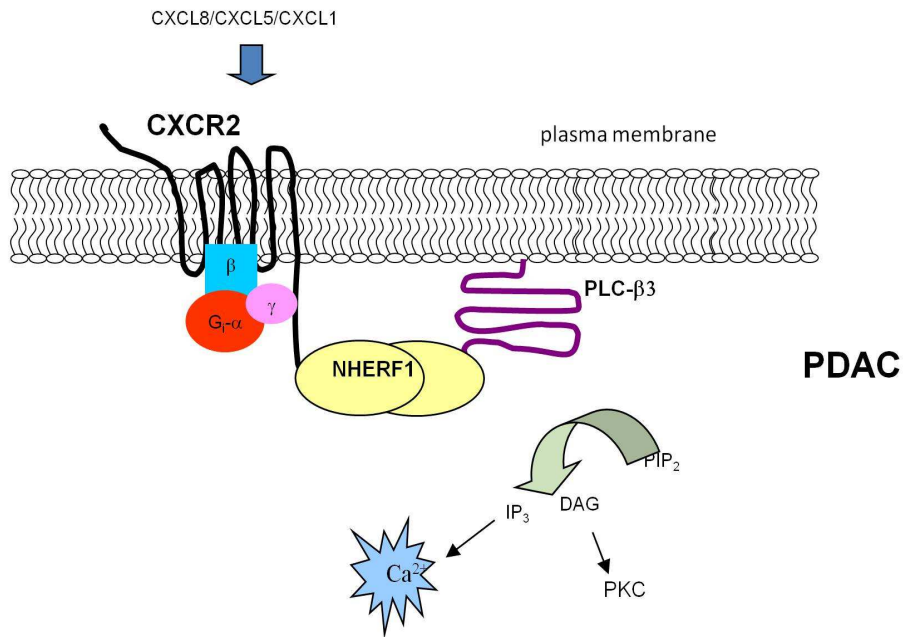


**Fig. 2-15. Proposed mechanism of the NHERF1-mediated coupling of CXCR2 to PLC-β3 signaling in PDAC cells.** Both CXCR2 and PLC-β3 directly interact with the PDZ scaffold protein NHERF1. NHERF1 clusters CXCR2 and PLC-β3 in close proximity via a PDZ-based interaction, thereby forming spatially compact signaling complexes beneath the plasma membrane. Consequently, the macromolecular signaling complex (CXCR2•NHERF1•PLC-β3) enables CXCR2 to transduce its signal to PLC-β3 with efficiency and specificity. Wang, S. *et al.* *CXCR2 macromolecular complex in pancreatic cancer: a potential therapeutic target in tumor growth.* *Translational oncology* 6, 216-225 (2013). © 2013 Neoplasia Press.

Recent advances regarding PDZ proteins have suggested that the specific inhibition of the protein-protein interaction mediated by PDZ domains, with subsequent intervention of the signaling pathways mediated by the PDZ proteins, appears to be a promising strategy for developing novel peptide inhibitors in cancer<sup>180</sup>. Furthermore, our studies have shown that our CXCR2 specific peptide (bearing the last 13 residues of the C-terminal sequence of CXCR2) exhibit significant inhibitory effect on the malignant cellular functions of pancreatic cancer<sup>125</sup>. However, before the clinical trials commence, our strategy still needs to be further investigated by addressing several challenges. The membrane permeability of the small peptide is one of the frequently questioned problems in novel inhibitor development<sup>180</sup>. Also, additional effort is also required on maximizing the binding affinity and specificity of the peptide inhibitors. Recent studies have reported that myristate, a saturated 14-carbon alkyl acid, would function as a promising delivery system for membrane transport<sup>181-183</sup>. Furthermore, it has been suggested that organic halogen modifications appear to be promising strategies to enhance the binding affinity and specificity of the novel peptide inhibitors, as the halogen atoms have been reported to enhance the stability of protein-ligand interaction<sup>184,185</sup>, increase the binding contacts<sup>186</sup>, and also improve the membrane permeability<sup>186</sup>. Dr. Mark Spaller's group from Dartmouth College recently reported a novel peptide targeting the PDZ domain of GAIP-interacting protein, C terminus (GIPC) bearing the last 8 residues of the C-terminal sequence of GAIP (N-myristoyl-PSQSKSKA). The peptide was modified by chemical substitution of two bromobenzoate moieties at the "-1" and "-3" positions<sup>180</sup>. The halogenated benzoyl-group has introduced

the new potential contacts between the “-1” and “-3” residues and the PDZ domain, resulting in the significantly increased inhibitory effect of this peptide compared to the non-modified peptide. Similar enhanced inhibitory effects of the halogenated modification have been observed in other peptide, such as flavopiridol<sup>187</sup>. Further studies should involve control peptides to test the specificity of the peptide inhibitor (peptide with scrambled sequences, or CXCR2 PDZ mutation peptide such as Myr-SGHTSAAA or Myr-SGHTS).

## Chapter III

### Crystallographic Analysis of NHERF1-PLC $\beta$ 3 Interaction Provides Structural Basis for CXCR2 Signaling in Pancreatic Cancer

© 2014 Elsevier

#### 3.1 Introduction:

CXC chemokine receptor 2 (CXCR2) was initially identified as the neutrophil receptor that is activated by binding to interleukin-8<sup>188</sup>. Besides the roles in mediating neutrophilic migration and positioning of oligodendrocyte precursors in developing spinal cord<sup>163,189,190</sup>, a growing body of evidence has suggested that the enhanced expression of CXCR2 correlates with aggressive stages and poor survival in pancreatic cancer patients<sup>62,191</sup>. More recent studies have also revealed that CXCR2 and its ligands (CXCL1, CXCL5, and CXCL8) are overexpressed in pancreatic ductal adenocarcinoma cell lines and enhance cell proliferation<sup>141,144,192</sup>. The evidence has made CXCR2 an attractive drug target for developing highly-specific inhibitors for pancreatic cancer.

Recent studies regarding protein-protein interactions suggested that CXCR2 interacts with other proteins, including ion channels, transporters, scaffolding proteins, and cytoskeletal elements to form macromolecular complexes at specific subcellular domains within cytoplasm<sup>163,192</sup>. These dynamic protein-protein interactions regulate CXCR2 signaling function as well as its localization and processing within cells<sup>193,194</sup>. In chapter 2, I have detected a macromolecular complex containing CXCR2, Na<sup>+</sup>/H<sup>+</sup> exchanger regulatory factor-1 (NHERF1), and phosphoinositide 3-kinase C- $\beta$ 3 (PLC- $\beta$ 3), at the plasma membrane of pancreatic cancer cells, which functionally initiated the CXCR2

signaling cascade through PLC- $\beta$ 3<sup>192</sup>. PLC- $\beta$ 3, a membrane bound enzyme, catalyzes the formation of inositol 1,4,5-trisphosphate and diacylglycerol from phosphatidylinositol 4,5-bisphosphate. NHERF1 is a PDZ domain-containing protein that typically functions as a scaffold to cluster transporters, receptors, and signaling molecules into macromolecular complexes<sup>195</sup>. In chapter 2, I have already demonstrated that the formation of the CXCR2 macromolecular complex is mediated by PDZ-binding through the PDZ domains in NHERF1 and the PDZ binding motifs from CXCR2 (-STTL-COOH) and PLC- $\beta$ 3 (-STQL-COOH). I also showed that disruption of this PDZ-mediated interaction attenuated the cellular functions (i.e. proliferation, invasion, and tumor growth) in pancreatic cancer, implicating that targeting the PDZ binding-mediated CXCR2-PLC- $\beta$ 3 interaction could provide new strategies for therapeutic interventions.

In general, PDZ domains recognize the C-terminal sequences of the target proteins (i.e. membrane receptors, ion channels, etc.) and bind to the targets via a canonically and structurally conserved PDZ peptide-binding pocket<sup>196</sup>, thereby mediating the protein-protein interactions and the formation of macromolecular complex. The specificity of the interactions is primarily determined by the amino acids at positions 0 and -2 of the C-terminal sequences of the target proteins, whereas other residues do not significantly contribute to the interaction (position 0 refers to as the extreme residue at the C-terminus)<sup>196</sup>. The characteristics of the side chains of the residues at 0 and -2 positions have led to the classification of the PDZ domains into two major classes: I, S/T)X(V/I/L) (X denoting any amino acid); class II, (F/Y)X(F/V/A)<sup>197-199</sup>. However, more recent studies have suggested that the specificity of the PDZ binding is unexpectedly

complicated, with the PDZ domain family recognizing up to 7 C-terminal residues and forming multiple PDZ binding classes<sup>200</sup>. The promiscuity of the binding between different PDZ binding motifs and distinct PDZ domains raises a challenging problem of how PDZ domains, which are structurally simple protein interaction modules, achieve the broad substrate specificity. In this chapter, crystal structure of the complex, NHERF1-PDZ1 with the PLC- $\beta$ 3 C-terminal peptide ENTQL, reveals that the PLC- $\beta$ 3 peptide binds to PDZ1 domain in an extended conformation with the last four residues making specific side chain contacts. The results that PLC- $\beta$ 3 can bind both NHERF1 PDZ1 and PDZ2 in PDAC cells (chapter 2), are consistent with the observation that the two PDZ domains, PDZ1 and PDZ2, share the peptide-binding pockets which are highly structurally conserved. The study in this chapter provides the structural basis of the PDZ interaction-mediated NHERF1-PLC $\beta$ 3 interaction, and provides the novel insights in development of novel therapeutic strategies against lethal pancreatic cancer.

## **3.2 Materials and Methods**

### **3.2.1 Protein Expression and Purification**

For X-ray crystallography, a DNA fragment encoding the human NHERF1 PDZ1 (residues 11–94) was amplified by PCR using the full-length human NHERF1 cDNA as a template. The C-terminal extension ENTQL that corresponds to residues 1230–1234 of human PLC $\beta$ 3 was created by inclusion of 15 extra bases in the reverse primer. The PCR products were cloned in the pSUMO vector containing an N-terminal His6-SUMO tag. The resulting clone was transformed into *Escherichia coli* BL21 Condon Plus (DE3) cells for protein expression. The transformants were grown to an OD<sub>600</sub> (optical density

at 600 nm) of 0.4 at 37 °C in LB medium, and then induced with 0.1 mM isopropylthio- $\beta$ -D-galactoside at 15 °C overnight. The cells were harvested by centrifugation and lysed by French Press. The soluble fraction was then subjected to Ni<sup>2+</sup> affinity chromatography purification, followed by the cleavage of the His6-SUMO tag with yeast SUMO Protease 1. PDZ1 proteins were separated from the cleaved tag by a second Ni<sup>2+</sup> affinity chromatography and further purified by size-exclusion chromatography. Finally, the proteins were concentrated to 30–40 mg/ml in a buffer containing 20 mM Tris-HCl (pH 8.0), 150 mM NaCl, 1 mM  $\beta$ -mercaptoethanol, and 5% glycerol. For pull-down experiments, glutathione S-transferase (GST) fusion proteins were generated by cloning NHERF1 PDZ1, PDZ2, or PDZ1-PDZ2 into the pGEX4T-1 vector<sup>163</sup>. His-S-tagged proteins were generated by cloning PLC $\beta$ 3 C-terminal fragment (residues 1135–1234) into the pET30 vector<sup>192</sup>. GST-PDZ proteins were purified using glutathione agarose beads (BD Biosciences) and eluted with 50 mM glutathione. His-S-PLC $\beta$ 3 was purified using Cobalt resins (Thermo Scientific) and eluted with 200 mM imidazole.

### 3.2.2 Crystallization, Data Collection and Structure Determination

Crystals were grown by the hanging-drop vapor-diffusion method by mixing the protein (~25 mg/ml) with an equal volume of a reservoir solution containing 100 mM sodium acetate, pH 4.6, 2.5 M sodium chloride at 20 °C. Crystals typically appeared overnight and continued to grow to their full size in 3–4 days. Prior to X-ray diffraction data collection, crystals were cryoprotected in a solution containing the mother liquor and 25% glycerol and flash cooled in liquid nitrogen. The data were collected at 100 K at beamline 21-ID-F at the Advanced Photon Source (Argonne, IL) and processed and scaled using the program XDS<sup>201</sup>. Crystals belong to the space group  $P3_121$  with unit



**Table 3-1.** Crystallographic data and refinement statistics

|                            |                            |
|----------------------------|----------------------------|
| <b>Data</b>                |                            |
| Space group                | $P2_1$                     |
| Cell parameters (Å)        |                            |
| a                          | 26.4                       |
| b                          | 40.3                       |
| c                          | 37.1                       |
| Wavelength (Å)             | 1.2719                     |
| Resolution (Å)             | 24.2-1.34 (1.37-           |
| $R_{merge}^a$              | 0.039 (0.250) <sup>b</sup> |
| Redundancy                 | 4.1 (4.0)                  |
| Unique reflections         | 17966                      |
| Completeness (%)           | 99.8 (99.6)                |
| $\langle I/\sigma \rangle$ | 15.3 (3.0)                 |
| <b>Refinement</b>          |                            |
| Resolution (Å)             | 24.2-1.34 (1.37-           |
| Molecules/AU               | 1                          |
| $R_{work}^c$               | 0.145 (0.268)              |
| $R_{free}^d$               | 0.177 (0.275)              |
| Ramachandran plot          |                            |
| Residues in favored        | 97.9%                      |
| Residues in allowed        | 2.1%                       |
| RMSD                       |                            |
| Bond lengths (Å)           | 0.007                      |
| Bond angles (°)            | 1.2                        |
| No. of atoms               |                            |
| Protein                    | 1347                       |
| Peptide                    | 73                         |
| Water                      | 143                        |
| Chloride                   | 2                          |
| B-factor (Å <sup>2</sup> ) |                            |
| Protein                    | 17.2                       |
| Peptide                    | 17.7                       |
| Water                      | 28.5                       |
| Chloride                   | 20.2                       |
| SCN                        | 12.4                       |

<sup>a</sup> $R_{merge} = \sum |I - \langle I \rangle| / \sum I$ , where  $I$  is the observed intensity and  $\langle I \rangle$  is the averaged intensity of multiple observations of symmetry-related reflections.

<sup>b</sup>Numbers in parentheses refer to the highest resolution shell.

<sup>c</sup> $R_{work} = \sum |F_o - F_c| / \sum |F_o|$ , where  $F_o$  is the observed structure factor,  $F_c$  is the calculated structure factor.

<sup>d</sup> $R_{free}$  was calculated using a subset (5%) of the reflection not used in the refinement.

cell dimensions  $a = b = 50.7 \text{ \AA}$ ,  $c = 66.7 \text{ \AA}$ , and one molecule in the asymmetric unit (Table 1). The structure was solved by the molecular replacement method with the program PHASER<sup>202</sup> using the PDZ1-CXCR2 structure (PDB code: 4JL7) as a search model. Structure modeling was carried out in COOT<sup>203</sup>, and refinement was performed with PHENIX<sup>204</sup>. To reduce the effects of model bias, iterative-build OMIT maps were used during model building and structure refinement. The final models were analyzed and validated with Molprobit<sup>205</sup>. All figures of 3D representations of the PDZ1-PLC $\beta$ 3 structure were made with PyMOL ([www.pymol.org](http://www.pymol.org)).

### 3.2.3 Protein Data Bank Accession Number

Coordinates and structure factors have been deposited in the Protein Data Bank with accession number 4PQW.

## 3.3 Results

### Binding specificity of NHERF1-PLC- $\beta$ 3 Interaction

The overall structure of NHERF1-PDZ1 is similar to other PDZ domains<sup>199,206</sup>, consisting of six  $\beta$  strands ( $\beta$ 1– $\beta$ 6) and two  $\alpha$ -helices ( $\alpha$ A and  $\alpha$ B) (Fig. 3-1 A and Fig. 3-1 B). The PLC- $\beta$ 3 peptide binds in the cleft between  $\beta$ 2 strand and  $\alpha$ B helix, burying a total solvent-accessible surface area of  $600 \text{ \AA}^2$ . The binding specificity of the PDZ1-PLC- $\beta$ 3 interaction is achieved through networks of hydrogen bonds and hydrophobic interactions (Fig. 3-1 C). At the ligand position 0, the side chain of Leu0 is nestled in a deep hydrophobic pocket formed by invariant residues Tyr24, Phe26, and Leu28 from  $\beta$ 2 and Val76 and Ile79 from  $\alpha$ B (Fig. 3-1 D). In the binding pocket, the position of Leu0

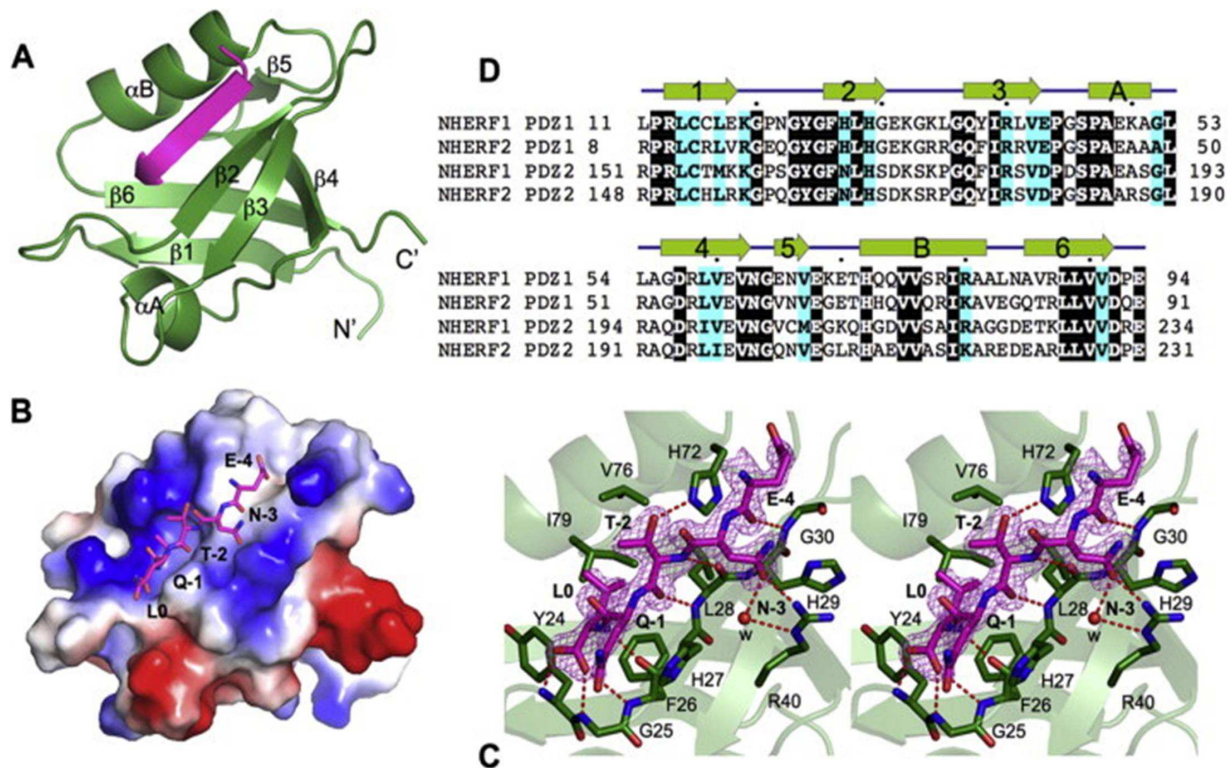


**Fig. 3-1. Structure of NHERF1 PDZ1 in complex with the PLC $\beta$ 3 C-terminal sequence ENTQL.** A) Ribbon diagram of the PDZ1–PLC $\beta$ 3 structure. PDZ1 is shown in green and the PLC $\beta$ 3 peptide is shown in magenta. Secondary structures of PDZ1,  $\alpha$ -helices, and  $\beta$ -strands are labeled and numbered according to their position in the sequence. (B) Surface representation of the PDZ1–PLC $\beta$ 3 structure. Surface coloring is according to the electrostatic potential: red, white, and blue correspond to negative, neutral, and positive potential, respectively. The vacuum electrostatics/protein contact potential was generated by PyMOL. The PLC $\beta$ 3 peptide is depicted by sticks. (C) Stereo view of the PDZ1 ligand-binding site bound to the PLC $\beta$ 3 C-terminal peptide. PDZ1 residues are represented by sticks with their carbon atoms colored in green. The PLC $\beta$ 3 peptide is depicted by sticks overlaid with  $2F_o - F_c$  omit map calculated at 1.47 Å and contoured at  $1.8\sigma$ . Hydrogen bonds are illustrated as red broken lines. (D) Sequence alignment of selected PDZ domains. The alignment was performed by ClustalW [30], including human NHERF1 and NHERF2. Identical residues are shown as white on black, and similar residues appear shaded in cyan. Secondary structure elements are displayed above the sequences and labeled according to the scheme in A. Sequence numbering is displayed to the left of the sequences, with every 10th residue marked by a dot shown above the alignment. (For interpretation of the references to color in this figure legend, the reader is referred to the web version of this article.). Jiang, Y., Wang, S. et al. Crystallographic Analysis of NHERF1-PLC $\beta$ 3 Interaction Provides Structural Basis for CXCR2 Signaling in Pancreatic Cancer. *Biochemical and biophysical research communications*, doi:10.1016/j.bbrc.2014.03.028 (2014). © 2014 Elsevier.

is further secured by both a hydrogen bond from its amide nitrogen to the Phe26 carbonyl oxygen and triplet hydrogen bonding between the Leu0 carboxylate and the amides of Tyr24, Gly25, and Phe26. Similar interactions have been observed in several other PDZ-mediated complexes<sup>199,206</sup>, which represent the most-conserved binding mode for terminal Leu recognition.

Residues at other positions also contribute to the PDZ1-PLC- $\beta$ 3 complex formation (Fig. 3-1 C). At the position -1, the aliphatic portion of the Gln-1 side chain makes Van der Waals interaction with the imidazole ring of His27. At position -2, Thr-2 makes one hydrogen bond to the His72 imidazole group and two hydrogen bonds to the highly conserved residue Leu28. At the position -3, the interactions with Asn-3 include a direct hydrogen bond from its side chain oxygen to the N $\eta$ 1 atom of Arg40 and a water-mediated hydrogen bond to the N $\epsilon$  atom of Arg40. The latter two interactions represent ligand specific interactions, as the small side chain of Ser-3 is recognized by His29 in PDZ1-CXCR2 complex<sup>129,207</sup>. Finally, the peptide residue Glu-4 engages in a main chain contact with Gly30, but does not participate in any specific side chain interactions. These observations indicate that the last four residues of PLC- $\beta$ 3 contribute to the binding specificity in the PDZ1-PLC- $\beta$ 3 complex formation.

To understand the structural basis of the bivalent binding, we performed a structural alignment between the structure of NHERF1 PDZ1 and the structure of NHERF1 PDZ2. The alignment reveals that NHERF1 PDZ1 and PDZ2 share highly similar overall structures and highly conserved ligand-binding pockets (Fig. 3-2). The root mean

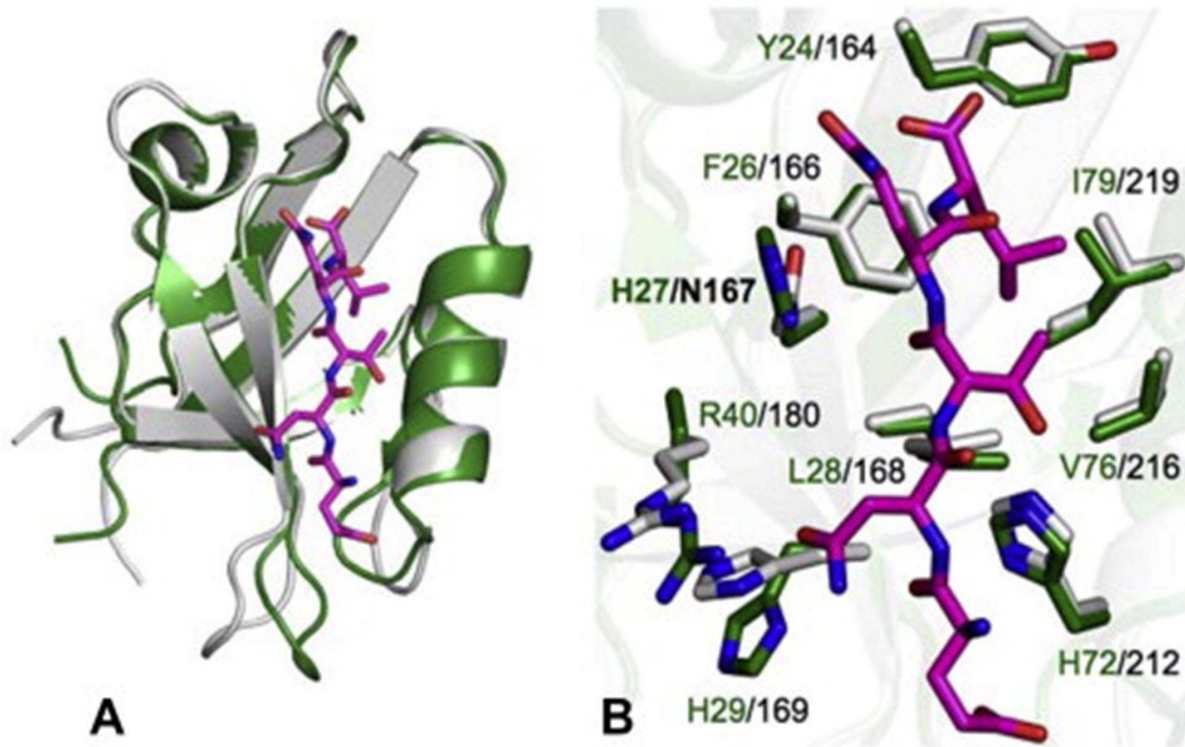


**Fig. 3-2. Structural comparison of NHERF1 PDZ1 and PDZ2.** (A) Superposition of the structures of PDZ1–PLCβ3 (green; PDB code: [4PQW](#)) and PDZ2 (gray; PDB code: [2OZF](#)). PDZ domains are represented by ribbons. Residues in PLCβ3 are displayed as sticks with the carbon atoms shown in magenta. (B) Superposition of the PDZ ligand binding pockets. Both PDZ and ligand residues are depicted by sticks and colored according to the scheme in A. *Jiang, Y., Wang, S. et al. Crystallographic Analysis of NHERF1-PLCβ3 Interaction Provides Structural Basis for CXCR2 Signaling in Pancreatic Cancer. Biochemical and biophysical research communications, doi:10.1016/j.bbrc.2014.03.028 (2014). © 2014 Elsevier.*

square (rms) difference is 0.63 Å for the overall structure (92 C $\alpha$  atoms), and for the ligand-interacting residues, 0.27 Å. The only distinct difference in the ligand-binding sites is residue 27, which is His in PDZ1 and Asn (residue 164) in PDZ2. It is noteworthy that this conserved substitution maintains the amino functionality of the side chain, which is not expected to disrupt the observed Van der Waals contact between PDZ1 and PLC- $\beta$ 3 (Fig. 3-1 C). Therefore, the comparison of PDZ1 and PDZ2 provides a structural explanation for the ability of PLC- $\beta$ 3 to bind to both PDZ domains.

### 3.4 Discussion

Our previous study has suggested that targeting the PDZ-mediated CXCR2 macromolecular complex have a therapeutic potential in PDAC treatment, as disruption of this interaction has been found to inhibit cellular functions both *in vitro* and tumor growth *in vivo*<sup>192</sup>. These findings highlight the significance of our present structure studies and also indicate that the structural details of the NHERF1-PLC- $\beta$ 3 interaction could open the new avenues in developing novel methods and strategies for selective drug design (i.e. design new NHERF1 inhibitors that could block the NHERF1-PLC- $\beta$ 3 interaction with high specificity). Such inhibitors have the potential to inhibit pancreatic tumor growth by suppressing CXCR2 signaling and preventing tumor cell proliferation and invasion. In addition, the fact that PLC- $\beta$ 3 binds to both PDZ domains of NHERF1 (Fig. 2-6), together with structural similarity of PDZ1 domain and PDZ2 domain (Fig. 3-2), suggests NHERF1 inhibitors may be capable of targeting PDZ1 and PDZ2 simultaneously. Such inhibitors might be advantageous in cancer treatment, as PDZ1 and PDZ2 have been shown to have differential roles during metastasis. NHERF1

PDZ2 promotes visceral metastasis via invadopodia-dependent invasion and anchorage-independent growth, as well as by inhibition of apoptosis, while PDZ1 promotes bone metastasis by stimulating podosome nucleation, motility, angiogenesis, and osteoclastogenesis in the absence of increased growth or invasion<sup>208</sup>. It is conceivable that simultaneous targeting of the PDZ domains could lead to a combinatorially synergetic effect that would prevent cellular functions in pancreatic cancer. The biological impact of the bivalent NHERF1-PLC- $\beta$ 3 interaction remains mysterious, which directs future studies toward the evaluation of its effect on CXCR2-mediated cellular functions in pancreatic cancer. Especially, it is worthy determining whether different PDZ domains could mediate the assembly of distinct CXCR2 signal transduction complexes.

## Chapter IV

### Conclusion and Future Directions

#### 4.1 Conclusion

Pancreatic cancer is a disease with poor prognosis, high level of mortality, significant high death rates, and accounting for 6 ~ 7% of all cancer-related deaths for both men and women in the United States. Thus, a more comprehensive understanding of the biology of PDAC and the mechanisms/factors that promote invasion and tumor growth may help identify new molecular targets for the development of diagnostics and/or therapeutics of pancreatic cancer.

My dissertation research study has identified a CXCR2 macromolecular complex (CXCR2•NHERF1•PLC- $\beta$ 3) in human pancreatic cancer cells, the scaffolding protein NHERF1 clusters CXCR2 and PLC- $\beta$ 3 in close proximity via a specific PDZ domain-based interaction, thereby forming spatially compact signaling complexes beneath the plasma membrane. Consequently, the CXCR2 macromolecular complex enables CXCR2 to transduce its signal to PLC- $\beta$ 3 with efficiency and specificity. Using various cellular functional assays and an *in vivo* model, we also demonstrated this CXCR2 macromolecular complex is critical for the malignant cellular functions of pancreatic cancer including cell proliferation, cell invasion, tumor-induced angiogenesis, and tumor growth *in vitro* and *in vivo*. We further tested a peptide inhibitor specifically designed based on CXCR2 PDZ-mediated protein-protein interaction, and showed that this



peptide inhibitor significantly inhibited the malignant cellular functions of pancreatic cancer cells, suggesting that it could be a promising strategy for further drug design.

Our findings of the functional significance and therapeutic potential of the interaction between CXCR2 and NHERF1 in pancreatic cancer may be valuable in the development of innovative strategies for targeted drug discovery. Systemic blockade of CXCR2 is the primary approach being used currently. However, the important roles of CXCR2 in regulation of normal physiology (including early tumor surveillance and immune system physiology) warrants the necessity to identify novel CXCR2 inhibitors, which can be more tissue-specific and/or disease-specific<sup>112</sup>. The results of this dissertation project have proved that the PDZ-mediated interaction between CXCR2 and NHERF1 is important in pancreatic cancer, and targeting this interaction could represent novel approach to tackle this lethal disease. Also, our subsequent structural analysis have revealed the structural specificity between NHERF1 and CXCR2/PLC- $\beta$ 3, and provided insights that would be valuable for designing CXCR2 inhibitors that are specific to the CXCR2-NHERF1 interaction without cross-inhibiting any of the other NHERF1-coordinated signaling events, considering the complexity of the NHERF1 interaction network and its versatile roles in regulation of many cellular processes essential to normal physiology<sup>130,131</sup>.

## **4.2 Future Directions**

### **4.2.1 Investigation of the effect of the CXCR2 macromolecular complex in CXCR2 signaling**

CXCR2 couples to the pertussis toxin-sensitive  $G_i$  proteins to stimulate phosphatidylinositide-specific phospholipase C (PLC) activities<sup>209</sup>. PLC molecules can be divided into six families of isozymes:  $\beta$ ,  $\gamma$ ,  $\delta$ ,  $\epsilon$ ,  $\eta$ , and  $\zeta$ <sup>210</sup>. The  $\beta$  family consists of four isoforms, PLC- $\beta$ 1 to PLC- $\beta$ 4. PLC- $\beta$ 2 has been detected primarily in hematopoietic cells, whereas PLC- $\beta$ 1 and PLC- $\beta$ 3 are found in a wide range of cells and tissue<sup>174</sup>. PLC- $\beta$ 4 is predominantly expressed in certain neuronal cells<sup>211,212</sup>. Activation of PLC- $\beta$  results in hydrolysis of the lipid phosphatidylinositol 4, 5-bisphosphate, generating diacylglycerol (DAG), which activates PKC isoforms, and inositol 1,3,4-triphosphate (IP3), which releases calcium from intracellular stores. Stimulation of PDAC cells with CXCR2 ligands (such as CXCL1, CXCL5, and CXCL8) results in increases in cytosolic calcium due to a combination of intracellular calcium release mediated by inositol 1,3,4-triphosphate (IP3) and an influx of extracellular calcium. Furthermore, we have already demonstrated that PLC- $\beta$ 3 and CXCR2 is nucleated by NHERF1 into a macromolecular complex (see section 2.3.7). The specific interactions of different PLC- $\beta$ 3 with NHERF1 may be responsible for the specific intracellular cell signaling (e.g. intracellular calcium mobilization) induced by CXCR2 biological axis. Our previous study also demonstrated that CXCR2 peptide (WT) disrupted the CXCR2 macromolecular complex and inhibited intracellular  $Ca^{2+}$  increase in neutrophils<sup>124</sup>. Therefore, this peptide may also have similar inhibitory effect on the CXCR2 ligands elicited calcium signals in pancreatic cancer cells. In order to test the effect of the CXCR2 peptide (WT) on CXCL5/8 induced intracellular calcium mobilization, I will deliver this peptide into pancreatic cancer cells, and then measure the intracellular calcium mobilization induced by CXCL5/8 as described above<sup>124</sup>. My prediction is that the CXCR2 peptide (WT), when delivered into

PDAC cells, will disrupt the macromolecular complex (CXCR2•NHERF1•PLC-β3) by competing with the endogenous CXCR2 for binding to NHERF1; and PDAC cells delivered with this peptide will show markedly reduced calcium signals compared to the control. The CXCR2 peptide ( $\Delta$ TTL) will be used in parallel to demonstrate whether the PDZ motif of CXCR2 is critical for the CXCL5/8-induced calcium mobilization.

Also, to confirm the specificity of the CXCR2 peptide in the CXCL5/8-induced calcium signal, other peptides (e.g. C-terminal peptides of CFTR, or LPAR2 receptor synthesized by Genemed Synthesis. *Please note:* all of these peptides contain the PDZ motif consensus at their C-termini<sup>154</sup>) will also be delivered into PDAC cells in parallel as controls, followed by measurement of the intracellular calcium mobilization induced by CXCL5/8. In addition, the effect of CXCR2 peptide will also be assessed in the other ligands-induced calcium mobilization in PDAC cells, such as bradykinin (BK), cholecystokinin (CCK)<sup>165</sup>. My prediction is that the CXCR2 peptide (both WT and  $\Delta$ TTL) will not affect the intracellular calcium signals induced by BK or CCK, but will only inhibit the CXCL5/8 induced calcium signals.

#### **4.2.2 Further Characterization of Interactions between NHERF1 and CXCR2 by Fluorescence Recovery After Photobleaching (FRAP)**

Fluorescence Recovery After Photobleaching (FRAP) is an optical technique for measuring membrane transport or two dimensional lateral diffusion of fluorescent molecules on the cell membrane<sup>213-215</sup>. The FRAP technique was initially developed back in the 70's, and was primarily used to investigate the lateral diffusion of the membrane proteins in single cells<sup>216-218</sup>. Recently, with the rapid development of the

fluorescent-fused protein technology, FRAP technique has been increasingly used in investigating the protein-protein interactions and macromolecular dynamics in the living cells. Qualitative assessment of the recovery rate (slower or faster) has been used to characterize specific perturbations of the protein-protein interaction<sup>219</sup>.

Briefly, all the fluorescent probes or fluorescent-fused proteins could emit light of one wave length (e.g. green) after the light of another wavelength (e.g. blue) was absorbed. However, the fluorescent probes or fluorescent proteins will be photo-bleached if a high density light is delivered. The bilayer membrane or a particular membrane protein is uniformly labeled with a fluorescent tag, or the membrane protein is fused with a fluorescent protein, such as green fluorescent protein (GFP) or yellow fluorescent protein (YFP). The fluorescence is initially evenly distributed on the cell membrane. A particular area on the cell membrane is selectively photo-bleached by a small fast light pulse. After the photo-bleach, due to the diffusion or active movements of the molecules on the cell membrane, the fluorescence intensity in the photo-bleached area will increase as the unbleached molecules continuously diffuse into this area, until the fluorescence intensity become stabilized over time. By monitoring the recovery of the fluorescence intensity after the photo-bleach, the lateral diffusion of the membrane proteins could be characterized.

I will make constructs of CXCR2-FL (WT,  $\Delta$ TTL, and AAA) with YFP tagged at N-terminus, and co-transfect PDAC cells with pEYFP-CXCR2 (WT,  $\Delta$ TTL, or AAA) and pcDNA3-NHERF1, and perform the FRAP assay to monitor CXCR2 motility. I anticipate

that PDAC cells co-overexpressing YFP-CXCR2 (WT) and NHERF1 will show the greatest  $T_{1/2}$  (lowest motility), because forming the spatially compact macromolecular complex will retard the motility (lateral diffusion) of CXCR2. Also, I will deliver CXCR2 peptides (WT or  $\Delta$ TTL) into PDAC cells co-overexpressing EYFP-CXCR2 (WT) and NHERF1, and perform the FRAP experiments. I anticipate that CXCR2 peptide (WT) will enhance the recovery, whereas CXCR2 peptide ( $\Delta$ TTL) will not.

Besides, I will transfect PDAC cells with pEYFP-CXCR2 (WT), and transduced with  $\alpha$ -NHERF1 lenti-shRNAs or control. Gene sequence-specific shRNA clones anti-NHERF1 and anti-NHERF2 (containing CTCGAG as the loop sequence)<sup>220</sup> have been constructed within the lentivirus plasmid vector pLKO.1-puromycin (obtained from Dr. Fei Sun at Physiology dept, and Dr. Fei Sun has the expertise with Lentivirus construction). The knockdown effect of anti-NHERF1 shRNA constructs have been confirmed by transient transfection into a pancreatic cancer cell L3.6pl (data not shown). All cells will be subjected to the FRAP experiments. My prediction is that the cells with NHERF1 knockdown will show the greatest recovery after photo-bleach, because the binding between NHERF1 and CXCR2 could stabilize CXCR2 in the membrane.

I have also planned an alternative approach due to the possibility that I might not detect the anticipated difference in my proposed FRAP assays, because FRAP only measures the average of the fluorescence recovery (lateral diffusion) in the photo-bleached region, not the individual behavior of the single receptor molecule (such as CXCR2). Therefore, I will also use single molecule imaging via Total Internal Reflection Fluorescence

Microscope (TIRFM) to study the molecular dynamics of individual CXCR2 in the plasma membrane. Briefly, PDAC cells will be transduced by Lenti-virus encoding 3HA-CXCR2-FL. PDAC cells stably expressing 3HA-CXCR2 will be overexpressed with NHERF1, and grown on 35-mm glass-bottom dishes. Then, the cells will be incubated with biotin  $\alpha$ -HA antibody (Sigma-Aldrich, St. Louis, MO), followed by a 2<sup>nd</sup> incubation with streptavidin-conjugated Qdot-655, which specifically binds to biotin, before mounted on an inverted fluorescence microscope. The images will be captured at 1 ~ 3 frames per second for 1 ~ 3min with 50-ms exposure time, 100x oil-immersion objective (NA 1.40). Data will be analyzed by SlideBook 4.2 software, which generates the diffusion coefficient (D) and mean squared displacement (MSD). To monitor the changes in lateral diffusion of CXCR2 with complex disruption, cells will be pre-delivered with CXCR2 peptide (WT or  $\Delta$ TTL).

## APPENDIX: CORRESPONDANCE

### Re: Copyright Permission Request on Translational Oncology

|                |   |
|----------------|---|
| <b>Subject</b> | <b>Re: Copyright Permission Request on Translational Oncology</b> |
| <b>From</b>    | TransOnc <transonc@transonc.com>                                  |
| <b>To</b>      | Wang, Shuo <shuwang@med.wayne.edu>                                |
| <b>Sent</b>    | Monday, March 17, 2014 8:27 AM                                    |

Dear Shuo,

Translational Oncology is happy to give permission for the use of figures and text, from your recent publication in the journal in your thesis submission.

Editorial Office

On Sat, Mar 15, 2014 at 11:19 AM, Wang, Shuo <[shuwang@med.wayne.edu](mailto:shuwang@med.wayne.edu)> wrote:

Dear Dr. Lawrence,

My name is Shuo Wang. I am a Ph.D. student at Wayne State University. I am writing for your permission to include the results of my recently-published paper in Translational Oncology in my dissertation (***Transl Oncol. 6(2):216-25 (2013)***, <http://www.transonc.com/pdf/manuscript/v06i02/neo13133.pdf>)

The dissertation will be made available to the public through the graduate school of Wayne State University, and will be available on ProQuest (formerly UMI). Please let me know if further information needed.

I really appreciate your time and help on this matter.

Thank you,

Shuo Wang  
 Ph.D. Candidate  
 Biochemistry & Molecular Biology  
 Wayne State University School of Medicine

© **Elsevier**: Authors can use either their accepted author manuscript or final published article for inclusion in a thesis or dissertation.

<http://www.elsevier.com/journal-authors/author-rights-and-responsibilities>

© **American Society for Biochemistry and Molecular Biology**: Authors need NOT contact the journal to obtain rights to reuse their own material. They are automatically granted permission to Use an article in a thesis and/or dissertation.

[http://www.jbc.org/site/misc/Copyright\\_Permission.xhtml](http://www.jbc.org/site/misc/Copyright_Permission.xhtml)

© **Plos One**: Open Access.



## REFERENCES

- 1 Gerard, C. & Rollins, B. J. Chemokines and disease. *Nature immunology* **2**, 108-115, doi:Doi 10.1038/84209 (2001).
- 2 Moser, B. & Willmann, K. Chemokines: role in inflammation and immune surveillance. *Annals of the rheumatic diseases* **63 Suppl 2**, ii84-ii89, doi:10.1136/ard.2004.028316 (2004).
- 3 Baggiolini, M. Chemokines in pathology and medicine. *J Intern Med* **250**, 91-104, doi:DOI 10.1046/j.1365-2796.2001.00867.x (2001).
- 4 Proudfoot, A. E. I. Chemokine receptors: Multifaceted therapeutic targets. *Nat Rev Immunol* **2**, 106-115, doi:Doi 10.1038/Nri722 (2002).
- 5 Murphy, P. M. & Tiffany, H. L. Cloning of Complementary-DNA Encoding a Functional Human Interleukin-8 Receptor. *Science* **253**, 1280-1283, doi:DOI 10.1126/science.1891716 (1991).
- 6 Allen, S. J., Crown, S. E. & Handel, T. M. Chemokine: Receptor structure, interactions, and antagonism. *Annu Rev Immunol* **25**, 787-820, doi:DOI 10.1146/annurev.immunol.24.021605.090529 (2007).
- 7 Nasser, M. W. *et al.* CXCR1 and CXCR2 activation and regulation - Role of aspartate 199 of the second extracellular loop of CXCR2 in CXCL8-mediated rapid receptor internalization. *Journal of Biological Chemistry* **282**, 6906-6915, doi:DOI 10.1074/jbc.M610289200 (2007).
- 8 Sai, J. Q., Walker, G., Wikswo, J. & Richmond, A. The IL sequence in the LLKIL motif in CXCR2 is required for full ligand-induced activation of Erk, Akt, and chemotaxis in HL60 cells. *Journal of Biological Chemistry* **281**, 35931-35941, doi:DOI 10.1074/jbc.M605883200 (2006).

- 9 Olson, T. S. & Ley, K. Chemokines and chemokine receptors in leukocyte trafficking. *American journal of physiology. Regulatory, integrative and comparative physiology* **283**, R7-28, doi:10.1152/ajpregu.00738.2001 (2002).
- 10 Murdoch, C. & Finn, A. Chemokine receptors and their role in inflammation and infectious diseases. *Blood* **95**, 3032-3043 (2000).
- 11 Charo, I. F. & Ransohoff, R. M. Mechanisms of disease - The many roles of chemokines and chemokine receptors in inflammation. *New Engl J Med* **354**, 610-621, doi:Doi 10.1056/Nejmra052723 (2006).
- 12 Monteclaro, F. S. & Charo, I. F. The amino-terminal extracellular domain of the MCP-1 receptor, but not the RANTES/MIP-1 alpha receptor, confers chemokine selectivity - Evidence for a two-step mechanism for MCP-1 receptor activation. *Journal of Biological Chemistry* **271**, 19084-19092 (1996).
- 13 Crump, M. P. *et al.* Solution structure and basis for functional activity of stromal cell-derived factor-1; dissociation of CXCR4 activation from binding and inhibition of HIV-1. *Embo J* **16**, 6996-7007, doi:DOI 10.1093/emboj/16.23.6996 (1997).
- 14 Rajagopalan, L. & Rajarathnam, K. Ligand selectivity and affinity of chemokine receptor CXCR1. Role of N-terminal domain. *The Journal of biological chemistry* **279**, 30000-30008, doi:10.1074/jbc.M313883200 (2004).
- 15 Kraemer, S. *et al.* MIF-chemokine receptor interactions in atherogenesis are dependent on an N-loop-based 2-site binding mechanism. *FASEB journal : official publication of the Federation of American Societies for Experimental Biology* **25**, 894-906, doi:10.1096/fj.10-168559 (2011).
- 16 Waugh, D. J. J. & Wilson, C. The Interleukin-8 Pathway in Cancer. *Clinical Cancer Research* **14**, 6735-6741, doi:Doi 10.1158/1078-0432.Ccr-07-4843 (2008).
- 17 Baggiolini, M. Chemokines and leukocyte traffic. *Nature* **392**, 565-568, doi:10.1038/33340 (1998).

- 18 Mei, J. J. *et al.* Cxcr2 and Cxcl5 regulate the IL-17/G-CSF axis and neutrophil homeostasis in mice. *J Clin Invest* **122**, 974-986, doi:Doi 10.1172/Jci60588 (2012).
- 19 Eash, K. J., Greenbaum, A. M., Gopalan, P. K. & Link, D. C. CXCR2 and CXCR4 antagonistically regulate neutrophil trafficking from murine bone marrow. *J Clin Invest* **120**, 2423-2431, doi:Doi 10.1172/Jci41649 (2010).
- 20 von Vietinghoff, S., Asagiri, M., Azar, D., Hoffmann, A. & Ley, K. Defective Regulation of CXCR2 Facilitates Neutrophil Release from Bone Marrow Causing Spontaneous Inflammation in Severely NF-kappa B-Deficient Mice. *J Immunol* **185**, 670-678, doi:DOI 10.4049/jimmunol.1000339 (2010).
- 21 Hosking, M. P., Tirotta, E., Ransohoff, R. M. & Lane, T. E. CXCR2 signaling protects oligodendrocytes and restricts demyelination in a mouse model of viral-induced demyelination. *PLoS One* **5**, e11340, doi:10.1371/journal.pone.0011340 (2010).
- 22 Zaja-Milatovic, S. & Richmond, A. CXC chemokines and their receptors: a case for a significant biological role in cutaneous wound healing. *Histology and histopathology* **23**, 1399-1407 (2008).
- 23 Di Stefano, A. *et al.* Association of increased CCL5 and CXCL7 chemokine expression with neutrophil activation in severe stable COPD. *Thorax* **64**, 968-975, doi:10.1136/thx.2009.113647 (2009).
- 24 Qiu, Y. S. *et al.* Biopsy neutrophilia, neutrophil chemokine and receptor gene expression in severe exacerbations of chronic obstructive pulmonary disease. *Am J Resp Crit Care* **168**, 968-975, doi:DOI 10.1164/rccm.200208-794OC (2003).
- 25 Traves, S. L., Culpitt, S. V., Russell, R. E., Barnes, P. J. & Donnelly, L. E. Increased levels of the chemokines GROalpha and MCP-1 in sputum samples from patients with COPD. *Thorax* **57**, 590-595 (2002).

- 26 de Boer, W. I. *et al.* Monocyte chemoattractant protein 1, interleukin 8, and chronic airways inflammation in COPD. *J Pathol* **190**, 619-626, doi:Doi 10.1002/(Sici)1096-9896(200004)190:5<619::Aid-Path555>3.0.Co;2-6 (2000).
- 27 Weathington, N. M. *et al.* A novel peptide CXCR ligand derived from extracellular matrix degradation during airway inflammation. *Nature medicine* **12**, 317-323, doi:10.1038/nm1361 (2006).
- 28 Keane, M. P. *et al.* Imbalance in the expression of CXC chemokines correlates with bronchoalveolar lavage fluid angiogenic activity and procollagen levels in acute respiratory distress syndrome. *J Immunol* **169**, 6515-6521 (2002).
- 29 Miller, E. J. *et al.* Elevated Levels of Nap-1/Interleukin-8 Are Present in the Airspaces of Patients with the Adult Respiratory-Distress Syndrome and Are Associated with Increased Mortality. *Am Rev Respir Dis* **146**, 427-432 (1992).
- 30 Kurdowska, A. *et al.* Anti-interleukin-8 autoantibodies in patients at risk for acute respiratory distress syndrome. *Crit Care Med* **30**, 2335-2337, doi:Doi 10.1097/01.Ccm.0000030442.30078.C7 (2002).
- 31 Kurdowska, A. *et al.* Anti-interleukin 8 autoantibody : interleukin 8 complexes in the acute respiratory distress syndrome - Relationship between the complexes and clinical disease activity. *Am J Resp Crit Care* **163**, 463-468 (2001).
- 32 Dean, T. P., Dai, Y., Shute, J. K., Church, M. K. & Warner, J. O. Interleukin-8 Concentrations Are Elevated in Bronchoalveolar Lavage, Sputum, and Sera of Children with Cystic-Fibrosis. *Pediatr Res* **34**, 159-161 (1993).
- 33 Puleston, J. *et al.* A distinct subset of chemokines dominates the mucosal chemokine response in inflammatory bowel disease. *Alimentary pharmacology & therapeutics* **21**, 109-120, doi:10.1111/j.1365-2036.2004.02262.x (2005).

- 34 Willson, T. A. *et al.* STAT3 Genotypic Variation and Cellular STAT3 Activation and Colon Leukocyte Recruitment in Pediatric Crohn Disease. *J Pediatr Gastr Nutr* **55**, 32-43, doi:Doi 10.1097/Mpg.0b013e318246be78 (2012).
- 35 MohanKumar, K. *et al.* Gut mucosal injury in neonates is marked by macrophage infiltration in contrast to pleomorphic infiltrates in adult: evidence from an animal model. *Am J Physiol-Gastr L* **303**, G93-G102, doi:DOI 10.1152/ajpgi.00016.2012 (2012).
- 36 Izzo, R. S. *et al.* Interleukin-8 and Neutrophil Markers in Colonic Mucosa from Patients with Ulcerative-Colitis. *Am J Gastroenterol* **87**, 1447-1452 (1992).
- 37 Daig, R. *et al.* Increased interleukin 8 expression in the colon mucosa of patients with inflammatory bowel disease. *Gut* **38**, 216-222 (1996).
- 38 Keshavarzian, A. *et al.* Increased interleukin-8 (IL-8) in rectal dialysate from patients with ulcerative colitis: Evidence for a biological role for IL-8 in inflammation of the colon. *Am J Gastroenterol* **94**, 704-712, doi:DOI 10.1111/j.1572-0241.1999.00940.x (1999).
- 39 King, R. C. *et al.* Reperfusion injury significantly impacts clinical outcome after pulmonary transplantation. *Ann Thorac Surg* **69**, 1681-1685, doi:Doi 10.1016/S0003-4975(00)01425-9 (2000).
- 40 Turunen, A. J. *et al.* Association of graft neutrophil sequestration with delayed graft function in clinical renal transplantation. *Transplantation* **77**, 1821-1826, doi:DOI 10.1097/01.tp.0000122231.43653.cc (2004).
- 41 Palatianos, G. M. *et al.* Neutrophil depletion reduces myocardial reperfusion morbidity. *Ann Thorac Surg* **77**, 956-961, doi:DOI 10.1016/j.athoracsur.2003.10.004 (2004).
- 42 Belperio, J. A. *et al.* CXCR2/CXCR2 ligand biology during lung transplant ischemia-reperfusion injury. *J Immunol* **175**, 6931-6939 (2005).
- 43 De Perrot, M. *et al.* Interleukin-8 release during early reperfusion predicts graft function in human lung transplantation. *Am J Respir Crit Care Med* **165**, 211-215 (2002).

- 44 Fisher, A. J. *et al.* Elevated levels of interleukin-8 in donor lungs is associated with early graft failure after lung transplantation. *Am J Respir Crit Care Med* **163**, 259-265, doi:10.1164/ajrccm.163.1.2005093 (2001).
- 45 Kalfin, R. E. *et al.* Induction of Interleukin-8 Expression during Cardiopulmonary Bypass. *Circulation* **88**, 401-406 (1993).
- 46 Reutershan, J. *et al.* Critical role of endothelial CXCR2 in LPS-induced neutrophil migration into the lung. *J Clin Invest* **116**, 695-702, doi:Doi 10.1172/Jci27009 (2006).
- 47 Johnston, R. A., Mizgerd, J. P. & Shore, S. A. CXCR2 is essential for maximal neutrophil recruitment and methacholine responsiveness after ozone exposure. *Am J Physiol-Lung C* **288**, L61-L67, doi:DOI 10.1152/ajplung.00101.2004 (2005).
- 48 Ahuja, N. *et al.* Circulating IL-6 mediates lung injury via CXCL1 production after acute kidney injury in mice. *American journal of physiology. Renal physiology* **303**, F864-872, doi:10.1152/ajprenal.00025.2012 (2012).
- 49 Herbold, W. *et al.* Importance of CXC Chemokine Receptor 2 in Alveolar Neutrophil and Exudate Macrophage Recruitment in Response to Pneumococcal Lung Infection. *Infect Immun* **78**, 2620-2630, doi:Doi 10.1128/iai.01169-09 (2010).
- 50 Kordonowy, L. L. *et al.* Obesity Is Associated with Neutrophil Dysfunction and Attenuation of Murine Acute Lung Injury. *Am J Resp Cell Mol* **47**, 120-127, doi:DOI 10.1165/rcmb.2011-0334OC (2012).
- 51 Seki, M. *et al.* Critical Role of IL-1 Receptor-Associated Kinase-M in Regulating Chemokine-Dependent Deleterious Inflammation in Murine Influenza Pneumonia. *J Immunol* **184**, 1410-1418, doi:DOI 10.4049/jimmunol.0901709 (2010).
- 52 Londhe, V. A. *et al.* CXCR2/CXCR2 ligand biological axis impairs alveologenesis during dsRNA-induced lung inflammation in mice. *Pediatr Res* **58**, 919-926, doi:Doi 10.1203/01.Pdr.0000181377.78061.3e (2005).

- 53 Buane, P. *et al.* Crucial pathophysiological role of CXCR2 in experimental ulcerative colitis in mice. *J Leukocyte Biol* **82**, 1239-1246, doi:Doi 10.1189/Jlb.0207118 (2007).
- 54 Kuboki, S. *et al.* Hepatocyte signaling through CXC chemokine receptor-2 is detrimental to liver recovery after ischemia/reperfusion in mice. *Hepatology* **48**, 1213-1223, doi:Doi 10.1002/Hep.22471 (2008).
- 55 Tarzami, S. T. *et al.* Opposing effects mediated by the chemokine receptor CXCR2 on myocardial ischemia-reperfusion injury - Recruitment of potentially damaging neutrophils and direct myocardial protection. *Circulation* **108**, 2387-2392, doi:Doi 10.1161/01.Cir.0000093192.72099.9a (2003).
- 56 Cugini, D. *et al.* Inhibition of the chemokine receptor CXCR2 prevents kidney graft function deterioration due to ischemia/reperfusion. *Kidney Int* **67**, 1753-1761, doi:DOI 10.1111/j.1523-1755.2005.00272.x (2005).
- 57 Ruan, J. W. *et al.* Human pituitary tumor-transforming gene 1 overexpression reinforces oncogene-induced senescence through CXCR2/p21 signaling in breast cancer cells. *Breast Cancer Res* **14**, doi:Artn R106  
Doi 10.1186/Bcr3226 (2012).
- 58 Han, L. *et al.* High expression of CXCR2 is associated with tumorigenesis, progression, and prognosis of laryngeal squamous cell carcinoma. *Med Oncol* **29**, 2466-2472, doi:DOI 10.1007/s12032-011-0152-1 (2012).
- 59 Rubie, C. *et al.* ELR plus CXC chemokine expression in benign and malignant colorectal conditions. *Bmc Cancer* **8**, doi:Artn 178  
Doi 10.1186/1471-2407-8-178 (2008).
- 60 Huang, J. T. *et al.* Differential expression of interleukin-8 and its receptors in the neuroendocrine and non-neuroendocrine compartments of prostate cancer. *Am J Pathol* **166**, 1807-1815, doi:Doi 10.1016/S0002-9440(10)62490-X (2005).

- 61 Murphy, C. *et al.* Nonapical and cytoplasmic expression of interleukin-8, CXCR1, and CXCR2 correlates with cell proliferation and microvessel density in prostate cancer. *Clin Cancer Res* **11**, 4117-4127, doi:Doi 10.1158/1078-0432.Ccr-04-1518 (2005).
- 62 Hussain, F. *et al.* The expression of IL-8 and IL-8 receptors in pancreatic adenocarcinomas and pancreatic neuroendocrine tumours. *Cytokine* **49**, 134-140 (2010).
- 63 Frick, V. O. *et al.* Enhanced ENA-78 and IL-8 expression in patients with malignant pancreatic diseases. *Pancreatology* **8**, 488-497, doi:Doi 10.1159/000151776 (2008).
- 64 Saintigny, P. *et al.* CXCR2 Expression in Tumor Cells Is a Poor Prognostic Factor and Promotes Invasion and Metastasis in Lung Adenocarcinoma. *Cancer Res* **73**, 571-582, doi:Doi 10.1158/0008-5472.Can-12-0263 (2013).
- 65 Yang, G. *et al.* CXCR2 Promotes Ovarian Cancer Growth through Dysregulated Cell Cycle, Diminished Apoptosis, and Enhanced Angiogenesis. *Clin Cancer Res* **16**, 3875-3886, doi:Doi 10.1158/1078-0432.Ccr-10-0483 (2010).
- 66 Horikawa, T., Kaizaki, Y., Kato, H., Furukawa, M. & Yoshizaki, T. Expression of interleukin-8 receptor A predicts poor outcome in patients with nasopharyngeal carcinoma. *Laryngoscope* **115**, 62-67, doi:DOI 10.1097/01.mlg.0000150675.37860.f7 (2005).
- 67 Korkolopoulou, P. *et al.* Expression of Interleukin-8 Receptor CXCR2 and Suppressor of Cytokine Signaling-3 in Astrocytic Tumors. *Mol Med* **18**, 379-388, doi:DOI 10.2119/molmed.2011.00449 (2012).
- 68 Ning, Y. *et al.* Interleukin-8 is associated with proliferation, migration, angiogenesis and chemosensitivity in vitro and in vivo in colon cancer cell line models. *Int J Cancer* **128**, 2038-2049, doi:Doi 10.1002/ijc.25562 (2011).
- 69 Asfaha, S. *et al.* Mice That Express Human Interleukin-8 Have Increased Mobilization of Immature Myeloid Cells, Which Exacerbates Inflammation and Accelerates Colon



- Carcinogenesis. *Gastroenterology* **144**, 155-166, doi:DOI 10.1053/j.gastro.2012.09.057 (2013).
- 70 Ogatai, H. *et al.* GRO alpha promotes invasion of colorectal cancer cells. *Oncol Rep* **24**, 1479-1486, doi:Doi 10.3892/or\_00001008 (2010).
- 71 Singh, J. K. *et al.* Targeting CXCR1/2 Significantly Reduces Breast Cancer Stem Cell Activity and Increases the Efficacy of Inhibiting HER2 via HER2-Dependent and -Independent Mechanisms. *Clin Cancer Res* **19**, 643-656, doi:Doi 10.1158/1078-0432.Ccr-12-1063 (2013).
- 72 Acharyya, S. *et al.* A CXCL1 Paracrine Network Links Cancer Chemoresistance and Metastasis. *Cell* **150**, 165-178, doi:DOI 10.1016/j.cell.2012.04.042 (2012).
- 73 Matsuo, Y. *et al.* CXC-chemokine/CXCR2 biological axis promotes angiogenesis in vitro and in vivo in pancreatic cancer. *Int J Cancer* **125**, 1027-1037, doi:Doi 10.1002/ijc.24383 (2009).
- 74 Li, A. H. *et al.* Overexpression of CXCL5 Is Associated With Poor Survival in Patients With Pancreatic Cancer. *Am J Pathol* **178**, 1340-1349, doi:DOI 10.1016/j.ajpath.2010.11.058 (2011).
- 75 Wente, M. N. *et al.* Blockade of the chemokine receptor CXCR2 inhibits pancreatic cancer cell-induced angiogenesis. *Cancer letters* **241**, 221-227, doi:DOI 10.1016/j.canlet.2005.10.041 (2006).
- 76 Keane, M. P., Belperio, J. A., Xue, Y. Y., Burdick, M. D. & Strieter, R. M. Depletion of CXCR2 inhibits tumor growth and angiogenesis in a murine model of lung cancer. *J Immunol* **172**, 2853-2860 (2004).
- 77 Singh, S., Varney, M. & Singh, R. K. Host CXCR2-Dependent Regulation of Melanoma Growth, Angiogenesis, and Experimental Lung Metastasis. *Cancer Res* **69**, 411-415, doi:Doi 10.1158/0008-5472.Can-08-3378 (2009).

- 78 Shen, H., Schuster, R., Lu, B., Waltz, S. E. & Lentsch, A. B. Critical and opposing roles of the chemokine receptors CXCR2 and CXCR3 in prostate tumor growth. *The Prostate* **66**, 1721-1728, doi:10.1002/pros.20476 (2006).
- 79 Saijo, Y. *et al.* Proinflammatory cytokine IL-1 beta promotes tumor growth of Lewis lung carcinoma by induction of angiogenic factors: In vivo analysis of tumor-stromal interaction. *J Immunol* **169**, 469-475 (2002).
- 80 Halpern, J. L., Kilbarger, A. & Lynch, C. C. Mesenchymal stem cells promote mammary cancer cell migration in vitro via the CXCR2 receptor. *Cancer Lett* **308**, 91-99, doi:DOI 10.1016/j.canlet.2011.04.018 (2011).
- 81 Gabellini, C. *et al.* Functional activity of CXCL8 receptors, CXCR1 and CXCR2, on human malignant melanoma progression. *Eur J Cancer* **45**, 2618-2627, doi:DOI 10.1016/j.ejca.2009.07.007 (2009).
- 82 Li, A. H., Varney, M. L. & Singh, R. K. Constitutive expression of growth regulated oncogene (gro) in human colon carcinoma cells with different metastatic potential and its role in regulating their metastatic phenotype. *Clin Exp Metastas* **21**, 571-579 (2004).
- 83 Jamieson, T. *et al.* Inhibition of CXCR2 profoundly suppresses inflammation-driven and spontaneous tumorigenesis. *J Clin Invest* **122**, 3127-3144, doi:Doi 10.1172/Jci61067 (2012).
- 84 Chapman, R. W. *et al.* A novel, orally active CXCR1/2 receptor antagonist, sch527123, inhibits neutrophil recruitment, mucus production, and goblet cell hyperplasia in animal models of pulmonary inflammation. *J Pharmacol Exp Ther* **322**, 486-493, doi:DOI 10.1124/jpet.106.119040 (2007).
- 85 Min, S. H. *et al.* Pharmacological targeting reveals distinct roles for CXCR2/CXCR1 and CCR2 in a mouse model of arthritis. *Biochem Bioph Res Co* **391**, 1080-1086, doi:DOI 10.1016/j.bbrc.2009.12.025 (2010).

- 86 Singh, S. *et al.* Small-molecule antagonists for CXCR2 and CXCR1 inhibit human melanoma growth by decreasing tumor cell proliferation, survival, and angiogenesis. *Clin Cancer Res* **15**, 2380-2386, doi:10.1158/1078-0432.CCR-08-2387 (2009).
- 87 Varney, M. L. *et al.* Small molecule antagonists for CXCR2 and CXCR1 inhibit human colon cancer liver metastases. *Cancer Lett* **300**, 180-188, doi:DOI 10.1016/j.canlet.2010.10.004 (2011).
- 88 Braber, S. *et al.* CXCR2 antagonists block the N-Ac-PGP-induced neutrophil influx in the airways of mice, but not the production of the chemokine CXCL1. *Eur J Pharmacol* **668**, 443-449, doi:DOI 10.1016/j.ejphar.2011.03.025 (2011).
- 89 Zhang, S. G. *et al.* Simvastatin regulates CXC chemokine formation in streptococcal M1 protein-induced neutrophil infiltration in the lung. *Am J Physiol-Lung C* **300**, L930-L939, doi:DOI 10.1152/ajplung.00422.2010 (2011).
- 90 Bohrer, L. R. & Schwertfeger, K. L. Macrophages Promote Fibroblast Growth Factor Receptor-Driven Tumor Cell Migration and Invasion in a Cxcr2-Dependent Manner. *Mol Cancer Res* **10**, 1294-1305, doi:Doi 10.1158/1541-7786.Mcr-12-0275 (2012).
- 91 Yu, M., Berk, R. & Kosir, M. A. CXCL7-Mediated Stimulation of Lymphangiogenic Factors VEGF-C, VEGF-D in Human Breast Cancer Cells. *Journal of oncology* **2010**, 939407, doi:10.1155/2010/939407 (2010).
- 92 Stevenson, C. S. *et al.* Characterization of cigarette smoke-induced inflammatory and mucus hypersecretory changes in rat lung and the role of CXCR2 ligands in mediating this effect. *Am J Physiol-Lung C* **288**, L514-L522, doi:DOI 10.1152/ajplung.00317.2004 (2005).
- 93 Lazaar, A. L. *et al.* SB-656933, a novel CXCR2 selective antagonist, inhibits ex vivo neutrophil activation and ozone-induced airway inflammation in humans. *British journal of clinical pharmacology* **72**, 282-293, doi:10.1111/j.1365-2125.2011.03968.x (2011).

- 94 Yang, L. *et al.* Abrogation of TGF beta signaling in mammary carcinomas recruits Gr-1+CD11b+ myeloid cells that promote metastasis. *Cancer Cell* **13**, 23-35, doi:DOI 10.1016/j.ccr.2007.12.004 (2008).
- 95 Acharyya, S. *et al.* A CXCL1 paracrine network links cancer chemoresistance and metastasis. *Cell* **150**, 165-178, doi:10.1016/j.cell.2012.04.042 (2012).
- 96 Traves, S. L., Smith, S. J., Barnes, P. J. & Donnelly, L. E. Specific CXC but not CC chemokines cause elevated monocyte migration in COPD: a role for CXCR2. *J Leukoc Biol* **76**, 441-450, doi:10.1189/jlb.1003495 (2004).
- 97 Ijichi, H. *et al.* Inhibiting Cxcr2 disrupts tumor-stromal interactions and improves survival in a mouse model of pancreatic ductal adenocarcinoma. *J Clin Invest* **121**, 4106-4117, doi:Doi 10.1172/Jci42754 (2011).
- 98 Cunha, T. M. *et al.* Treatment with DF 2162, a non-competitive allosteric inhibitor of CXCR1/2, diminishes neutrophil influx and inflammatory hypernociception in mice. *Brit J Pharmacol* **154**, 460-470, doi:Doi 10.1038/Bjp.2008.94 (2008).
- 99 Coelho, F. M. *et al.* The chemokine receptors CXCR1/CXCR2 modulate antigen-induced arthritis by regulating adhesion of neutrophils to the synovial microvasculature. *Arthritis Rheum* **58**, 2329-2337, doi:Doi 10.1002/Art.23622 (2008).
- 100 Barsante, M. M. *et al.* Blockade of the chemokine receptor CXCR2 ameliorates adjuvant-induced arthritis in rats. *Br J Pharmacol* **153**, 992-1002, doi:10.1038/sj.bjp.0707462 (2008).
- 101 Russo, R. C. *et al.* Role of the Chemokine Receptor CXCR2 in Bleomycin-Induced Pulmonary Inflammation and Fibrosis. *Am J Resp Cell Mol* **40**, 410-421, doi:DOI 10.1165/rcmb.2007-0364OC (2009).
- 102 Podechard, N. *et al.* Interleukin-8 induction by the environmental contaminant benzo(a)pyrene is aryl hydrocarbon receptor-dependent and leads to lung inflammation. *Toxicol Lett* **177**, 130-137, doi:DOI 10.1016/j.toxlet.2008.01.006 (2008).

- 103 Liu, X. *et al.* G31P, an Antagonist against CXC Chemokine Receptors 1 and 2, Inhibits Growth of Human Prostate Cancer Cells in Nude Mice. *Tohoku J Exp Med* **228**, 147-156, doi:Doi 10.1620/Tjem.228.147 (2012).
- 104 Tazzyman, S. *et al.* Inhibition of neutrophil infiltration into A549 lung tumors in vitro and in vivo using a CXCR2-specific antagonist is associated with reduced tumor growth. *Int J Cancer* **129**, 847-858, doi:Doi 10.1002/ijc.25987 (2011).
- 105 Wilson, C. *et al.* Constitutive and Treatment-Induced CXCL8-Signalling Selectively Modulates the Efficacy of Anti-Metabolite Therapeutics in Metastatic Prostate Cancer. *PloS one* **7**, doi:ARTN e36545  
DOI 10.1371/journal.pone.0036545 (2012).
- 106 Allegretti, M. *et al.* Allosteric inhibitors of chemoattractant receptors: opportunities and pitfalls. *Trends Pharmacol Sci* **29**, 280-286, doi:DOI 10.1016/j.tips.2008.03.005 (2008).
- 107 Proudfoot, A. E. I., Power, C. A. & Schwarz, M. K. Anti-chemokine small molecule drugs: a promising future? *Expert Opin Inv Drug* **19**, 345-355, doi:Doi 10.1517/13543780903535867 (2010).
- 108 Holz, O. *et al.* SCH527123, a novel CXCR2 antagonist, inhibits ozone-induced neutrophilia in healthy subjects. *Eur Respir J* **35**, 564-570, doi:Doi 10.1183/09031936.00048509 (2010).
- 109 Chapman, R. W. *et al.* CXCR2 antagonists for the treatment of pulmonary disease. *Pharmacol Therapeut* **121**, 55-68, doi:DOI 10.1016/j.pharmthera.2008.10.005 (2009).
- 110 Moss, R. B. *et al.* Safety and early treatment effects of the CXCR2 antagonist SB-656933 in patients with cystic fibrosis. *Journal of cystic fibrosis : official journal of the European Cystic Fibrosis Society* **12**, 241-248, doi:10.1016/j.jcf.2012.08.016 (2013).
- 111 Norman, P. Evidence on the identity of the CXCR2 antagonist AZD-5069. *Expert Opin Ther Pat* **23**, 113-117, doi:Doi 10.1517/13543776.2012.725724 (2013).

- 112 Hertzner, K. M., Donald, G. W. & Hines, O. J. CXCR2: a target for pancreatic cancer treatment? *Expert opinion on therapeutic targets* **17**, 667-680, doi:10.1517/14728222.2013.772137 (2013).
- 113 Thelen, M. & Stein, J. V. How chemokines invite leukocytes to dance. *Nature immunology* **9**, 953-959, doi:Doi 10.1038/Ni.F.207 (2008).
- 114 Neel, N. F. *et al.* IQGAP1 Is a Novel CXCR2-Interacting Protein and Essential Component of the "Chemosynapse". *PloS one* **6**, doi:ARTN e23813
- 115 Fan, G. H., Yang, W., Sai, J. Q. & Richmond, A. Hsc/Hsp70 interacting protein (Hip) associates with CXCR2 and regulates the receptor signaling and trafficking. *Journal of Biological Chemistry* **277**, 6590-6597, doi:DOI 10.1074/jbc.M110588200 (2002).
- 116 Fan, G. H., Lapierre, L. A., Goldenring, J. R. & Richmond, A. Differential regulation of CXCR2 trafficking by Rab GTPases. *Blood* **101**, 2115-2124, doi:DOI 10.1182/blood-2002-07-1965 (2003).
- 117 Neel, N. F., Lapierre, L. A., Goldenring, J. R. & Richmond, A. RhoB plays an essential role in CXCR2 sorting decisions. *J Cell Sci* **120**, 1559-1571, doi:Doi 10.1242/Jcs.03437 (2007).
- 118 Fan, G. H., Lapierre, L. A., Goldenring, J. R., Sai, J. Q. & Richmond, A. Rab11-family interacting protein 2 and myosin Vb are required for CXCR2 recycling and receptor-mediated chemotaxis. *Mol Biol Cell* **15**, 2456-2469, doi:DOI 10.1091/mbc.E03-09-0706 (2004).
- 119 Richardson, R. M., Marjoram, R. J., Barak, L. S. & Snyderman, R. Role of the cytoplasmic tails of CXCR1 and CXCR2 in mediating leukocyte migration, activation, and regulation. *J Immunol* **170**, 2904-2911 (2003).
- 120 Barlic, J. *et al.* Regulation of tyrosine kinase activation and granule release through beta-arrestin by CXCR1. *Nature immunology* **1**, 227-233, doi:Doi 10.1038/79767 (2000).

- 121 Neel, N. F. *et al.* VASP is a CXCR2-interacting protein that regulates CXCR2-mediated polarization and chemotaxis. *J Cell Sci* **122**, 1882-1894, doi:Doi 10.1242/Jcs.039057 (2009).
- 122 Raman, D., Sai, J. Q., Neel, N. F., Chew, C. S. & Richmond, A. LIM and SH3 Protein-1 Modulates CXCR2-Mediated Cell Migration. *PloS one* **5**, doi:ARTN e10050
- 123 Baugher, P. J. & Richmond, A. The Carboxyl-terminal PDZ Ligand Motif of Chemokine Receptor CXCR2 Modulates Post-endocytic Sorting and Cellular Chemotaxis. *Journal of Biological Chemistry* **283**, 30868-30878, doi:DOI 10.1074/jbc.M804054200 (2008).
- 124 Wu, Y. N. *et al.* A Chemokine Receptor CXCR2 Macromolecular Complex Regulates Neutrophil Functions in Inflammatory Diseases. *Journal of Biological Chemistry* **287**, 5744-5755, doi:DOI 10.1074/jbc.M111.315762 (2012).
- 125 Wang, S. *et al.* CXCR2 Macromolecular Complex in Pancreatic Cancer: A Potential Therapeutic Target in Tumor Growth. *Translational oncology* **6**, 216-225, doi:Doi 10.1593/Tlo.13133 (2013).
- 126 Yanning Wu, S. M. F., Shuo Wang, Xiaoqing Guan, Yanxia Liu, Yuning Hou, Robert M. Strieter, Ali S. Arbab, Chunying Li. A critical role of CXCR2 PDZ-mediated interactions in endothelial progenitor cell neovascularization. *Angiogenesis* **2013**, 253, doi:10.1007/s10456-012-9326-5 (2013).
- 127 Su, Y. J. *et al.* Altered CXCR2 signaling in beta-arrestin-2-deficient mouse models. *J Immunol* **175**, 5396-5402 (2005).
- 128 Lu, G. R. *et al.* Structural Insights into Neutrophilic Migration Revealed by the Crystal Structure of the Chemokine Receptor CXCR2 in Complex with the First PDZ Domain of NHERF1. *Plos One* **8**, doi:ARTN e76219

- 129 Jiang, Y. *et al.* New Conformational State of NHERF1-CXCR2 Signaling Complex Captured by Crystal Lattice Trapping. *PloS one* **8**, e81904, doi:10.1371/journal.pone.0081904 (2013).
- 130 Weinman, E. J., Minkoff, C. & Shenolikar, S. Signal complex regulation of renal transport proteins: NHERF and regulation of NHE3 by PKA. *Am J Physiol-Renal* **279**, F393-F399 (2000).
- 131 Wang, B., Yang, Y. M., Abou-Samra, A. B. & Friedman, P. A. NHERF1 Regulates Parathyroid Hormone Receptor Desensitization: Interference with beta-Arrestin Binding. *Mol Pharmacol* **75**, 1189-1197, doi:DOI 10.1124/mol.108.054486 (2009).
- 132 Siegel, R., Naishadham, D. & Jemal, A. Cancer statistics, 2012. *CA Cancer J Clin* **62**, 10-29, doi:10.3322/caac.20138 (2012).
- 133 Huang, Z. Q., Saluja, A. K., Dudeja, V., Vickers, S. M. & Buchsbaum, D. J. Molecular targeted approaches for treatment of pancreatic cancer. *Current pharmaceutical design* **17**, 2221-2238 (2011).
- 134 Wang, S. & Li, C. Tumor Microenvironment and Pancreatic Cancer. *Journal of Molecular Biology* **1**, e104, doi:10.4172/2168-9547.1000e104 (2012).
- 135 Xie, K., Wei, D. & Huang, S. Transcriptional anti-angiogenesis therapy of human pancreatic cancer. *Cytokine & growth factor reviews* **17**, 147-156, doi:10.1016/j.cytogfr.2006.01.002 (2006).
- 136 Xiong, H. Q. *et al.* NF-kappaB activity blockade impairs the angiogenic potential of human pancreatic cancer cells. *International journal of cancer. Journal international du cancer* **108**, 181-188, doi:10.1002/ijc.11562 (2004).
- 137 Shi, Q. *et al.* Constitutive and inducible interleukin 8 expression by hypoxia and acidosis renders human pancreatic cancer cells more tumorigenic and metastatic. *Clinical cancer research : an official journal of the American Association for Cancer Research* **5**, 3711-3721 (1999).



- 138 Zhu, V. F., Yang, J., Lebrun, D. G. & Li, M. Understanding the role of cytokines in Glioblastoma Multiforme pathogenesis. *Cancer Lett* **316**, 139-150, doi:10.1016/j.canlet.2011.11.001 (2012).
- 139 Waugh, D. J. & Wilson, C. The interleukin-8 pathway in cancer. *Clinical cancer research : an official journal of the American Association for Cancer Research* **14**, 6735-6741, doi:10.1158/1078-0432.CCR-07-4843 (2008).
- 140 Hussain, F. *et al.* The expression of IL-8 and IL-8 receptors in pancreatic adenocarcinomas and pancreatic neuroendocrine tumours. *Cytokine* **49**, 134-140, doi:DOI 10.1016/j.cyto.2009.11.010 (2010).
- 141 Takamori, H., Oades, Z. G., Hoch, O. C., Burger, M. & Schraufstatter, I. U. Autocrine growth effect of IL-8 and GROalpha on a human pancreatic cancer cell line, Capan-1. *Pancreas* **21**, 52-56 (2000).
- 142 Hidaka, H. *et al.* Curcumin inhibits interleukin 8 production and enhances interleukin 8 receptor expression on the cell surface: impact on human pancreatic carcinoma cell growth by autocrine regulation. *Cancer* **95**, 1206-1214, doi:10.1002/cncr.10812 (2002).
- 143 Kuwada, Y. *et al.* Potential involvement of IL-8 and its receptors in the invasiveness of pancreatic cancer cells. *Int J Oncol* **22**, 765-771 (2003).
- 144 Miyamoto, M. *et al.* Effect of interleukin-8 on production of tumor-associated substances and autocrine growth of human liver and pancreatic cancer cells. *Cancer immunology, immunotherapy : CII* **47**, 47-57 (1998).
- 145 Wu, D., Jiang, H., Katz, A. & Simon, M. I. Identification of critical regions on phospholipase C-beta 1 required for activation by G-proteins. *J Biol Chem* **268**, 3704-3709 (1993).
- 146 Fanning, A. S. & Anderson, J. M. PDZ domains: fundamental building blocks in the organization of protein complexes at the plasma membrane. *Journal of Clinical Investigation* **103**, 767-772 (1999).

- 147 Li, C. Y. & Naren, A. P. CFTR chloride channel in the apical compartments: spatiotemporal coupling to its interacting partners. *Integr Biol-Uk* **2**, 161-177, doi:Doi 10.1039/B924455g (2010).
- 148 Jelen, F., Oleksy, A., Smietana, K. & Otlewski, J. PDZ domains - common players in the cell signaling. *Acta Biochim Pol* **50**, 985-1017, doi:035004985 (2003).
- 149 Songyang, Z. *et al.* Recognition of unique carboxyl-terminal motifs by distinct PDZ domains. *Science* **275**, 73-77 (1997).
- 150 Doyle, D. A. *et al.* Crystal structures of a complexed and peptide-free membrane protein-binding domain: Molecular basis of peptide recognition by PDZ. *Cell* **85**, 1067-1076 (1996).
- 151 Karthikeyan, S., Leung, T., Birrane, G., Webster, G. & Ldias, J. A. A. Crystal structure of the PDZ1 domain of human Na<sup>+</sup>/H<sup>+</sup> exchanger regulatory factor provides insights into the mechanism of carboxyl-terminal leucine recognition by class IPDZ domains. *Journal of Molecular Biology* **308**, 963-973 (2001).
- 152 Daniels, D. L., Cohen, A. R., Anderson, J. M. & Brunger, A. T. Crystal structure of the hCASK PDZ domain reveals the structural basis of class II PDZ domain target recognition. *Nature Structural Biology* **5**, 317-325 (1998).
- 153 Naren, A. P. *et al.* A macromolecular complex of beta(2) adrenergic receptor, CFTR, and ezrin/radixin/moesin-binding phosphoprotein 50 is regulated by PKA. *Proceedings of the National Academy of Sciences of the United States of America* **100**, 342-346, doi:DOI 10.1073/pnas.0135434100 (2003).
- 154 Li, C. Y. *et al.* Lysophosphatidic acid inhibits cholera toxin-induced secretory diarrhea through CFTR-dependent protein interactions. *Journal of Experimental Medicine* **202**, 975-986, doi:Doi 10.1084/Jem.20050421 (2005).

- 155 Li, C. Y. *et al.* Spatiotemporal coupling of cAMP transporter to CFTR chloride channel function in the gut epithelia. *Cell* **131**, 940-951, doi:DOI 10.1016/j.cell.2007.09.037 (2007).
- 156 Li, C., Schuetz, J. D. & Naren, A. P. Tobacco carcinogen NNK transporter MRP2 regulates CFTR function in lung epithelia: implications for lung cancer. *Cancer Lett* **292**, 246-253, doi:10.1016/j.canlet.2009.12.009 (2010).
- 157 Wu, Y., Wang, S. & Li, C. In vitro analysis of PDZ-dependent CFTR macromolecular signaling complexes. *Journal of visualized experiments : JoVE*, doi:10.3791/4091 (2012).
- 158 Hwang, J. I. *et al.* The interaction of phospholipase C-beta 3 with Shank2 regulates mGluR-mediated calcium signal. *Journal of Biological Chemistry* **280**, 12467-12473, doi:DOI 10.1074/jbc.M410740200 (2005).
- 159 Choi, J. W. *et al.* Subtype-specific role of phospholipase C-beta in bradykinin and LPA signaling through differential binding of different PDZ scaffold proteins. *Cell Signal* **22**, 1153-1161, doi:DOI 10.1016/j.cellsig.2010.03.010 (2010).
- 160 Donowitz, M. *et al.* Alterations in the proteome of the NHERF1 knockout mouse jejunal brush border membrane vesicles. *Physiol Genomics* **42A**, 200-210, doi:10.1152/physiolgenomics.00001.2010 (2010).
- 161 Hwang, J. I. *et al.* Regulation of phospholipase C-beta 3 activity by Na<sup>+</sup>/H<sup>+</sup> exchanger regulatory factor 2. *Journal of Biological Chemistry* **275**, 16632-16637 (2000).
- 162 Suh, P. G., Hwang, J. I., Ryu, S. H., Donowitz, M. & Kim, J. H. Breakthroughs and views - The roles of PDZ-containing proteins in PLC-beta-mediated signaling. *Biochemical and Biophysical Research Communications* **288**, 1-7 (2001).
- 163 Wu, Y. *et al.* A chemokine receptor CXCR2 macromolecular complex regulates neutrophil functions in inflammatory diseases. *The Journal of biological chemistry* **287**, 5744-5755, doi:10.1074/jbc.M111.315762 (2012).

- 164 Zhang, Y., Vogel, W. K., McCullar, J. S., Greenwood, J. A. & Filtz, T. M. Phospholipase C-beta3 and -beta1 form homodimers, but not heterodimers, through catalytic and carboxyl-terminal domains. *Molecular pharmacology* **70**, 860-868, doi:10.1124/mol.105.021923 (2006).
- 165 Guha, S. *et al.* Broad-spectrum G protein-coupled receptor antagonist, [D-Arg1,D-Trp5,7,9,Leu11]SP: a dual inhibitor of growth and angiogenesis in pancreatic cancer. *Cancer Res* **65**, 2738-2745, doi:10.1158/0008-5472.CAN-04-3197 (2005).
- 166 Morales, F. C. *et al.* NHERF1/EBP50 head-to-tail intramolecular interaction masks association with PDZ domain ligands. *Molecular and cellular biology* **27**, 2527-2537, doi:10.1128/MCB.01372-06 (2007).
- 167 Georgescu, M. M., Morales, F. C., Molina, J. R. & Hayashi, Y. Roles of NHERF1/EBP50 in cancer. *Current molecular medicine* **8**, 459-468 (2008).
- 168 Matsuo, Y. *et al.* CXCL8/IL-8 and CXCL12/SDF-1alpha co-operatively promote invasiveness and angiogenesis in pancreatic cancer. *International journal of cancer. Journal international du cancer* **124**, 853-861, doi:10.1002/ijc.24040 (2009).
- 169 Hill, K. S. *et al.* Met Receptor Tyrosine Kinase Signaling Induces Secretion of the Angiogenic Chemokine Interleukin-8/CXCL8 in Pancreatic Cancer. *PLoS One* **7**, doi:ARTN e40420
- 170 Li, M. *et al.* Interleukin-8 increases vascular endothelial growth factor and neuropilin expression and stimulates ERK activation in human pancreatic cancer. *Cancer science* **99**, 733-737, doi:10.1111/j.1349-7006.2008.00740.x (2008).
- 171 Yamamoto, M. *et al.* TSU68 prevents liver metastasis of colon cancer xenografts by modulating the premetastatic niche. *Cancer Res* **68**, 9754-9762, doi:10.1158/0008-5472.CAN-08-1748 (2008).

- 172 Kim, J. K. *et al.* Subtype-specific roles of phospholipase C-beta via differential interactions with PDZ domain proteins. *Advances in enzyme regulation* **51**, 138-151, doi:10.1016/j.advenzreg.2010.10.004 (2011).
- 173 Kim, C. G., Park, D. & Rhee, S. G. The role of carboxyl-terminal basic amino acids in Gqalpha-dependent activation, particulate association, and nuclear localization of phospholipase C-beta1. *Journal of Biological Chemistry* **271**, 21187-21192 (1996).
- 174 Rhee, S. G. Regulation of phosphoinositide-specific phospholipase C. *Annu Rev Biochem* **70**, 281-312 (2001).
- 175 Lee, C. W., Lee, K. H., Lee, S. B., Park, D. & Rhee, S. G. Regulation of phospholipase C-beta 4 by ribonucleotides and the alpha subunit of Gq. *Journal of Biological Chemistry* **269**, 25335-25338 (1994).
- 176 Tang, Y. *et al.* Association of mammalian trp4 and phospholipase C isozymes with a PDZ domain-containing protein, NHERF. *J Biol Chem* **275**, 37559-37564, doi:10.1074/jbc.M006635200
- 177 E, S. Y. *et al.* Lysophosphatidic Acid 2 Receptor-mediated Supramolecular Complex Formation Regulates Its Antiapoptotic Effect. *Journal of Biological Chemistry* **284**, 14558-14571, doi:DOI 10.1074/jbc.M900185200 (2009).
- 178 Maudsley, S. *et al.* Platelet-derived growth factor receptor association with Na<sup>+</sup>/H<sup>+</sup> exchanger regulatory factor potentiates receptor activity. *Molecular and Cellular Biology* **20**, 8352-8363 (2000).
- 179 Davare, M. A. *et al.* A beta(2) adrenergic receptor signaling complex assembled with the Ca<sup>2+</sup> channel Ca(v)1.2. *Science* **293**, 98-101, doi:DOI 10.1126/science.293.5527.98 (2001).

- 180 Patra, C. R. *et al.* Chemically modified peptides targeting the PDZ domain of GIPC as a therapeutic approach for cancer. *ACS chemical biology* **7**, 770-779, doi:10.1021/cb200536r (2012).
- 181 Sankaram, M. B. Membrane Interaction of Small N-Myristoylated Peptides - Implications for Membrane Anchoring and Protein-Protein Association. *Biophysical journal* **67**, 105-112 (1994).
- 182 Peitzsch, R. M. & Mclaughlin, S. Binding of Acylated Peptides and Fatty-Acids to Phospholipid-Vesicles - Pertinence to Myristoylated Proteins. *Biochemistry-Us* **32**, 10436-10443, doi:Doi 10.1021/Bi00090a020 (1993).
- 183 Losonczi, J. A., Tian, F. & Prestegard, J. H. Nuclear magnetic resonance studies of the N-terminal fragment of adenosine diphosphate ribosylation factor 1 in micelles and bicelles: Influence of N-myristoylation. *Biochemistry-Us* **39**, 3804-3816, doi:Doi 10.1021/Bi9923050 (2000).
- 184 Lu, Y. X., Wang, Y. & Zhu, W. L. Nonbonding interactions of organic halogens in biological systems: implications for drug discovery and biomolecular design. *Phys Chem Chem Phys* **12**, 4543-4551, doi:Doi 10.1039/B926326h (2010).
- 185 Halogen Bonding: Fundamentals and Applications. *Struct Bond* **126**, 1-221, doi:Doi 10.1007/978-3-540-74330-9 (2008).
- 186 Greenbaum, D. C. *et al.* Synthesis and structure-activity relationships of parasiticidal thiosemicarbazone cysteine protease inhibitors against Plasmodium falciparum, Trypanosoma brucei, and Trypanosoma cruzi. *J Med Chem* **47**, 3212-3219, doi:Doi 10.1021/Jm030549j (2004).
- 187 Krystof, V. *et al.* 4-arylazo-3,5-diamino-1H-pyrazole CDK inhibitors: SAR study, crystal structure in complex with CDK2, selectivity, and cellular effects. *J Med Chem* **49**, 6500-6509, doi:Doi 10.1021/Jm0605740 (2006).

- 188 Addison, C. L. *et al.* The CXC chemokine receptor 2, CXCR2, is the putative receptor for ELR+ CXC chemokine-induced angiogenic activity. *J Immunol* **165**, 5269-5277 (2000).
- 189 Chapman, R. W. *et al.* CXCR2 antagonists for the treatment of pulmonary disease. *Pharmacol Ther* **121**, 55-68 (2009).
- 190 Tsai, H. H. *et al.* The chemokine receptor CXCR2 controls positioning of oligodendrocyte precursors in developing spinal cord by arresting their migration. *Cell* **110**, 373-383 (2002).
- 191 Li, A. *et al.* Overexpression of CXCL5 is associated with poor survival in patients with pancreatic cancer. *Am J Pathol* **178**, 1340-1349 (2011).
- 192 Wang, S. *et al.* CXCR2 macromolecular complex in pancreatic cancer: a potential therapeutic target in tumor growth. *Translational oncology* **6**, 216-225 (2013).
- 193 Magalhaes, A. C., Dunn, H. & Ferguson, S. S. Regulation of GPCR activity, trafficking and localization by GPCR-interacting proteins. *Br J Pharmacol* **165**, 1717-1736 (2012).
- 194 Neel, N. F. *et al.* VASP is a CXCR2-interacting protein that regulates CXCR2-mediated polarization and chemotaxis. *J Cell Sci* **122**, 1882-1894 (2009).
- 195 Shenolikar, S., Voltz, J. W., Cunningham, R. & Weinman, E. J. Regulation of ion transport by the NHERF family of PDZ proteins. *Physiology (Bethesda)* **19**, 362-369 (2004).
- 196 Harris, B. Z. & Lim, W. A. Mechanism and role of PDZ domains in signaling complex assembly. *J Cell Sci* **114**, 3219-3231 (2001).
- 197 Sheng, M. & Sala, C. PDZ domains and the organization of supramolecular complexes. *Annu Rev Neurosci* **24**, 1-29 (2001).
- 198 Lee, H. J. & Zheng, J. J. PDZ domains and their binding partners: structure, specificity, and modification. *Cell Commun Signal* **8**, 8 (2010).

- 199 Karthikeyan, S., Leung, T. & Ladas, J. A. Structural basis of the Na<sup>+</sup>/H<sup>+</sup> exchanger regulatory factor PDZ1 interaction with the carboxyl-terminal region of the cystic fibrosis transmembrane conductance regulator. *J Biol Chem* **276**, 19683-19686 (2001).
- 200 Tonikian, R. *et al.* A specificity map for the PDZ domain family. *PLoS Biol* **6**, e239 (2008).
- 201 Kabsch, W. Xds. *Acta Crystallogr D Biol Crystallogr* **66**, 125-132 (2010).
- 202 McCoy, A. J. *et al.* Phaser crystallographic software. *J Appl Crystallogr* **40**, 658-674 (2007).
- 203 Emsley, P. & Cowtan, K. Coot: model-building tools for molecular graphics. *Acta Crystallogr D Biol Crystallogr* **60**, 2126-2132 (2004).
- 204 Adams, P. D. *et al.* PHENIX: a comprehensive Python-based system for macromolecular structure solution. *Acta Crystallogr D Biol Crystallogr* **66**, 213-221 (2010).
- 205 Chen, V. B. *et al.* MolProbity: all-atom structure validation for macromolecular crystallography. *Acta Crystallogr D Biol Crystallogr* **66**, 12-21 (2010).
- 206 Runyon, S. T. *et al.* Structural and functional analysis of the PDZ domains of human HtrA1 and HtrA3. *Protein Sci* **16**, 2454-2471 (2007).
- 207 Lu, G. *et al.* Structural insights into neutrophilic migration revealed by the crystal structure of the chemokine receptor CXCR2 in complex with the first PDZ domain of NHERF1. *PLoS One* **8**, e76219 (2013).
- 208 Cardone, R. A. *et al.* NHERF1 acts as a molecular switch to program metastatic behavior and organotropism via its PDZ domains. *Mol Biol Cell* **23**, 2028-2040 (2012).
- 209 Wu, D., LaRosa, G. J. & Simon, M. I. G protein-coupled signal transduction pathways for interleukin-8. *Science* **261**, 101-103 (1993).
- 210 Harden, T. K., Hicks, S. N. & Sondek, J. Phospholipase C isozymes as effectors of Ras superfamily GTPases. *J Lipid Res* **50**, S243-S248, doi:DOI 10.1194/jlr.R800045-JLR200 (2009).



- 211 Jiang, H. P. *et al.* Phospholipase C beta 4 is involved in modulating the visual response in mice. *Proceedings of the National Academy of Sciences of the United States of America* **93**, 14598-14601, doi:DOI 10.1073/pnas.93.25.14598 (1996).
- 212 Kano, M. *et al.* Phospholipase C beta 4 is specifically involved in climbing fiber synapse elimination in the developing cerebellum. *Proceedings of the National Academy of Sciences of the United States of America* **95**, 15724-15729, doi:DOI 10.1073/pnas.95.26.15724 (1998).
- 213 Axelrod, D., Koppel, D. E., Schlessinger, J., Elson, E. & Webb, W. W. Mobility measurement by analysis of fluorescence photobleaching recovery kinetics. *Biophysical journal* **16**, 1055-1069, doi:10.1016/S0006-3495(76)85755-4 (1976).
- 214 Sprague, B. L., Pego, R. L., Stavreva, D. A. & McNally, J. G. Analysis of binding reactions by fluorescence recovery after photobleaching. *Biophysical journal* **86**, 3473-3495, doi:10.1529/biophysj.103.026765 (2004).
- 215 Houtsmuller, A. B. & Vermeulen, W. Macromolecular dynamics in living cell nuclei revealed by fluorescence redistribution after photobleaching. *Histochemistry and cell biology* **115**, 13-21 (2001).
- 216 Edidin, M., Zagayansky, Y. & Lardner, T. J. Measurement of membrane protein lateral diffusion in single cells. *Science* **191**, 466-468 (1976).
- 217 Schlessinger, J. *et al.* Lateral transport on cell membranes: mobility of concanavalin A receptors on myoblasts. *Proceedings of the National Academy of Sciences of the United States of America* **73**, 2409-2413 (1976).
- 218 Liebman, P. A. & Entine, G. Lateral Diffusion of Visual Pigment in Photoreceptor Disk Membranes. *Science* **185**, 457-459, doi:DOI 10.1126/science.185.4149.457 (1974).
- 219 Dou, Y. L., Bowen, J., Liu, Y. F. & Gorovsky, M. A. Phosphorylation and an ATP-dependent process increase the dynamic exchange of H1 in chromatin. *J Cell Biol* **158**, 1161-1170, doi:DOI 10.1083/jcb.200202131 (2002).

- 220 Sarker, R. *et al.* NHERF1 and NHERF2 are necessary for multiple but usually separate aspects of basal and acute regulation of NHE3 activity. *Am J Physiol-Cell Ph* **300**, C771-C782, doi:DOI 10.1152/ajpcell.00119.2010 (2011).

**ABSTRACT****CXCR2 MACROMOLECULAR COMPLEX IN PANCREATIC CANCER: A POTENTIAL THERAPEUTIC TARGET IN TUMOR GROWTH**

by

**SHUO WANG****May 2014****Advisor:** Dr. Chunying Li**Major:** Biochemistry & Molecular Biology**Degree:** Doctor of Philosophy

The signaling mediated by the chemokine receptor CXCR2 plays an important role in promoting the progression of many cancers, including pancreatic cancer, one of the most lethal human malignancies. CXCR2 possesses a consensus PSD-95/DlgA/ZO-1 (PDZ) motif at its carboxyl termini, which might interact with potential PDZ scaffold/adaptor proteins. We have previously reported that CXCR2 PDZ motif-mediated protein interaction is an important regulator for neutrophil functions. Here, using a series of biochemical assays, we demonstrate that CXCR2 is physically coupled to its downstream effector phospholipase C- $\beta$ 3 (PLC- $\beta$ 3) that is mediated by PDZ scaffold protein Na(+)/H(+) exchange regulatory factor 1 (NHERF1) into a macromolecular signaling complex both *in vitro* and in pancreatic cancer cells. We also observe that disrupting the CXCR2 complex, by gene delivery or peptide delivery of exogenous CXCR2 C-tail, significantly inhibits the biologic functions of pancreatic cancer cells (i.e., proliferation and invasion) in a PDZ motif-dependent manner. In addition, using a human pancreatic tumor xenograft model, we show that gene delivery of CXCR2 C-tail sequence (containing the PDZ motif) by adeno-

associated virus type 2 viral vector potently suppresses human pancreatic tumor growth in a subcutaneous xenograft mouse model. In summary, our results suggest the existence of a physical and functional coupling of CXCR2 and PLC- $\beta$ 3 mediated through NHERF1, forming a macromolecular complex that is critical for efficient and specific CXCR2 signaling in pancreatic cancer progression. Disrupting this CXCR2 complex could represent a novel and effective treatment strategy against pancreatic cancer.

## AUTOBIOGRAPHICAL STATEMENT

### SHUO WANG

#### Contact Information:

Department of Biochemistry & Molecular Biology, Wayne State University School of Medicine. 540 E. Canfield St., Detroit, MI-48201  
[shuwang@med.wayne.edu](mailto:shuwang@med.wayne.edu)

#### Education:

Aug. 2009 ~ May 2014      Ph.D. in Biochemistry & Molecular Biology,  
 Wayne State University School of Medicine

#### Publications:

1. Yanning Wu, **Shuo Wang**, Chunying Li. *In Vitro Analysis of PDZ-dependent CFTR Macromolecular Signaling Complexes. Journal of Visualized Experiments.* 2012 Aug 13;(66). pii: 4091. doi: 10.3791/4091
2. Yanning Wu\*, **Shuo Wang\***, Shukkur Muhammed Farooq\* (**\* Equal contributions**), Marcello Pasquale Castelvete, Yuning Hou, Jiliang Gao, Javier V. Navarro, David Oupicky, Fei, Sun, Chunying Li. *A Chemokine Receptor CXCR2 Macromolecular Complex Regulates Neutrophil Functions in Inflammatory Diseases. Journal of Biological Chemistry.* 2012 Feb 17; 287(8):5744-55. doi: 10.1074/jbc.M111.315762. Recommended and rated "Top 2%" of published articles in biology and medicine by **Faculty of 1000**.
3. **Shuo Wang**, Chunying Li. *Tumor Microenvironment and Pancreatic Cancer. Mol. Biol. doi: 10.4172/2168-9547.1000e104* (2012)
4. **Shuo Wang**, Yanning Wu, Yuning Hou, Marcello P. Castelvete, Xiaoqing Guan, Jacob J. Oblak, Sanjeev Banerjee, Theresa M. Filtz, Fazlul H. Sarkar, Xuequn Chen, Bhanu P. Jena, Chunying Li. *CXCR2 Macromolecular Complex in Pancreatic Cancer: A Potential Therapeutic Target in Tumor growth. Translational Oncology.* 2013 Apr;6(2):216-25. Highlighted by **Pancreatic Cell News**.
5. Yanning Wu, Shukkur M. Farooq, **Shuo Wang**, Xiaoqing Guan, Yanxia Liu, Yuning Hou, Robert M. Strieter, Ali S. Arbab, Chunying Li. *A critical role of CXCR2 PDZ-mediated interactions in endothelial progenitor cell neovascularization. Angiogenesis (2012).* DOI 10.1007/s10456-012-9326-5.
6. Guorong Lu, Yanning Wu, Yuanyuan Jiang, **Shuo Wang**, Yuning Hou, Xiaoqing Guan, Joseph Brunzelle, Nualpun Sirinupong, Shijie Sheng, Chunying Li, Zhe Yang. *Structural Insights into Neutrophilic Migration Revealed by the Crystal Structure of the Chemokine Receptor CXCR2 in Complex with the First PDZ Domain of NHERF1. PLoS ONE* 8(10): e76219. doi:10.1371/journal.pone.0076219.
7. Yuanyuan Jiang, Guorong Lu, Laura Trescott, Yuning Hou, Xiaoqing Guan, **Shuo Wang**, Angelique Stamenkovich, Joseph Brunzelle, Nualpun Sirinupong, Mark Spaller, Chunying Li, Zhe Yang. *New Conformational State of NHERF1-CXCR2 Signaling Complex Captured by Crystal Lattice Trapping. PLoS ONE* 8(12): e81904. doi:10.1371/journal.pone.0081904.
8. Yuanyuan Jiang<sup>#</sup>, **Shuo Wang<sup>#</sup>**, (**# Equal Contributions**) Joshua Holcomb, Laura Trescott, Xiaoqing Guan, Yuning Hou, Joseph Brunzelle, Nualpun Sirinupong, Chunying Li, Zhe Yang. *Crystallographic Analysis of NHERF1-PLCbeta3 Interaction Provides Structural Basis for CXCR2 Signaling in Pancreatic Cancer. Biochemical and biophysical research communications,* doi:10.1016/j.bbrc.2014.03.028 (2014)